

**VIRAL REGULATION OF CAP-DEPENDENT MESSENGER RNA TRANSLATION
INHIBITOR 4E-BP1 DURING MITOSIS**

by

Celestino Velásquez

B.S. in Biomedical Chemistry, Oral Roberts University, 2013

Submitted to the Graduate Faculty of
University of Pittsburgh School of Medicine
Program in Integrative Molecular Biology
in partial fulfillment
of the requirements for the degree of
Doctor of Philosophy

University of Pittsburgh

2017

UNIVERSITY OF PITTSBURGH
SCHOOL OF MEDICINE

This dissertation was presented

by

Celestino Velásquez

It was defended on

June 12, 2017

and approved by

Gary Thomas, Ph.D., Professor, Department of Microbiology and Molecular Genetics

Jeffrey L. Brodsky, Ph.D., Professor, Department of Biological Sciences

Saleem A. Khan, Ph.D., Professor, Department of Microbiology and Molecular
Genetics

Christopher J. Bakkenist, Ph.D., Associate Professor, Department of Pharmacology
and Chemical Biology

Dissertation Advisor: Patrick S. Moore, M.D., M.P.H., Distinguished Professor,
Department of Microbiology and Molecular Genetics

Copyright © by Celestino Velásquez

2017

**VIRAL REGULATION OF CAP-DEPENDENT MESSENGER RNA TRANSLATION
INHIBITOR 4E-BP1 DURING MITOSIS**

Celestino Velásquez

University of Pittsburgh, 2017

The work described in this dissertation started in 2013 and focuses on the activation of cap-dependent mRNA translation and regulation of the translation inhibitor protein 4E-BP1 during mitosis. By investigating the viral oncoprotein Merkel cell polyomavirus small T antigen (MCV sT), an alternative pathway for cap-dependent mRNA translation regulation through the CDK1 kinase was discovered. In addition, a novel phosphorylation site of 4E-BP1—Ser83—was identified in mitotic cells, and a polyclonal antibody against this phosphorylation site was generated. The phospho-Ser83 4E-BP1 antibody is a useful tool that can be used as a bona fide mitotic marker by various assays: immunoblotting, immunofluorescence, and flow cytometry. Overall, this work provokes a reassessment of protein synthesis regulation during cell division, hints at additional undescribed functions for 4E-BP1, and suggests that certain mRNAs translated in this phase of the cell cycle may contribute to cell proliferation and tumorigenesis.

TABLE OF CONTENTS

ACKNOWLEDGMENTS	XIII
1.0 INTRODUCTION.....	1
1.1 REGULATION OF TRANSLATION INITIATION.....	1
1.2 MECHANISMS OF TRANSLATION INITIATION.....	2
1.2.1 Cap-Dependent Translation.....	2
1.2.2 Cap-Independent Translation	3
1.3 CIS-ACTING RNA FACTORS.....	7
1.3.1 5' 7-Methyl-Guanine Cap and 3' Poly-Adenine Tail.....	7
1.3.2 Untranslated Regions.....	8
1.4 TRANS-ACTING PROTEIN FACTORS	11
1.4.1 Eukaryotic Initiation Factor 4E	11
1.4.2 Eukaryotic Initiation Factor 4G.....	13
1.4.3 Eukaryotic Initiation Factor 4A.....	14
1.5 EUKARYOTIC INITIATION FACTOR 4E BINDING PROTEIN 1	16
1.5.1 Expression	16
1.5.2 Regulation of 4E-BP1 Translation Inhibition	17
1.5.3 Signaling Pathways	21
1.5.4 Cell Cycle Progression.....	27

1.6	TRANSLATION IN CANCER	30
1.6.1	eIF4E Overexpression	31
1.6.2	4E-BP1 Hyperphosphorylation	32
1.6.3	Tumor Viruses.....	33
1.6.4	Merkel Cell Polyomavirus	34
2.0	CDK1 SUBSTITUTES FOR MTOR KINASE TO ACTIVATE CAP-DEPENDENT PROTEIN TRANSLATION DURING MITOSIS.....	45
2.1	INTRODUCTION	47
2.2	MATERIALS AND METHODS	50
2.2.1	Cell Culture and Transfection/Transduction	50
2.2.2	Kinase Inhibitors.....	50
2.2.3	Plasmids and Transfections	50
2.2.4	Immunoblotting and Antibodies.....	51
2.2.5	Immunoprecipitation	51
2.2.6	Two-Dimensional Electrophoresis	52
2.2.7	Flow Cytometry.....	52
2.2.8	Cell Cycle Synchronization and Mitotic Cell Enrichment.....	53
2.2.9	In vitro Phosphorylation Assays	53
2.2.10	m7GTP Cap Binding Assay	54
2.2.11	In vitro mRNA Synthesis and Translation	54
2.2.12	Nascent Protein Synthesis Analysis.....	55
2.2.13	Statistical Analysis	56
2.3	RESULTS.....	57

2.3.1	MCV sT increases mitogenesis by targeting the cellular anaphase promoting complex E3 ligase.....	57
2.3.2	MCV sT induces mTOR-independent 4E-BP1 phosphorylation.	61
2.3.3	CDK1/CYCB1 directly phosphorylates 4E-BP1, in the presence and absence of sT, to the δ isoform during mitosis.	62
2.3.4	δ 4E-BP1 is induced in mitosis during normal cell cycling.	69
2.3.5	CDK1 activates cap-dependent translation during mitosis.	73
2.4	DISCUSSION	80
3.0	MITOTIC PROTEIN KINASE CDK1 PHOSPHORYLATION OF MESSENGER RNA TRANSLATION REGULATOR 4E-BP1 SER83 MAY CONTRIBUTE TO CELL TRANSFORMATION	85
3.1	INTRODUCTION	87
3.2	MATERIALS AND METHODS	90
3.2.1	Cell Culture and Transfection/Transduction	90
3.2.2	Plasmids.....	90
3.2.3	Fluorescence Quantification	92
3.2.4	In vitro Translation Assay.....	92
3.2.5	Lentiviral Transduction	93
3.2.6	Immunoblotting and Antibodies.....	93
3.2.7	Cell Cycle Synchronization.....	94
3.2.8	Kinase Inhibitors.....	94
3.2.9	Flow Cytometry.....	94
3.2.10	Mass Spectrometry.....	95

3.2.11	Two-Dimensional Electrophoresis	96
3.2.12	In Vitro Protein Phosphorylation Assay	96
3.2.13	Immunofluorescence.....	96
3.2.14	m7GTP Cap Binding Assay	97
3.2.15	Foci Formation Assays	97
3.3	RESULTS.....	98
3.3.1	δ -4E-BP1 hyperphosphorylation is a feature of mitosis across multiple cancer cell lines.....	98
3.3.2	S83 phosphorylation is a component of δ -4E-BP1 and is mediated by CDK1/CYCB.	99
3.3.3	S83-phosphorylated 4E-BP1 colocalizes with centrosomes during mitosis and peaks at metaphase.	106
3.3.4	Mutation of 4E-BP1 at S83 does not affect general cap-dependent translation but partially reverses MCV sT-induced Rat-1 cell transformation.....	112
3.4	DISCUSSION	119
4.0	CONCLUSION AND PERSPECTIVES.....	123
4.1	CDK1 REGULATION OF CAP-DEPENDENT TRANSLATION.....	124
4.2	S83-PHOSPHORYLATED 4E-BP1 AND MITOTIC TRANSIT	127
4.3	TUMOR VIRUS INDUCTION OF MITOTIC TRANSLATION.....	129
4.4	FUTURE DIRECTIONS	130
5.0	BIBLIOGRAPHY.....	132

LIST OF TABLES

Table 1. Primers used for in vitro site-directed mutagenesis of HA-tagged 4E-BP1. 91

Table 2. Plasmids constructs used for HA-tagged 4E-BP1 and MCV sT expression. ... 92

LIST OF FIGURES

Figure 1. Mechanism of Cap-Dependent mRNA Translation	3
Figure 2. Internal Ribosome Entry Site (IRES) Mediated Translation.....	5
Figure 3. Anatomy of a Eukaryotic Messenger RNA	7
Figure 4. Architecture of the Scaffold Protein eIF4G	14
Figure 5. Schematic of the PI3K-AKT-mTOR Pathway	17
Figure 6. Architecture of Human 4E-Binding Proteins 1, 2, and 3	18
Figure 7. Sequential Phosphorylation of 4E-BP1 by mTORC1	19
Figure 8. Relative Position of Phosphorylation Sites on eIF4E-Bound 4E-BP1.....	21
Figure 9. Signaling Pathways Targeting the mTORC1-4E-BP1 Axis	26
Figure 10. Wild-Type Merkel Cell Polyomavirus Genome	37
Figure 11. MCV Large T and Small T Antigen Domain Architecture	39
Figure 12. MCV sT increases mitotic entry by targeting APC/C E3-ubiquitin ligases. ...	58
Figure 13. MCV sT increases mitogenesis in 293 cells.	60
Figure 14. MCV sT stabilizes APC/C targets (AURKA and CYCB1) in nocodazole- arrested 293 cells.	60
Figure 15. MCV sT induces cellular 4E-BP1 hyperphosphorylation.	61
Figure 16. CDK1/CYCB1 phosphorylates 4E-BP1 during mitosis.	63
Figure 17. Mitotic slippage with mitotic kinase inhibition.	66

Figure 18. δ -4E-BP1 phospho-isoform expression in sT-expressing mitotic cells.	67
Figure 19. 4E-BP1 β , γ , and δ isoforms are completely lost after lambda phosphatase treatment.	68
Figure 20. 4E-BP1 is hyperphosphorylated to the δ isoform during mitosis.	70
Figure 21. Flow cytometry, with PI and phospho-H3 ^{S10} staining, of 293 cells synchronized by double-thymidine release.	71
Figure 22. δ -4E-BP1 induction during mitosis in synchronized U2OS cells.....	72
Figure 23. eIF4F formation on the m7GTP cap and direct measurement of cap-dependent protein translation during mitosis (M) and interphase (I).	75
Figure 24. eIF4F formation on the m7GTP cap is inhibited by CDK1 inhibition in mitosis-enriched HeLa cells.....	77
Figure 25. The 293 cell-nascent protein synthesis is sensitive to PP242.	78
Figure 26. Nocodazole inhibits mitotic protein translation.	79
Figure 27. Model for cell cycle dependent 4E-BP1 regulation of cap-dependent mRNA translation.....	82
Figure 28. δ -4E-BP1 hyperphosphorylation is a common feature of mitosis across multiple cancer cell lines.	98
Figure 29. LC-MS/MS spectrum for phospho-S83 4E-BP1 peptide identified only in mitotic HeLa cells.	100
Figure 30. p4E-BP1 ^{S83} rabbit antiserum specificity screen against 4E-BP1 phosphorylation mutants.	102
Figure 31. S83 phosphorylation is a component of δ -4E-BP1 and is mediated by CDK1/CYCB.....	103

Figure 32. p4E-BP1 ^{S83} flow cytometry staining of HeLa cells.....	105
Figure 33. S83-phosphorylated 4E-BP1 colocalizes with centrosomes during mitosis and peaks at metaphase.	107
Figure 34. p4E-BP1 ^{S83} immunofluorescence staining of U2OS cells.	109
Figure 35. Epitope competition assays with antigen pre-absorbed p4E-BP1 ^{S83} antiserum.	110
Figure 36. p4E-BP1 ^{T37/T46} phosphorylation is maintained during interphase and mitosis.	111
Figure 37. Mutation of 4E-BP1 at S83 does not affect general cap-dependent translation initiation complex formation.....	114
Figure 38. Mutation of 4E-BP1 at S83 does not affect general cap-dependent translation initiation complex formation but partially reverses MCV sT-induced Rat-1 cell transformation.	116
Figure 39. Expression of HA-tagged 4E-BP1 in Rat-1 cells used for transformation assays.....	118
Figure 40. Novel mitosis-specific phosphorylation of 4E-BP1 Ser83 by CDK1.	119
Figure 41. 4E-BP1 S83 is part of the loop binding the lateral pocket of eIF4E.....	125
Figure 42. S83-phosphorylated 4E-BP1 is a novel mitotic marker.	128

ACKNOWLEDGMENTS

I would like to express my deepest gratitude to everyone who has helped me throughout this scientific journey: Dr. Patrick S. Moore and Dr. Yuan Chang for their mentorship, patience, and generosity; Dr. Masahiro Shuda, Dr. Erdong Cheng, Dr. Hyun Jin Kwun, Dr. Laura Wasil, Dr. Kathleen Richards, Dr. Daniel Cordek, and Felicia Taylor for their teaching, support, and friendship; my dissertation committee members for their time, advice, and evaluation; my PIMB, ISB, and IBGP friends for their laughs and complaints; my longtime friends Col. Lance Turner, Annette Turner, Scott Stephens, Cindy Stephens, and families for things innumerable; my mother María de la Cruz García Enamorado, my sister Celeste Marycruz Velásquez García, and my brother Fernando Velásquez García for their love, motivation, and understanding.

1.0 INTRODUCTION

1.1 REGULATION OF TRANSLATION INITIATION

Eukaryotic messenger RNA (mRNA) translation is a complex process that is tightly regulated by various protein and non-protein components. mRNA translation undergoes regulation at each of its four distinct phases: initiation, elongation, termination, and ribosome recycling (1). Translation initiation is the most highly regulated and complicated phase, and thus, it is the rate-limiting step (2). It requires the highest number of protein factors in order to recruit the ribosome to the mRNA for protein synthesis (2). The 80S ribosome is assembled on the message through a canonical series of events as follows: mRNA 5' cap binding by the eukaryotic initiation factor 4F (eIF4F) complex, 43S pre-initiation complex (PIC) formation, 40S ribosome recruitment to mRNA, start codon localization, and 60S ribosome joining. This introduction reviews the regulation of translation initiation and the role of the eukaryotic initiation factor 4E binding protein 1 (4E-BP1) in the context of cell cycle progression and viral and non-viral induced tumorigenesis.

1.2 MECHANISMS OF TRANSLATION INITIATION

In eukaryotic organisms, most mRNA translation follows the canonical cap-dependent mechanism of translation (3). A portion of cellular mRNAs rely on alternative mechanisms that bypass the canonical requirements for translation initiation (4, 5). Nonetheless, the objective of all these mechanisms is the same—recruiting the ribosome to the 5' untranslated region to begin the synthesis of functional proteins.

1.2.1 Cap-Dependent Translation

Cap-dependent translation is the main mechanism by which most mRNAs are translated in eukaryotic cells. The term “cap-dependent” refers to the first step in this mechanism, where the translation initiation factors assemble at the 5' cap of an mRNA and form the eukaryotic initiation factor 4F (eIF4F) complex (**Figure 1**). The cap-binding protein eIF4E directs translation initiation complex assembly at the 5' untranslated region (5' UTR) of an mRNA (6, 7). The 5' cap-bound eIF4E protein then recruits the essential eIF4G protein, which serves as a large scaffold for the various cap complex members (8, 9). This scaffold protein performs several functions: it binds eIF4A, an RNA helicase that resolves secondary RNA structures near the 5'-cap (10); it recruits the 43S pre-initiation complex (containing the 40S ribosome subunit, initiator Met-tRNA, and ribosome binding proteins eIF2 and eIF3) (11-18); and it circularizes and facilitates translation of mRNA by interacting with the 3' end poly-adenine (poly(A)) binding protein (PABP) (19, 20). The 43S pre-initiation complex then scans the 5' UTR, in the 5' to 3' direction, to find the start codon and attract the 60S ribosomal subunit to initiate

translation (21). The translation initiation factors dissociate from the 40S ribosomal subunit and allow it to complex with the 60S subunit, forming the full 80S ribosome loaded with the initiation Met-tRNA (10). Polypeptide chain elongation begins with the addition of amino acids to the start methionine at the AUG codon, and peptide synthesis is terminated when the 80S ribosome meets a stop codon (21).

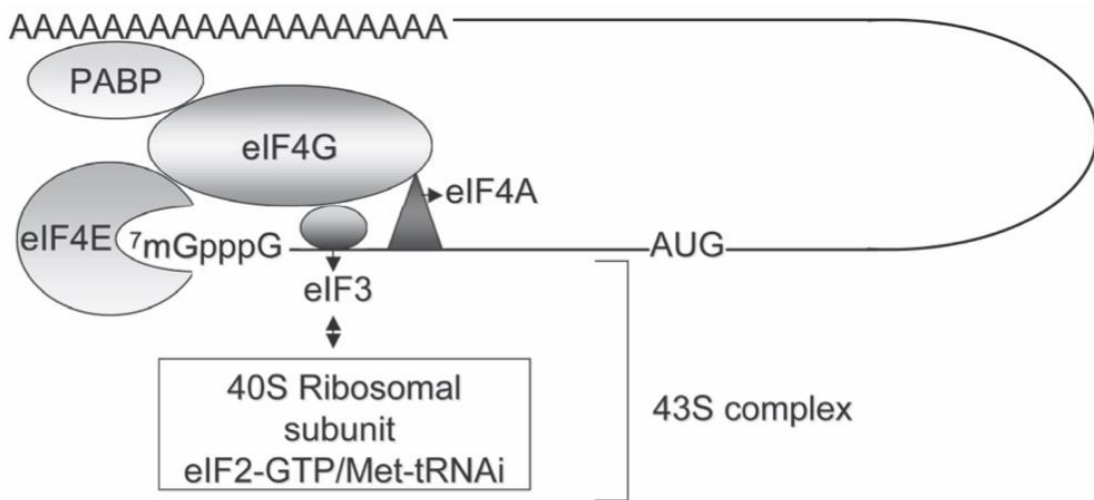


Figure 1. Mechanism of Cap-Dependent mRNA Translation

Cap-dependent mRNA translation is initiated by the formation of the eIF4F complex on the 5' cap of mRNA, which recruits the 43S pre-initiation complex that forms between the 40S ribosomal subunit, eIF2, and eIF3. The full initiation complex scans for the first start codon and recruits the 60S ribosomal subunit upon encountering it, forming the 80S ribosome to begin translation (From López-Lastra et al. 2005 (22)).

1.2.2 Cap-Independent Translation

Internal Ribosome Entry Site (IRES)-Mediated Translation

Some mRNAs are not translated through the cap-dependent translation mechanism and rely mainly on internal ribosome entry site (IRES)-mediated translation. IRESes are structured RNA elements found at 5' UTRs that allow mRNAs to be translated through

an alternative mechanism under conditions that suppress cap-dependent protein synthesis, such as viral infection (23-25), stress (26, 27), apoptosis (28), and mitosis (29, 30).

While most eukaryotic transcripts contain a 5' cap and a poly(A) tail, IRES-containing cellular mRNAs are mainly translated through IRES-mediated translation but can also be translated, albeit less efficiently, through cap-dependent translation (31-33). First identified in the single-stranded positive-sense RNA poliovirus genome, IRES structures at mRNA 5' UTRs recruit the ribosome and some translation initiation factors internally, bypassing the translation initiation complex eIF4F that forms at the 5' cap (**Figure 2**) (23, 34). Some proto-oncogenes contain 5' IRES sequences, such as c-Myc (35, 36), ornithine decarboxylase (ODC) (30), vascular endothelial growth factor (VEGF) (26), X-linked inhibitor of apoptosis (XIAP) (28), and fibroblast growth factor 2 (FGF-2) (37), which allow them to overcome cap-dependent translation regulation.

The requirements for IRES-mediated translation vary across cellular and viral transcripts. Despite their similarities in function, IRES elements are not homologous in sequence nor structure and initiate translation by recruiting a plethora of different canonical and non-canonical factors (4, 38). A group of RNA-binding proteins, called IRES-trans-acting factors (ITAFs), are also reported to stimulate this translation mechanism by providing binding sites for some translation initiation factors (39).

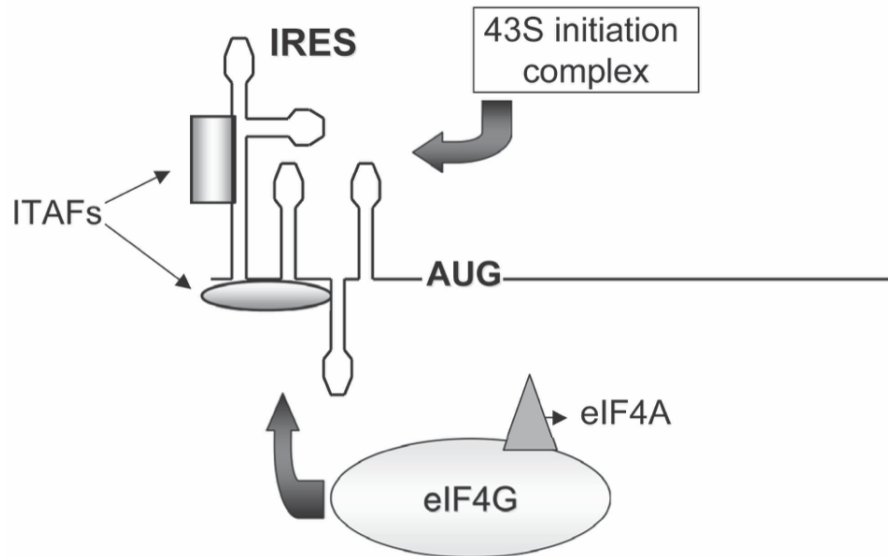


Figure 2. Internal Ribosome Entry Site (IRES) Mediated Translation

Internal translation initiation permits the 43S pre-initiation complex to be recruited directly to the structured 5' UTR of some cellular mRNAs, circumventing the 5' cap complex. Different IRESes require different translation initiation factors and ITAFs, to aid in their function to attract the ribosome and any other translation initiation components other than eIF4E (From López-Lastra et al. 2005 (22)).

N6-methyladenosine (m6A)-Mediated Translation

A novel mechanism for eukaryotic translation initiation—N6-methyladenosine-mediated translation—has been proposed in recent years. Similar to IRES structures, N6-methyladenosine (m6A) modifications in mRNA can also initiate translation internally by recruiting the ribosome to the message. m6A is the most abundant internal modification in the mammalian transcriptome, found predominantly in the 3' UTR of more than 7,000 human transcripts (40, 41). In 2015 Wang et al. reported that m6A modifications in the 3' UTR provide a binding site for the YTH domain-containing protein YTHDF1 (42). YTHDF1 interacts with eIF3 and thus attracts the 43S pre-initiation complex directly to the 5' UTR, forming a closed-loop mRNA structure (42). A couple of concurrent studies showed that uncapped mRNAs containing a single m6A in their 5' UTR can be

translated in vitro unlike their unmodified counterparts (5, 43). m6A modifications located in the 5' UTR of mRNAs provide a binding site for eIF3, which can be reversed by overexpression of the mRNA demethylase FTO and knockdown of the N6-adenosine-methyltransferase METTL3 (5, 43, 44). Furthermore, mRNA with 5' UTR m6A modifications can still be translated efficiently under heat stress conditions that suppress cap-dependent translation (43). This novel mechanism of mRNA translation initiation suggests that alternative mechanisms, besides IRES-mediated translation, take over protein synthesis control under abnormal cellular conditions and allow cells to survive until normal conditions are restored.

1.3 CIS-ACTING RNA FACTORS

Translation initiation efficiency is regulated by the intrinsic composition of the mRNA (cis-acting factors) and initiation protein factor availability (trans-acting factors) (10, 45-49). Cis-acting features outside of the mRNA main open reading frame (ORF), such as the 7-methyl-guanine cap, poly-adenine tail, and 5' and 3' UTRs (**Figure 3**), contain primary sequence and secondary structure elements that control its accessibility to the eIF4F complex and can be unique to the message or family of messages (45).



Figure 3. Anatomy of a Eukaryotic Messenger RNA

Eukaryotic mRNAs are modified post-transcriptionally with a 7-methyl-guanine cap at the 5' end and with a poly-adenine tail at the 3' end. The protein coding sequence is found in a region called the main ORF, which begins at the AUG start codon and ends with a stop codon, UGA, UAA, or UAG. The 5' and 3' UTRs flank the main ORF.

1.3.1 5' 7-Methyl-Guanine Cap and 3' Poly-Adenine Tail

Mature cellular mRNAs contain a 7-methyl-guanine cap structure at their 5' end (50, 51), which is added post-transcriptionally by the RNA guanylyltransferase 5' triphosphatase RNGTT and the RNA guanine-7-methyltransferase RNMT (52-54). The 7-methyl-guanine cap serves multiple purposes: it protects the message from 5' exonuclease-mediated degradation (55, 56), facilitates nuclear export (57-59), increases polyadenylation efficiency (60), and attracts the translation initiation complex (7). The eukaryotic initiation factor 4E (eIF4E) binds this cap structure and attracts the

trans-acting elements required to start translation (7, 61). The 5' cap consists of a guanine nucleotide methylated at the 7' position (62) and connected to the mRNA by a 5'-to-5' triphosphate linkage (63). While the 7-methyl-guanine cap is necessary for efficient mRNA translation, it is dispensable in some mRNAs that rely on other structural features to recruit the ribosome (64).

Another post-transcriptional modification found in mature mRNAs is the polyadenine (poly(A)) tail, which is added on the 3' end of all cellular transcripts but those encoding histones (65). Like the 5' cap structure, the poly(A) tail protects mRNA from exonuclease-mediated degradation and enhances translation by interacting with the 5' cap-associated eukaryotic initiation factor 4G (eIF4G) protein through the poly(A)-binding protein (PABP) (19, 66, 67). This interaction forms a stable closed-loop mRNA structure that facilitates translation in vitro (20, 68, 69).

1.3.2 Untranslated Regions

Translation begins when the ribosome recognizes the first AUG triplet on the mRNA, termed the start codon. Although the rate of translation initiation depends largely on the availability of trans-acting initiation factors that allow the ribosome to find the start codon (70), sequence and structural features in the non-coding regions can also determine how efficiently an mRNA is translated (71, 72).

Sequence

The length and composition of the 5' UTR affects the translation efficiency of a message. The shorter the 5' UTR of an mRNA is, the more efficiently it can be

translated by the ribosome (73). The nucleotide sequence composition of the 5' UTR can also affect mRNA translation efficiency. For instance, genes that are critical for protein synthesis and ribosomal biogenesis contain a short stretch of pyrimidine nucleotides at the beginning of their 5' UTR that facilitates their translation (74). This sequence, called the 5' terminal oligopyrimidine (TOP) motif, is composed of 6-12 pyrimidines at the 5' end of the mRNA (75). Transcripts encoding translation initiation and elongation factors and ribosomal proteins are known to contain 5' TOP motifs (76-78). These are reported to be mainly sensitive to cell proliferation signaling by mTORC1 (79, 80). When mTORC1 signaling is inhibited pharmacologically, the levels of proteins translated from 5' TOP-containing mRNAs decreases.

Another regulatory sequence found in the 5' UTR, upstream open reading frames (uORFs) prevent translation of the downstream main ORF (81). Normally, eukaryotic translation begins at the first AUG start codon found in the optimal Kozak consensus sequence context GCC(A/G)CCAUGG (21, 82, 83). Transcripts that contain uORFs, on the other hand, initiate translation through alternative start codons, mainly the cognate CUG triplet (21, 84, 85). The primary function of uORFs seems to be reducing the synthesis of physiologically functional proteins by encoding short non-functional peptides that are 5-30 amino acids in length (81).

The 3' UTR is another regulatory region located downstream of the protein coding sequence of every mRNA, which includes the poly(A) tail (2, 86, 87). While the 5' UTR plays a prominent role in regulating translation initiation, the 3' UTR regulates primarily the stability of the mRNA (87). The only clear impact that the 3' UTR may have on translation initiation is through the poly(A) tail. This tract of adenines provides a

binding site for several PABP molecules (68), which enhance in vitro translation initiation by interacting with the 5' cap complex protein eIF4G (88).

Structure

Secondary RNA structures at the 5' UTR also regulate translation initiation. Secondary structures form when complementary regions of RNA form base pairs and adopt stable hairpin structures (89). These structures sterically hinder the 43S ribosome pre-initiation complex from finding the start codon since the 40S ribosome subunit can only accommodate single-stranded RNA (89, 90). In order to translate highly structured 5' UTR mRNAs, the translation initiation complex relies on the activity of its RNA helicase eIF4A to resolve the secondary structures, which retards the ribosome from reaching the start codon and thus decreases the translation rate of the mRNA (10).

Some mRNAs, on the other hand, possess an IRES structure that permits their translation by an alternative process. This specialized secondary RNA structure allows capped or uncapped mRNAs to recruit the translation machinery to an internal site upstream of their coding region, bypassing the translation initiation complex assembled at their 5' end (23, 91-93). IRES elements are present in the 5' UTR of 3-5% of all cellular mRNAs (64, 94). Secondary structures have also been identified in the 3' UTR of various transcripts, but whether they affect translation initiation is unknown (95).

1.4 TRANS-ACTING PROTEIN FACTORS

Translation initiation is also regulated by trans-acting factors, which mainly consist of the eukaryotic initiation factor 4 (eIF4) proteins eIF4E, eIF4G, and eIF4A (1). Together these three proteins and several other accessory proteins form the eIF4F translation initiation complex and are responsible for recruiting the ribosome to the mRNA. The molecular interactions between these proteins and the 5' UTR of mRNAs are modular and allow for rapid regulation of gene expression (2).

1.4.1 Eukaryotic Initiation Factor 4E

The eukaryotic initiation factor 4E (eIF4E) is the eIF4F complex protein that interacts directly with the 7-methyl-guanine cap at the 5' end of mRNA (7). eIF4E has a molecular weight of 24 kDa, and it is the least abundant translation initiation factor and thus the limiting one (6). eIF4E is highly conserved in eukaryotic organisms, and mammalian organisms possess three isoforms: eIF4E-1 (eIF4E), eIF4E-2 (or 4EHP), and eIF4E-3 (96). eIF4E-1 is the predominant 4E family member and binds to the 5' cap with much higher affinity than eIF4E-2 and eIF4E-3 (97, 98). Thus, eIF4E-1 is the most studied cap-binding protein and is simply referred to as eIF4E.

The cap-binding protein eIF4E has two main binding partners: the eukaryotic initiation factor 4G (eIF4G) and the eukaryotic initiation factor 4E binding proteins (4E-BPs) (99, 100). The canonical binding site for eIF4G and 4E-binding proteins (4E-BPs) is found on the eIF4E dorsal region, near residue W73 of human eIF4E (101). When this residue is mutated to alanine, the interaction with eIF4G is completely ablated and

the translation initiation complex cannot assemble on the cap structure (101). Unlike eIF4E-1, eIF4E-2 cannot interact with eIF4G and eIF4E-3 cannot interact with 4E-BPs (96). Given its inability to associate with eIF4G, eIF4E-2 is suspected to inhibit mRNA translation by competing with eIF4E-1 for cap-binding. A recent study has shown that 3' UTR-associated RNA-induced silencing complexes (RISCs) recruit eIF4E-2 to the 5' cap through the deadenylating complex CCR4-NOT, forming a closed-loop structure that inhibits the translation initiation complex assembly (102).

The interaction between eIF4E and eIF4G is inhibited by the 4E-BPs, which are molecular mimics of eIF4G (100, 103). Sharing the conserved eIF4E binding sequence as is found in eIF4G, YXXXXLΦ (where X is any amino acid residue and Φ is a hydrophobic residue) (100), 4E-BPs (4E-BP1-3) compete with eIF4G for eIF4E occupancy on the dorsal binding pocket and prevent the formation of the translation initiation complex, thereby inhibiting protein synthesis (103, 104). In addition to interacting with eIF4E dorsally, 4E-BP1 binds the lateral surface of eIF4E through a novel motif consisting of residues ⁷⁹PGVTS⁸³ (105-107).

eIF4E engages the 5' cap of mRNA through two tryptophan residues, W56 and W102, located on its ventral side (101). Mutation of W56 to alanine abolishes eIF4E interaction with the 5' cap structure (101). eIF4G binding to eIF4E seems to allosterically increase the affinity of eIF4E for the 5' cap. Studies in yeast have shown that interaction with eIF4G induces a conformational change in eIF4E that tightens its grip on the 7-methyl-guanine cap (108, 109).

1.4.2 Eukaryotic Initiation Factor 4G

The eukaryotic initiation factor protein 4G (eIF4G) is the largest protein in the eIF4F complex and serves as a scaffold with docking sites for the multiple proteins that make up the translation initiation complex (110-113). It has a molecular weight of 220 kDa (114), and it binds eIF4E, the RNA helicase eIF4A, the poly(A) binding protein PABP, and eIF3, which connects the eIF4F-mRNA complex to the 43S ribosome pre-initiation complex (110). In mammals, two functionally redundant eIF4G isoforms exist, eIF4G I and eIF4G II. Two smaller eIF4G isoforms also exist—the PABP interacting protein-1 (Paip-1) and the death-associated protein-5 (Dap-5)—that lack the conserved eIF4E binding site and only share homologous eIF4A and eIF3 binding sites (110). The former has been shown to bind eIF3 and enhance translation initiation (9, 115), while the latter appears to promote IRES-mediated translation (116).

eIF4G has multiple docking sites for protein factors necessary for translation initiation activation (**Figure 4**). The N-terminus of the eIF4G protein contains the binding sites for eIF4E and PABP (117-119). The eIF4E binding site is located in this region at amino acids 572-578, and its human sequence is the conserved YDREFLL (100). The PABP binding site is located at amino acids 172-200 (120), and allows the 5' end-associated eIF4G to form a closed-loop mRNA structure with the 3' poly(A)-bound PABP proteins (19, 20). Circularization of mRNA by the eIF4G-PABP interaction enhances mRNA translation in vitro, but this has yet to be confirmed in vivo.

Like many other large complex scaffold proteins, eIF4G possesses multiple HEAT (Huntingtin, EF3, PP2A, and TOR) repeats located in its central and C-terminal regions (**Figure 4**) (121). These fragments encompass binding sites for the eukaryotic

initiation factor 4A (eIF4A) between amino acids 650-1000 and amino acids 1200-1400 (8, 118, 122), the eukaryotic initiation factor 3 (eIF3) between amino acids 1000-1100 (8, 11), and the MNK1/2 kinases between amino acids 1400-1600 (123, 124). Interaction of eIF4G to the RNA helicase eIF4A aids in resolving secondary RNA structures in the 5' UTR (125), while interaction with eIF3 recruits the 40S ribosome subunit (9). eIF4G recruits the MNK1/2 kinases through its C-terminal end to phosphorylate cap-bound eIF4E at S209, whose function remains unclear (123, 124). Additionally, eIF4G is also able to bind RNA directly through a central RNA recognition motif (RRM) that lies between amino acids 740-940 (25, 111).

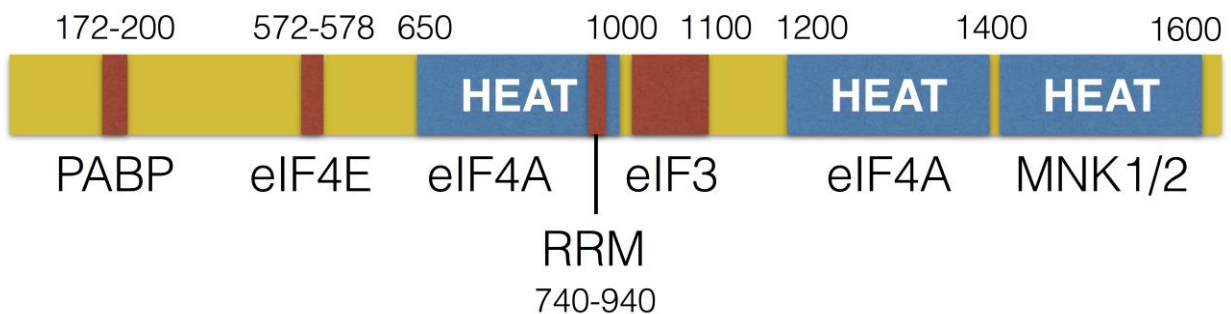


Figure 4. Architecture of the Scaffold Protein eIF4G

The schematic shows the amino acid positions of the various binding sites on eIF4G for PABP, eIF4E, eIF3, eIF4A, and MNK1/2 kinases located at HEAT repeats, and for RNA at the RNA recognition motif (RRM).

1.4.3 Eukaryotic Initiation Factor 4A

eIF4A is the only member of the eIF4F complex possessing enzymatic activity—RNA-dependent ATPase activity (126). It has a molecular weight of 46 kDa (127), and it acts as an RNA helicase. eIF4A unwinds secondary RNA structures at the 5' UTR of mRNA

to permit ribosome binding and scanning for the start codon (128-131). In mammals, there are three eIF4A isoforms—eIF4A I, eIF4A II, and eIF4A III—which are members of the Aspartate-Glutamine-Alanine-Aspartate (DEAD)-box family (132-134). The first two, eIF4A I and eIF4A II, are functionally redundant and homologous (135). eIF4A interacts with eIF4G through a recombinase A-like domain located in its C-terminus (136). By stabilizing the interaction of eIF4A with RNA, eIF4G enhances the helicase activity of eIF4A (9, 136, 137). Two accessory proteins, eIF4B and eIF4H, have also been identified to stimulate eIF4A RNA processing (138, 139).

1.5 EUKARYOTIC INITIATION FACTOR 4E BINDING PROTEIN 1

Sonenberg et al. discovered a set of three small binding proteins, called eIF4E(4E)-BPs (4E-BP1, 4E-BP2, and 4E-BP3), that inhibit cap-dependent translation by interacting with the mRNA 5'-cap-binding eukaryotic initiation factor eIF4E (7, 99, 104). 4E-BP1 and 4E-BP2 are functionally redundant in terms of their impact on translation initiation and are regulated in a similar manner (100, 140, 141). However, very little is known about 4E-BP3 (142), and most studies have focused on 4E-BP1 and a few on 4E-BP2 (140, 141, 143).

1.5.1 Expression

mRNA expression of 4E-BP1 and 4E-BP2 is ubiquitous in mammals, but their expression level appears to vary across different tissues (144). For instance, 4E-BP1 is found to be highly expressed in the pancreas, skeletal muscle, and white adipose tissue, while 4E-BP2 is predominantly expressed in the central nervous system (2, 145, 146). Some transcription factors have been identified to regulate 4E-BP1 gene expression in human cells. Transcription factors ATF4 and SMAD4 upregulate 4E-BP1 transcription to protect pancreatic cells from endoplasmic reticulum stress and inhibit cell proliferation, respectively (145, 147). In prostate cancer cells, the transcription factor c-Myc induces 4E-BP1 mRNA expression upon treatment with the mTOR inhibitor rapamycin (148). The one transcription factor that has been identified to downregulate 4E-BP1 transcription is the p38/MAPK- and PI3K-dependent transcription factor EGR1, which promotes cell proliferation in hematopoietic stem cells (149, 150).

1.5.2 Regulation of 4E-BP1 Translation Inhibition

The best characterized eIF4E binding protein is 4E-BP1, and it has a molecular weight of 15 kDa (151). 4E-BP1 competes with eIF4G for eIF4E binding, preventing the recruitment of the translation initiation machinery to the 5' UTR of mRNA (152). The interaction between 4E-BP1 and eIF4E thus inhibits cap-dependent protein synthesis. However, this interaction is reversible, and it is regulated through phosphorylation mediated canonically by the mammalian target of rapamycin (mTOR) kinase in response to metabolic and growth-related signaling (**Figure 5**) (153).

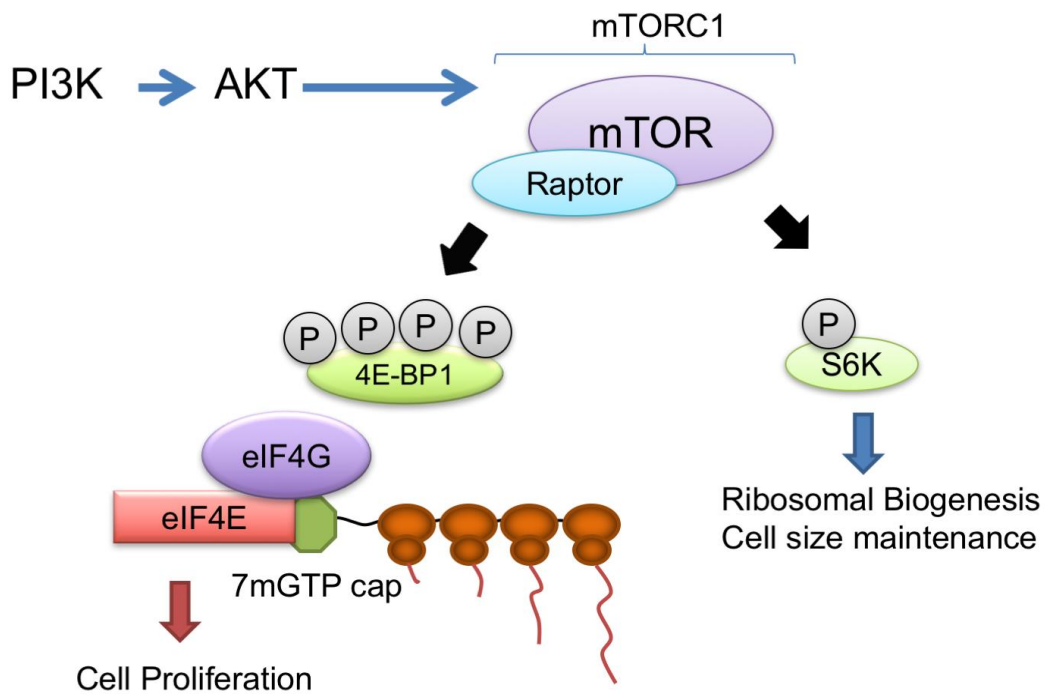


Figure 5. Schematic of the PI3K-AKT-mTOR Pathway

The PI3K-AKT pathway activates the mTORC/Raptor (mTORC1) kinase complex that phosphorylates and activates S6K and phosphorylates and inhibits 4E-BP1, which prevents 4E-BP1 from binding eIF4E and inhibiting cap-dependent translation initiation.

The phosphatidylinositol-3 kinase (PI3K)-AKT pathway regulates the repressor function of 4E-BP1 by activating the mammalian target of rapamycin (mTOR) kinase (**Figure 5**) (154-158). The mTOR kinase forms two complexes, mTORC1 and mTORC2, in association with adaptor proteins Raptor and Rictor, respectively, which aid in substrate recognition (159-162). Activated mTORC1 phosphorylates 4E-BP1 at various serine and threonine residues and releases eIF4E from sequestration (163).

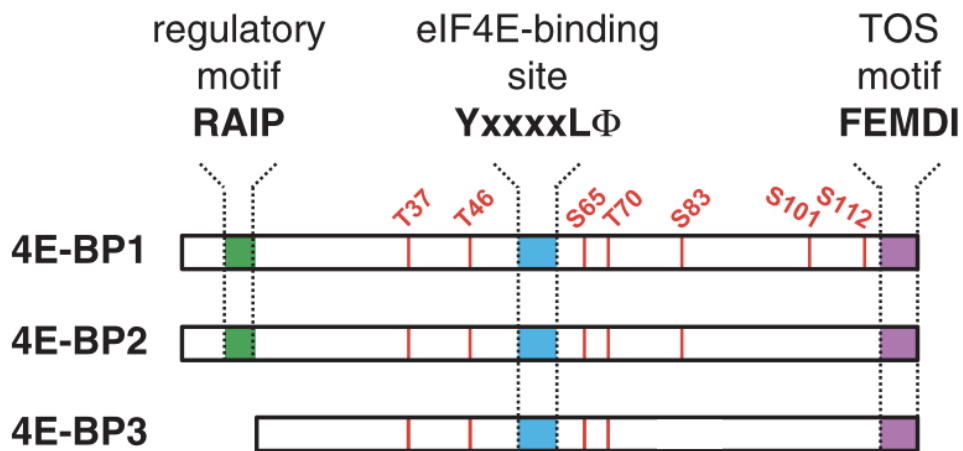


Figure 6. Architecture of Human 4E-Binding Proteins 1, 2, and 3

The eIF4E-binding site (blue) and the Raptor binding TOS motif (purple) are conserved in all human 4E-BPs. The Raptor binding regulatory RAIP motif is absent in 4E-BP3. Threonine (T) and serine (S) residues identified on these proteins are indicated in red, where T37, T46, S65, and T70 are shared across all human 4E-BPs (Reprinted and adapted by permission from Macmillan Publishers Ltd: *Oncogene* 32(6):671-677, 2013, Martineau et al. (144)).

4E-BP1 has two short mTORC1 binding motifs, the C-terminal mTOR signaling (TOS) motif and the N-terminal RAIP motif, which regulate Raptor association (**Figure 6**) (164-169). All 4E-BPs—1, 2, and 3—share the TOS motif that serves as a docking site for the mTOR adaptor protein Raptor and is also present in another mTORC1

substrate, the ribosomal protein S6 kinase S6K1 (**Figure 5**) (100, 169). Raptor interaction with the TOS motif allows the mTOR kinase to phosphorylate 4E-BP1 at residues T37, T46, S65, and T70 (153, 163, 165). 4E-BP1 and 4E-BP2 contain an N-terminal RAIP motif, which is also important for Raptor interaction and is absent in 4E-BP3 (164, 166, 167). Intact mTORC1 binding motifs are crucial for 4E-BP1 phosphorylation and cap-dependent translation activation. Alanine substitutions of the TOS and RAIP motifs (F114A and I15A, respectively) abrogate mTORC1 binding and inhibit 4E-BP1 phosphorylation (164, 167).

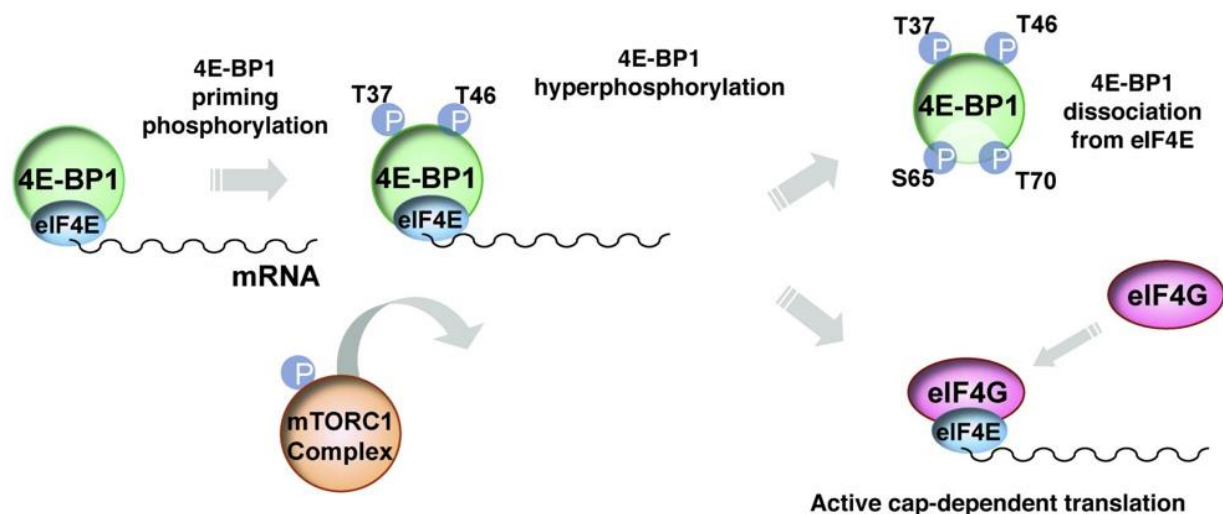


Figure 7. Sequential Phosphorylation of 4E-BP1 by mTORC1

Priming phosphorylation of 4E-BP1 at residues T37 and T46 by mTORC1 allows for sequential phosphorylation at S65 and T70 (153), which leads to its dissociation from eIF4E and cap-dependent translation activation (Reprinted and adapted by permission from American Society for Clinical Investigation: *J Clin Invest* 121(9):3623-3634, 2011, Shuda et al. (170)).

Furthermore, human 4E-BP1 interacts with eIF4E through two binding motifs. 4E-BP1 binds eIF4E mainly through the canonical binding site ⁵⁴YDRKFLM⁶⁰, located

between mTOR-targeted phosphorylation sites T46 and S65, which contacts the dorsal surface of eIF4E (122, 171). 4E-BP1 shares this binding site with eIF4G—the conserved eIF4E-binding motif YXXXXLΦ (100). Mutation of key residues Y54 and L59 to alanines abolish 4E-BP1 binding to eIF4E (165). Recent studies have reported that 4E-BP1 also interacts with the lateral surface of eIF4E through the secondary binding site ⁷⁹PGVTS⁸³ (106), which confers to 4E-BP1 a competitive advantage over eIF4G and contributes to its translation inhibitory function (105). Priming phosphorylation at 4E-BP1 T37 and T46 near the canonical binding site (**Figure 8**) allows for subsequent phosphorylation at T70 and S65 (**Figure 7**) (153). Sequential phosphorylation of 4E-BP1 at these four residues decreases its affinity for eIF4E and allows eIF4G docking to eIF4E to bring the translational machinery to the mRNA (172, 173). Double alanine substitutions of critical T37 and T46 phosphorylation sites of 4E-BP1 inhibit its hyperphosphorylation, rendering a constitutively active 4E-BP1 that strongly binds eIF4E and is insensitive to mTOR inhibition (156, 174).

Three additional 4E-BP1 phosphorylation sites have also been identified—S83, S101, and S112—whose regulation mechanism has remained unknown, except for that of the first one in recent years (**Figure 6**) (154, 175, 176). S83 is phosphorylated during mitosis by the CDK1 kinase and is located in the non-canonical binding motif that interacts with eIF4E (**Figure 8**) (177). Whether phosphorylation of this residue affects the interaction between 4E-BP1 and eIF4E has yet to be determined.

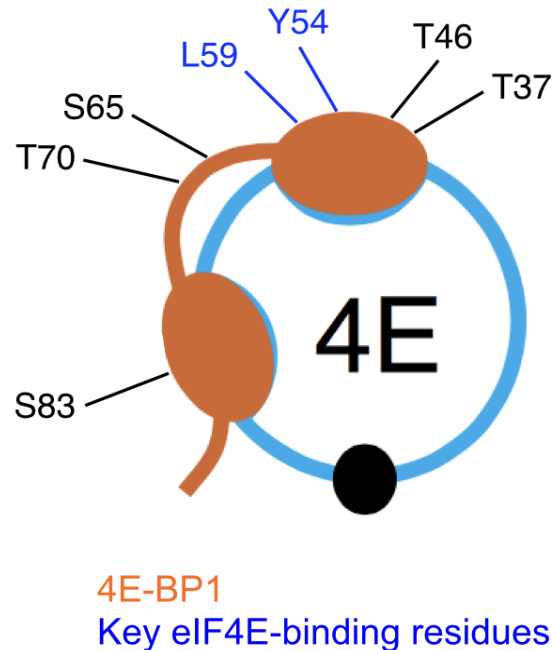


Figure 8. Relative Position of Phosphorylation Sites on eIF4E-Bound 4E-BP1
(Modified from Igreja et al. 2014 (107)).

1.5.3 Signaling Pathways

4E-BP1 phosphorylation is affected by various signaling pathways that converge on mTORC1, such as metabolic signaling, stress conditions, and growth factors and cytokines (178-180). Regulation of 4E-BP1 activity through various stimuli allows the cell to regulate protein synthesis as needed.

Metabolic Signaling

Metabolic inputs, such as ATP, oxygen, amino acids, glucose, and lipids, regulate 4E-BP1 phosphorylation and mRNA translation through mTORC1 modulation (**Figure 9**). Protein synthesis is an energy-intensive process, and for that reason, cells need to regulate their energy expenditure when ATP levels are low (181-183). The 5'-AMP-

regulated kinase AMPK, detect the ratios of cellular AMP:ATP and ADP:ATP (184). When ATP levels are low, AMPK inhibits mTORC1 by phosphorylating the adaptor protein Raptor and activating the tuberous sclerosis proteins 1 and 2 (TSC1/2), which inhibit mTORC1 indirectly by stimulating the GTPase activity of the Ras homolog enriched in brain protein (Rheb) (185, 186). When ATP levels are restored, mTORC1 is activated and increases ATP production by increasing mitochondrial biogenesis in a positive feedback loop (187).

Amino acid, glucose, and lipid signaling also regulates 4E-BP1 phosphorylation through mTORC1 (**Figure 9**). Amino acids are essential for protein synthesis and cell proliferation (188). The presence of amino acids inside lysosomes activates the GTP-binding protein Rheb on the lysosomal membrane, and in turn, recruits and activates mTORC1 through Raptor interaction (189-191). Similar to amino acid signaling, glucose recruits mTORC1 to the lysosomal membrane through Rag GTPases that allow for mTORC1 to interact with the GTP-bound Rheb (192). Furthermore, lipid signaling via phosphatidic acids (PAs) stabilizes the assembly and activity of the mTOR-Raptor (mTORC1) and mTOR-Rictor (mTORC2) complexes (162, 193). All these metabolic pathways converge by increasing 4E-BP1 phosphorylation through mTORC1 activation, thus coupling increased protein synthesis to increased nutrient availability.

Stress Conditions

Certain stress conditions, such as hypoxia, genotoxicity, and apoptosis, lead to mTORC1 inactivation and result in decreased 4E-BP1 phosphorylation and inhibited cap-dependent mRNA translation (**Figure 9**) (178). Low levels of oxygen—hypoxia—

leads to mTORC1 inactivation by decreasing cellular ATP levels and consequently activating AMPK (194-199). Low oxygen also stimulates transcription of the stress and hypoxia inducible gene REDD1, another negative regulator of mTORC1 that activates TSC2 and prevents association of Rheb with mTORC1 (195, 198, 199). Genotoxic stress activates the DNA-damage responsive transcription factor p53 and contributes to AMPK activation and increased phosphatase and tensin homolog (PTEN) expression, which negatively regulates the PI3K-AKT signaling pathway (200, 201). p53 activation leads to dephosphorylation and truncation of 4E-BP1, which cannot be phosphorylated and binds eIF4E with higher affinity than the full-length protein (202, 203). Furthermore, apoptosis signaling also blocks translation initiation through 4E-BP1 dephosphorylation by mTORC1 inhibition and caspase-cleavage of the N-terminal RAIP motif of 4E-BP1 (204, 205). As in conditions of p53 activation, the truncated 4E-BP1 protein cannot be phosphorylated effectively and becomes a dominant inhibitor of mRNA translation. Unlike metabolic signaling, these stress conditions shut off cap-dependent translation by decreasing 4E-BP1 phosphorylation.

Growth Factors and Cytokines

Extracellular signaling through growth factors and cytokines promotes mTORC1 activity. Insulin promotes cell proliferation by stimulating growth factor receptors on the cell surface that activate downstream intracellular signaling pathways, including the PI3K-AKT-mTOR pathway, which leads to increased 4E-BP1 phosphorylation and protein synthesis (104, 175). Pro-inflammatory cytokines TNF α and I κ B kinase- β (IKK β) also induce 4E-BP1 phosphorylation by interacting with and inactivating the mTORC1

inhibitor TSC2 (206). These observations have suggested that other intracellular pathways may target 4E-BP1 through kinases other than mTORC1.

Non-Canonical 4E-BP1 Kinases

In recent years various groups have identified kinases, other than mTORC1, that phosphorylate 4E-BP1: CDK1 (177, 207-209), PLK1 (210), Pim 2 (211), GSK3- β (212, 213), p38MAPK (212, 213), ERK1/2 (155, 214), LRRK2 (215, 216), ATM (217), and CK1 ϵ (218). The mitotic cyclin-dependent kinase 1 (CDK1) phosphorylates 4E-BP1 at T70 only in mitotic cells (207, 208). CDK1 can also phosphorylate mTOR-targeted residues T37, T46, and S65, and also the novel S83, which is not regulated by mTOR (177, 209). Another mitotic kinase, polo-like kinase 1 (PLK1), is able to phosphorylate 4E-BP1 in vitro, but the exact phosphorylation sites have not been determined (210). The Pim 1/2/3 kinases have been shown to be active in cells resistant to mTOR inhibitor rapamycin treatment (212, 213), and Pim 2, specifically, phosphorylates 4E-BP1 at S65 (211). Furthermore, the glycogen synthase kinase 3 β (GSK3- β) phosphorylates 4E-BP1 at its priming sites T37 and T46 and promotes cap-dependent protein synthesis and cell proliferation (219). In response to UV irradiation, apoptosis, and viral infection, the mitogen-activated protein kinase p38 (p38MAPK) phosphorylates mouse 4E-BP1 at T36, T45, S64, and T69 (220-222). Related to the p38MAPK kinase, the ERK1/2 kinases also phosphorylate 4E-BP1 at S65 and increase mTORC1 activity by inhibiting the mTORC1-suppressing TSC1/2 proteins (155, 214). Furthermore, the leucine-rich repeat kinase 2 (LRRK2) phosphorylates 4E-BP1 at the T37 and T46 sites (215, 216). Interestingly, a couple of enzymes that phosphorylate at non-mTORC1-regulated sites

have also been identified. First, the ataxia-telangiectasia mutated kinase (ATM) is normally activated by ionizing radiation and double-stranded DNA breaks and also phosphorylates 4E-BP1 at S112 following insulin stimulation (217). Second, the casein kinase 1 ϵ (CK1 ϵ) phosphorylates 4E-BP1 at T41 and T50 in breast cancer cells and appears to promote mRNA translation (218). The existence of other 4E-BP1 kinases could explain mTOR inhibitor resistance in cancer cells of various tumor types (223-225), and it also suggests that several signaling pathways converge on 4E-BP1 and regulate its function independently of mTORC1.

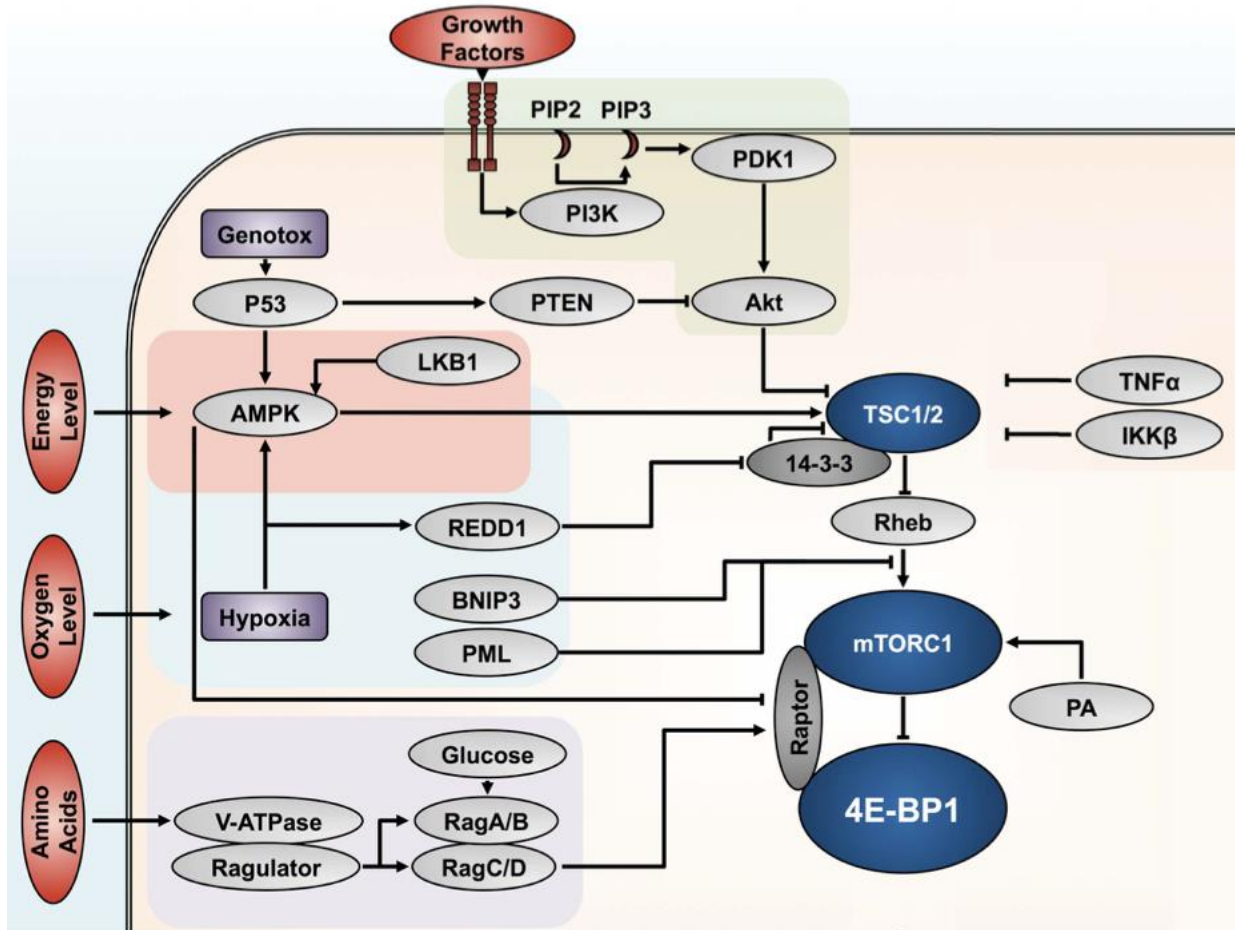


Figure 9. Signaling Pathways Targeting the mTORC1-4E-BP1 Axis

mTORC1 kinase activity inhibits 4E-BP1 by phosphorylation, thereby activating cap-dependent mRNA translation. Multiple upstream regulators, such as growth factors, nutrients, and stress, stimulate mTORC1 and regulate protein synthesis and cell proliferation via 4E-BP1 (Reprinted and adapted by permission from Macmillan Publishers Ltd: *Oncogene* 35(36):4675-4688, 2016, Musa et al. (143)).

1.5.4 Cell Cycle Progression

The PI3K-AKT-mTORC1 pathway is well known to regulate both cell growth and cell cycle progression, which are necessary for cell proliferation (226). mTORC1 inhibition by rapamycin blocks cell cycle progression and preferentially arrests cells transiting through the G1 phase (160, 227). Furthermore, raptor knockdown and serum starvation impair G1/S progression by inhibiting mTORC1 activity (228, 229). Some reports indicate that mTORC1 exerts its influence on cell cycle progression by modulating the activity of cyclin-dependent kinases, the gatekeepers of the cell cycle (230, 231). Cells from dTOR (*Drosophila* target of rapamycin)-null fruit flies express lower levels of cyclin E than the wild type cells and, as a result, are arrested in the G1/S transition (231). Downstream of mTORC1, 4E-BP1 hyperphosphorylation has been linked to an increase in CDK1 and CDK2 and cyclin E, D1, and B1 protein levels, which can be reversed by mTOR inhibition (230). Furthermore, overexpression of a non-phosphorylatable 4E-BP1 mutant also leads to G1/S phase arrest, decreased cell size, and thus decreased cell proliferation (174, 232). Conversely, eIF4E overexpression and increased S6K1 activity contributes to S phase progression and increased cell size (10, 141, 233, 234). These observations indicate the mTORC1, through 4E-BP1 targeting, is regulating not only cell growth but also cell cycle progression. Translation inhibition by 4E-BP1 of mRNAs encoding pro-proliferative genes, such as c-Myc, ODC, VEGF, cyclins, and CDKs, could explain this phenomenon (141, 230).

Translation During Mitosis

Global mRNA translation has long been assumed to be inhibited during mitosis. Several studies have shown that protein synthesis is decreased in HeLa cells (235, 236) and Chinese hamster ovary (CHO) cells (237) that were arrested in mitosis by treatment with nocodazole, a drug that destabilizes microtubules. One report shows that 4E-BP1 is dephosphorylated in nocodazole-arrested mitosis cells and provides additional evidence that translation is suppressed (236). Interestingly, IRES-containing poliovirus mRNA translation was unaffected in mitosis-arrested HeLa cells (238, 239), and mTORC1 activity was preserved during mitosis (229). These findings indicated that a subset of the global mRNA population, transcripts containing IRES structures in their 5' UTR, can escape the global translational suppression during mitosis. To determine whether cellular mRNAs containing IRES structures could escape the observed translational suppression, subsequent studies examined the translation of the ornithine decarboxylase enzyme (ODC), important for polyamine biosynthesis (30). ODC expression is translationally regulated in a cell cycle-dependent manner, peaking at the G1/S transition and at the G2/M transition (240). Like the poliovirus transcripts, ODC mRNA translation is not suppressed during mitosis and does not depend on eIF4E (30). The p53-activated tumor suppressor protein 14-3-3 σ has been reported to enhance the cap-independent translation of the IRES-containing p58 PITSLRE and p27 Kip1 transcripts during mitosis by targeting the translation initiation factors eIF4B and eIF2 (241). One of the eIF4F complex members crucial for cap-dependent translation, eIF4G, is phosphorylated at Ser1232 by CDK1 during mitosis, which prevents its association with eIF4A and may also explain the observed translational suppression (242).

In recent years, the idea that cap-dependent mRNA translation is suppressed during mitosis has been challenged by various groups and work presented in the following chapters (177, 209, 243, 244). Emerging ribosomal profiling studies (79, 80, 244) and sensitive single-cell metabolic labeling assays (209) have shown that mitotic mRNA translation is predominantly cap-dependent. In line with these observations, multiple studies have shown that 4E-BP1 is in fact hyperphosphorylated and inactivated during mitosis (177, 207-209, 243). The discrepancy between previous and recent studies has been attributed to the cell cycle synchronization method employed to arrest cells in mitosis. Previous studies utilized microtubule-destabilizing drugs, such as nocodazole, which has been reported to inhibit global mRNA translation (243). This would explain why only IRES-containing transcripts were able to be translated in the mitotic cell population. On the other hand, recent studies have resorted to mild synchronization methods to enrich mitotic cells, such as manual mitotic shake-off, S-phase arrest and release by double-thymidine block, and G2/M arrest and release by CDK inhibitor RO-3306 treatment (177, 209, 243-245).

1.6 TRANSLATION IN CANCER

Dysregulation of cap-dependent mRNA translation has been recognized to play an important role in cancer cell proliferation and survival (159). The signaling pathway responsible for activating protein synthesis, the PI3K-AKT-mTOR, is often overactivated in tumorigenesis, and has indicated that cap-dependent mRNA translation is increased in cancer cells, resulting in the overproduction of proteins that support cell proliferation and protect from cell death (246). This kind of dysregulation is attributed to the modulation of translation initiation effectors eIF4E and 4E-BP1 in favor of increased mRNA translation (143). Over the last couple of decades, the level of expression and phosphorylation of the cap-binding protein eIF4E and translation inhibitor 4E-BP1 have been identified as useful prognostics for multiple cancers (247-249). Interestingly, some tumor viruses, particularly the Merkel cell polyomavirus, have been shown to target 4E-BP1 to activate mRNA translation (170, 250-253), which highlights the importance of translational dyscontrol in non-viral and viral induced cancers alike.

1.6.1 eIF4E Overexpression

Due to its importance for cap-dependent mRNA translation of genes necessary for cell proliferation, eIF4E has been shown to act as a proto-oncogene (234, 254). eIF4E overexpression and upregulation lead to malignant transformation of rodent fibroblasts induced by other oncogenes, such as E1A, v-myc, and Ras (233, 234, 255-257). Knockdown of eIF4E reverses the tumorigenic phenotype of these transformed cells (258, 259). eIF4E is also overexpressed in various human cancers (260) and is regulated transcriptionally by c-Myc (261) and post-translationally by trans-acting translation initiation protein factors (262), ubiquitin-mediated protein degradation (263), and MNK1/2-mediated phosphorylation (123).

Mitogen-activated protein kinases (MAPK)-interacting protein kinases MNK1 and MNK2 bind eIF4G and phosphorylate human eIF4E at S209 (123, 146, 264, 265). The function of this phosphorylation is not yet clear, as it has not yet been determined whether it affects the affinity of eIF4E for the 5' cap or translation initiation. MNK1/2 double knockout in lymphoma and glioma mouse models does not exhibit any effects on cell growth when eIF4E S209 is not phosphorylated, but it appears to prevent cells from undergoing transformation (146). In line with this observation, phospho-defective eIF4E S209A knock-in mouse cells are resistant to transformation (266). The MNK1/2 kinases are able to phosphorylate eIF4E by binding to the C-terminus of eIF4G, which is bound to eIF4E when the eIF4F translation initiation complex has assembled on the 5' cap (123, 267). These observations suggest that eIF4E S209 phosphorylation may enhance cap-dependent translation in tumorigenesis, which may be disrupted upon 4E-BP1 displacing eIF4G and, in turn, preventing MNK1/2 from phosphorylating eIF4E.

1.6.2 4E-BP1 Hyperphosphorylation

Multiple signaling pathways that are dysregulated in cancer, such as the PI3K-AKT-mTOR and RAS-MAPK pathways, have been found to inactivate 4E-BP1 by phosphorylation. Increased protein synthesis through eIF4F-mediated translation leads to increased cell growth and proliferation. Thus, 4E-BP1 is a critical contributor to cell transformation, which has been shown to be dependent on sufficient eIF4F activity (268). In particular, eIF4F promotes cap-dependent translation of mRNAs encoding proteins that play a vital role in cell survival, proliferation, and migration (262).

The PI3K-AKT-mTOR pathway is commonly dysregulated in cancers and leads to increased 4E-BP1 phosphorylation and enhanced cap-dependent translation (141). Interestingly, phosphorylated 4E-BP1 protein levels are augmented in tumors in response to this signaling (248). Moreover, expression of a non-phosphorylatable 4E-BP1 antagonizes the tumorigenic phenotype of cancer cells in which the PI3K-AKT-mTOR pathway is constitutively activated (269). Double knockout of 4E-BP1 and 4E-BP2 in mouse embryonic fibroblasts leads to increased cell proliferation and renders the cells insensitive to mTOR inhibitor treatment (223). By phosphorylating 4E-BP1, the PI3K-AKT-mTOR frees its ultimate target eIF4E and allows it to recruit the rest of the translation initiation machinery to synthesize pro-proliferative proteins.

Another pathway that is activated in cancer is the RAS-MAPK pathway, which activates the MNK1/2 kinases that phosphorylate eIF4E at S209 (223, 264, 265). MNK1/2 can only phosphorylate eIF4E when eIF4G is bound to it (123). Expression of a non-phosphorylatable 4E-BP1 mutant in non-small cell lung cancer cells inhibits eIF4E phosphorylation by displacing eIF4G and preventing the recruitment of MNK1/2 (270).

RAS-MAPK signaling also appears to induce 4E-BP1 phosphorylation independently of PI3K-AKT signaling (223, 271). In tumor cells in which the two pathways are activated, 4E-BP1 phosphorylation is only abrogated when both pathways are inhibited (223). Notably, colon cancer cells become insensitive to RAS-MAPK and PI3K-AKT signaling when eIF4E is overexpressed or 4E-BP1 is knocked down (223). These findings suggest that the PI3K-AKT-mTOR and RAS-MAPK signaling pathways work together to activate both 4E-BP1 and eIF4E phosphorylation.

Finally, the tumor suppressor p53, which induces cell cycle arrest, DNA repair, senescence, and apoptosis, downregulates protein synthesis by inhibiting mTORC1 activity, which leads to 4E-BP1 dephosphorylation and truncation and thus increases the interaction between 4E-BP1 and eIF4E (200, 204, 205). The p53 gene is often mutated in various cancers, and some studies performed in cells with a p53 defect show that the acquisition of a tumorigenic phenotype is attributed to eIF4E overexpression or loss of 4E-BP1/2 expression and activity (214, 272). These results suggest that mutations that inhibit the tumor suppressor function of p53 allow for the phosphorylation and inactivation of 4E-BP1 through a dysregulated PI3K-AKT-mTOR pathway.

1.6.3 Tumor Viruses

Some cancer-causing viruses—HPV, HCV, KSHV, and MCV—are known to target the cap-dependent translation initiation machinery to promote the synthesis of their own proteins (273). The cervical cancer-causing human papilloma virus (HPV) encodes two major oncoproteins E6 and E7 (274). Essential for HPV replication and transformation, HPV E7 mRNA translation is activated by mTOR-mediated phosphorylation and

inactivation of the translation inhibitor 4E-BP1 (251). Furthermore, E6 upregulates the transcription of the 5' cap-binding protein eIF4E, which contributes to its tumorigenic activity (250). The hepatitis C virus (HCV), which causes hepatocellular carcinoma, encodes the nonstructural protein 5A (NS5A) that activates the mTORC1 kinase and induces 4E-BP1 phosphorylation and inactivation (253).

The two most recently discovered tumor viruses, KSHV and MCV, cause cancers associated with immunosuppression and also target cap-dependent mRNA translation initiation. The Kaposi sarcoma-associated herpesvirus (KSHV) causes Kaposi sarcoma (275) and activates mRNA translation by inducing 4E-BP1 phosphorylation (252), which leads to the synthesis of paracrine signaling proteins that are essential for tumor growth, namely VEGF-A and interleukin 6 (IL-6) (276). The Merkel cell polyomavirus (MCV) (277), which causes most Merkel cell carcinomas, encodes a small T antigen (sT) oncoprotein that also induces 4E-BP1 phosphorylation and activates cap-dependent translation (170, 209). Cap-dependent mRNA translation activation, thus, appears to be a critical target for the synthesis of tumor virus proteins and their transforming activities.

1.6.4 Merkel Cell Polyomavirus

Hundreds of thousands of viruses have been discovered, but only seven viruses are known to cause human cancers (278). Identifying a novel virus that causes a human cancer provides a new model to understand tumorigenesis. Nearly a decade ago, a novel cancer virus was discovered in Merkel cell carcinoma. Merkel cell carcinoma (MCC) is a very rare and aggressive skin cancer with a mortality rate of ~30% and an incidence of at least 1,500 cases per year in the United States, which has tripled in the

last two decades (279-281). MCC appears to arise from transformed Merkel cells, which are mechanoreceptor cells found in the basal layer of the epidermis (282). It is more prevalent in the elderly population, and risk factors for MCC occurrence include UV exposure and immunosuppression, particularly due to organ transplantation and the acquired immunodeficiency syndrome (AIDS) (283-285).

Due to its association with immunosuppression, the origin of MCC was suspected to be infectious. In 2008 a bioinformatics technique called digital transcriptome subtraction (DTS) was developed to search for viral sequences in cDNA libraries generated from MCC tumors (277). After transcripts that corresponded to human sequences were subtracted, databases containing only sequences of infectious origin remained. A non-human sequence that was highly homologous to the African green monkey lymphotropic polyomavirus was identified (277). Rapid amplification of cDNA ends (3'-RACE) revealed that a polyomavirus genome, eventually termed Merkel cell polyomavirus (MCPyV), was clonally integrated into the genome of 80% of the MCC tumors tested (277). Studies performed four years later with enhanced detection methods showed that 97% of MCCs are associated with this virus, suggesting that possibly all MCCs are caused by MCPyV (286).

Animal polyomavirus research has been central in cancer research. The first two polyomaviruses that were identified—the simian virus 40 (SV40) and the mouse polyomavirus (MPyV)—transform cells and can cause cancer in animals. Research on the SV40 large T antigen revealed the importance of two host cell tumor suppressor proteins, p53 and Rb (287). Studies on the SV40 small T antigen found the tumor suppressor function of the protein phosphatase PP2A, which is a negative regulator of

the AKT-mTOR pathway (288). Furthermore, mouse polyomavirus research on its middle T antigen revealed the critical role of the proto-oncogenic PI3K signaling pathway, which also targets the AKT-mTOR pathway (289). However, these viruses are not oncogenic in humans (290). Various polyomaviruses besides MCV have been identified in humans besides MCV. Although these viruses have a high seroprevalence in various human populations, they are not implicated in cancer (291-294), except for the BK virus that is associated with some genitourinary tumors in transplant patients (295). MCV is the first and only polyomavirus known to cause human cancer and has become a novel model to understand how cancers arise.

Genome

MCV, like other polyomaviruses, possesses a characteristic circular double-stranded DNA genome (approximately 5.4 kb) with an early region encoding two major overlapping tumor (T) antigens, small T (sT) and large T (LT), and a late region encoding three capsid proteins, VP1, VP2, and VP3 (**Figure 10**) (284). The tumor antigens LT and sT are the major oncoproteins encoded by MCV and are expressed in MCC tumors. Expression of these T antigens is required for MCC tumor cell growth, proliferation, and survival (296, 297). In addition to the major LT and sT, the early region also encodes the understudied 57kT antigen and the alternate frame of the LT ORF protein (ALTO) (298). Early and late coding regions are a common feature of DNA viruses and provide temporal regulation for viral gene expression. Polyomavirus tumor antigen genes are expressed upon viral entry to start viral DNA replication, after which the late viral capsid genes are expressed to produce new virions (299). MCV genome

has a non-coding regulatory region (NCRR) that separates the early and late genes and contains the viral origin of replication (Ori) and bidirectional transcription promoters for the two regions (300). In addition to these genes, MCV encodes a 22-nt microRNA, named MCPyV-miR-M1-5p, that has been identified in 50% of MCV-positive MCCs and may play a role in viral replication regulation and immune invasion (301, 302).

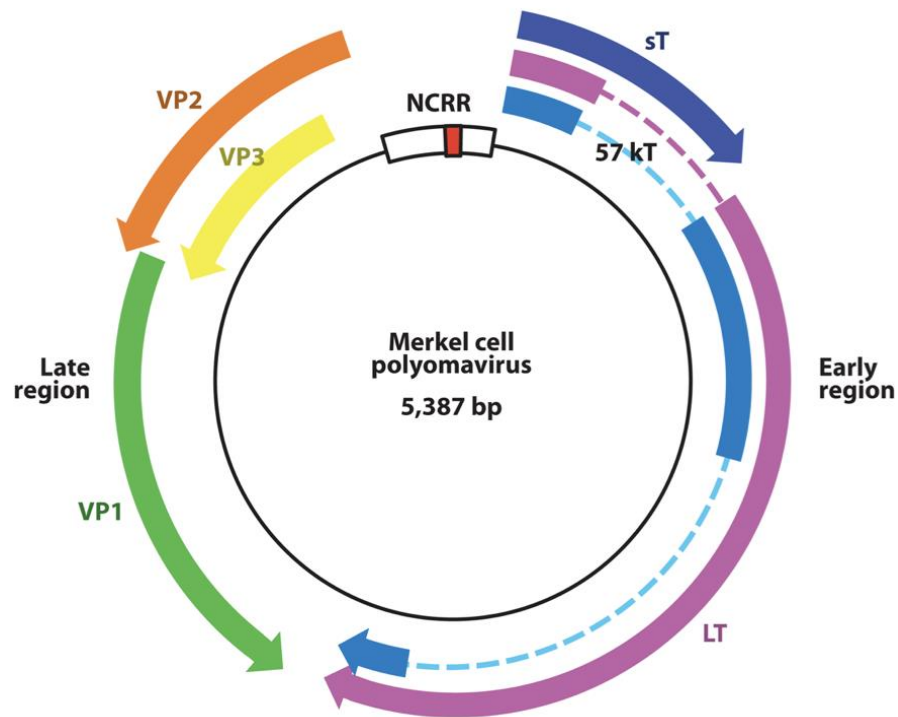


Figure 10. Wild-Type Merkel Cell Polyomavirus Genome

The wild-type Merkel cell polyomavirus genome is 5,387 bp long and contains early and late coding regions separated by the noncoding regulatory region (NCRR) that has an origin of replication (red) and promoters for bidirectional transcription. The early region encodes the early proteins large T antigen (LT), small T antigen (sT), and 57-kT antigen. The late region encodes the capsid viral protein genes 1, 2, and 3 (VP1, VP2, and VP3) (From Chang and Moore 2012 (284)).

Capsid Proteins

The MCV late region encodes the major capsid proteins VP1 and VP2 (**Figure 10**) (303). Expression of VP1 alone is sufficient for virus-like particle (VLP) production, which are ~40-55 nm in size, but assembly of both VP1 and VP2 is necessary for in vitro infection (304-306). Unlike the VP1 and VP2 genes, the VP3 gene is not expressed in MCV infection (304, 307). While the cell surface receptor for other polyomaviruses has been determined to be the ganglioside Gt1b sialic acids (308, 309), MCV pseudovirions rely on heparan sulfate, a sulfated glycosaminoglycan, for viral entry (306). Structural studies on VP1 protein complexes indicate that MCV uses primarily glycosaminoglycans for attachment and a sialylated glycan for internalization, which suggests a two-step entry process that is different from other polyomaviruses (310).

Large Tumor Antigen

The proteins encoded by DNA virus early genes target host cell cycle regulators and tumor suppressors in order to promote viral DNA replication (287, 288, 311, 312). The full-length MCV large T antigen (LT) is a large protein consisting of 817 amino acids and has various domains whose functions are important for MCV replication (**Figure 11**) (313). The DnaJ and CR1 domains in the N-terminus of LT bind the transcription inactivating chaperone protein Hsc70 (314, 315). This interaction between LT and Hsc70 has been shown to be permissive for MCV replication in vitro (316). Additionally, the LT antigen has a nuclear localization signal (NLS) and a conserved Rb-binding motif (LXCXE) between amino acids 100-300—a region different from other polyomaviruses and unique to MCV (317). Termed the MCV T antigen unique region (MUR), this stretch

of amino acids has been shown to interact with the vacuolar sorting protein Vam6p, which leads to nuclear translocation of this protein and lysosomal clustering (318). Expression of a Vam6p binding mutant LT enhances viral replication, while overexpression of human Vam6p inhibits this process (300). These findings suggest that the interaction between LT and Vam6p may help establish latency in the host cell.

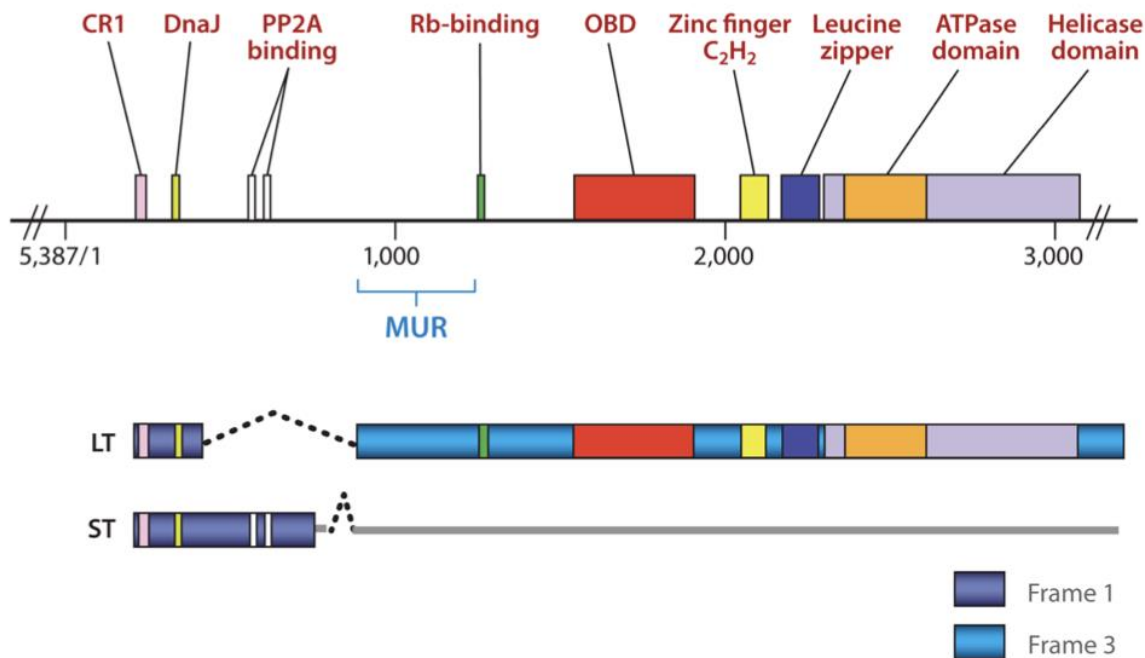


Figure 11. MCV Large T and Small T Antigen Domain Architecture

The full-length MCV LT schematic shows the location of its different domains, particularly its Rb-binding and origin-binding (OBD) domains. The MCV sT shares the DnaJ binding domain with LT and possesses a PP2A binding site (Modified from Chang and Moore 2012 (284)).

As in other polyomavirus T antigens, the conserved LXCXE motif allows MCV LT to bind the tumor suppressor retinoblastoma protein Rb (315, 319). This interaction is important to drive the cells into S phase by upregulating the transcription of E2F target genes, particularly cyclin-dependent kinases, cyclins, checkpoint regulators, and DNA

repair and replication proteins (317, 320, 321). An intact LXCXE is critical for MCC cell growth, as expression of an Rb-binding mutant LT in MCV LT-knockdown MCC cells cannot rescue their growth (322). Furthermore, expression of a LT protein with an intact LXCXE motif upregulates the expression of anti-apoptotic protein survivin, whose pharmacological inhibition in MCC xenograft mice increases their survival (321, 323).

The regions necessary for viral replication are found in the MCV LT C-terminal half (**Figure 11**). The origin binding domain (OBD) recognizes and binds the 71-bp origin of replication located in the NCRR (324). Two phosphorylation sites, T297 and T299, regulate the ability of LT to start DNA replication in opposite ways (325). Phosphorylation of T297 inhibits LT interaction with the origin of replication. On the other hand, phosphorylation of T299 is necessary for LT to initiate replication. Also on the C-terminal half of LT resides a helicase domain, between amino acids 441-817, that is required for LT oligomerization and replication initiation at the origin in the NCRR (320). Interestingly, the LT C-terminus is found to be truncated in MCC tumors, which eliminates the replication function of LT (315, 326). Recent findings have shed light on the anti-proliferative potential of the MCV LT C-terminus and may provide an additional explanation for its truncation in tumors. The helicase domain of LT is reportedly capable of inducing the host DNA-damage response (327). Phosphorylation of S816 in this domain by DNA-damage response ATM kinase induces apoptosis (328). Furthermore, the growth of MCC cells and SV40-immortalized human fibroblasts is suppressed by the expression of a fragment containing the last 100 residues of the LT C-terminus (329).

Small Tumor Antigen

The MCV small T antigen (sT) is the second major protein encoded by the MCV early region, and it shares the first 78 amino acids of the LT N-terminus and has a length of 186 amino acids (**Figure 11**) (313). Unlike LT in MCC, MCV sT is unaffected by tumor mutations, and its coding region is found intact (315). In the SV40 model of transformation, LT is the primary oncoprotein (290), whereas MCV-driven tumorigenesis relies mainly on sT, whose expression alone is sufficient to transform rodent fibroblasts (170) and induces tumor formation in transgenic mouse models (330, 331).

The C-terminus of MCV sT possesses a protein phosphatase 2A binding site that is conserved across polyomavirus sT antigens (288). For instance, the SV40 sT interacts with PP2A and inhibits the dephosphorylation of AKT, constitutively activating its downstream targets (332-334). While MCV sT can bind PP2A subunits and PP4C (335, 336), its transformation activity is independent of this interaction (170). Expression of this viral protein has modest effects on AKT-activating S473 phosphorylation but no effect on mTOR expression (170). On the other hand, the interaction of MCV sT and PP4C has been shown to inhibit the nuclear translocation of NF- κ B essential modulator (NEMO), which consequently blocks host inflammatory signaling (335). Another reported consequence of this interaction is facilitating cell migration by destabilizing microtubules through targeting of the cytoskeletal regulator stathmin (337).

MCV sT also promotes viral replication by stabilizing the LT protein (300, 316). sT inhibits the E3 ubiquitin ligase SCF Fbw7, which targets LT for proteasomal degradation and thus inhibits MCV replication (338). In addition, sT also stabilizes other Fbw7 substrates, cyclin E and c-Myc, that are contributors to cell transformation (338).

The LT stabilizing domain (LSD), mapped between amino acids 91-95, is important not only for MCV sT binding and inactivating of Fbw7, but also for its transformation activity (330, 338). MCV sT has also been shown to coordinate iron/sulfur clusters through two CXCXXC cysteine motifs, which are required for LT-mediated viral replication (339).

Furthermore, MCV sT targets host cap-dependent translation by inducing the hyperphosphorylation-inactivation of cap-dependent translation inhibitor 4E-BP1 in an mTOR-independent manner (170). It is speculated that the known consequences of 4E-BP1 inactivation, such as increased eIF4E activity and cap-dependent translation, might be key contributors to tumorigenesis caused by MCV (170). Knockdown of MCV sT in MCV-positive MCC cell lines decreases translation initiation complex assembly at the 7-methyl-guanine cap (170). Moreover, expression of a constitutively active, non-phosphorylatable 4E-BP1 abolishes MCV sT-induced rodent fibroblast transformation, indicating that 4E-BP1 inhibition is required for sT cell transformation activity (170).

Recent studies, included in the subsequent chapters of this dissertation, have clarified the mechanism of MCV sT targeting of 4E-BP1. MCV sT promotes mitogenesis by inhibiting another E3 ubiquitin ligase, the mitotic checkpoint APC/C cdc20 (209). This results in the activation of the mitotic CDK1 kinase to hyperphosphorylate 4E-BP1 and activate cap-dependent translation (209). MCV sT induction of mitosis revealed that mitotic cells in general express a unique hyperphosphorylated form of 4E-BP1, that contains a novel phosphorylation at S83 (177). Expression of an alanine mutant of S83 modestly reverses MCV sT-induced cell transformation (177). These findings suggest that mitotic cap-dependent mRNA translation activated by CDK1 phosphorylation of 4E-

BP1 is permissive for viral-induced tumorigenesis and possibly for non-viral-induced tumorigenesis as well.

The studies presented in this dissertation focused on the regulation of cap-dependent mRNA translation inhibitor protein 4E-BP1 during normal mitosis and mitosis enforced by the MCV sT oncoprotein. Chapter 2 shows that: 1) MCV sT increases mitogenesis by targeting the cellular anaphase promoting complex E3 ligase; 2) MCV sT induces mTOR-independent 4E-BP1 hyperphosphorylation; 3) CDK1 directly phosphorylates 4E-BP1 at T37, T46, S65, and T70 during mitosis, forming a high molecular weight δ phospho-species; 4) δ -4E-BP1 is induced in mitosis during normal cell cycling; and 5) CDK1 activates cap-dependent translation during mitosis. Chapter 3 shows that: 1) δ -4E-BP1 hyperphosphorylation is a feature of mitosis across multiple cancer cell lines; 2) CDK1 phosphorylates 4E-BP1 at S83; 3) S83-phosphorylated 4E-BP1 colocalizes with centrosomes during mitosis and peaks at metaphase; and 4) mutation of 4E-BP1 S83 does not affect global cap-dependent translation but partially reverses MCV sT-induced rodent cell transformation. Both studies provide evidence that cap-dependent mRNA translation is active during mitosis and reveal the role of CDK1 as a novel regulator of the protein synthesis gate-keeper 4E-BP1.

2.0 CDK1 SUBSTITUTES FOR MTOR KINASE TO ACTIVATE CAP-DEPENDENT PROTEIN TRANSLATION DURING MITOSIS

Work described in this chapter was published in the Proceedings of the Academy of
Sciences

Proc Natl Acad Sci U S A. 2015 May 12;112(19):5875-82

**with authors Masahiro Shuda, Celestino Velásquez, Erdong Cheng, Daniel
G. Cordek, Hyun Jin Kwun, Yuan Chang, and Patrick S. Moore**

Masahiro Shuda, Celestino Velásquez, Erdong Cheng, Daniel G. Cordek, and Hyun Jin Kwun performed experiments and analyzed the data. Masahiro Shuda, Celestino Velásquez, Erdong Cheng, Daniel G. Cordek, Hyun Jin Kwun, Yuan Chang, and Patrick S. Moore designed experiments. Masahiro Shuda, Celestino Velásquez, Erdong Cheng, Yuan Chang, and Patrick S. Moore wrote the manuscript.

This chapter describes an alternative control mechanism for maintaining cap-dependent translation during mitosis revealed by a viral oncoprotein, the Merkel cell polyomavirus small T antigen (MCV sT). We find MCV sT to be a promiscuous E3 ligase inhibitor targeting the anaphase promoting complex, which increases cell mitogenesis. MCV sT binds through its LSD region to Cdc20 and, possibly, Cdh1 E3 ligase adapters. This activates cyclin-dependent kinase 1/Cyclin B1 (CDK1/CYCB1) to directly hyperphosphorylate 4E-BP1 at authentic sites, generating a mitosis-specific, mTOR-inhibitor resistant δ phospho-isoform not present in G1-arrested cells. Recombinant 4E-BP1 inhibits capped mRNA reticulocyte translation, which is partially reversed by CDK1/CYCB1 phosphorylation of 4E-BP1. eIF4G binding to the eIF4E-m7GTP cap complex is resistant to mTOR inhibition during mitosis but sensitive during interphase. Flow cytometry, with and without sT, reveals an orthogonal pH3^{S10+} mitotic cell population having higher inactive p4E-BP1^{T37/T46+} saturation levels than pH3^{S10-} interphase cells. Using a Click-iT flow cytometric assay to directly measure mitotic protein synthesis, we find that most new protein synthesis during mitosis is cap-dependent, a result confirmed using the eIF4E/4G-inhibitor drug 4E1RCat. For most cell lines tested, cap-dependent translation levels were generally similar between mitotic and interphase cells and the majority of new mitotic protein synthesis was cap-dependent. Mitosis is commonly thought to be associated with reduced cap-dependent protein translation. These findings suggest that mitotic cap-dependent translation is generally sustained during mitosis by CDK1 phosphorylation of 4E-BP1 even under conditions of reduced mTOR signaling.

2.1 INTRODUCTION

Eukaryotic initiation factor 4E (eIF4E)-binding protein, 4E-BP1, is a principal target for mTORC1 (mechanistic target of rapamycin complex (159, 223, 269). mTOR regulates a variety of metabolic signaling pathways related to ribosomal biosynthesis and autophagy that contribute to cancer cell survival (159, 223, 246, 248, 340). Increasing evidence indicates that direct mTORC1 phosphorylation of 4E-BP1 may be the key event in mTOR-associated tumorigenesis (269). In the absence of activated mTOR, hypophosphorylated 4E-BP1 sequesters eIF4E to prevent assembly of eIF4F complex components onto capped mRNA, inhibiting cap-dependent translation. When 4E-BP1 is phosphorylated by mTOR (156), first at critical priming threonine (T)37 and T46 residues and then at other sites, 4E-BP1 is inactivated and releases eIF4E to allow initiation of cap-dependent translation (172). Other non-mTOR kinases, including cyclin-dependent kinase 1 (CDK1), have been shown to be able to phosphorylate 4E-BP1 (163, 207, 210, 219) but have not been extensively examined *in vivo* for their effects on 4E-BP1 regulated cap-dependent translation.

Protein synthesis has been described to decrease during mitosis relative to interphase in reports dating back to the 1960s (341, 342). There are two issues, however, with this conclusion: 1) Mitotic cells represent less than 1% of the total cell population in bulk culture and even under stringent conditions, high levels of interphase cell contamination can occur. 2) Many studies of mitotic cap-dependent translation rely on cell cycle synchronization studies with microtubule inhibitors, e.g., nocodazole, which are also mitotic translation inhibitors (243). Under these conditions, comparisons of interphase and mitotic translation can be imprecise. Single-cell measurements, such as

flow cytometry, can potentially overcome these concerns. Additionally, a highly hyperphosphorylated 4E-BP1 isoform called δ -4E-BP1 is present in mitotic cells (207, 208). This hyperphosphorylated isoform is predicted to promote rather than inhibit cap-dependent protein translation and is therefore inconsistent with the standard model.

Our studies on Merkel cell polyomavirus (MCV) provide insights into these issues. MCV is a small double-stranded DNA virus discovered in 2008 by our lab that causes most cases of the human skin cancer, Merkel cell carcinoma (MCC) ((277); for review see (284, 303, 343)). The 19-kDa MCV small T (sT) antigen is a transforming oncoprotein required for MCC cell growth (170, 296). A region of the sT protein spanning amino acid residues 91-95 called the LSD (Large T stabilization domain), promotes δ -4E-BP1 hyperphosphorylation (336), rodent cell transformation (338) and fibroblast proliferation in a mouse transgenic model (170, 330). Expression of the phosphorylation-defective, dominant-positive (DP)-4E-BP1 (153) with alanine substitution mutations at priming T37/T46 (4E-BP1^{T37A/T46A}) reverses sT-induced rodent fibroblast transformation, suggesting a direct link between 4E-BP1 phosphorylation status and sT-induced transformation (170). Surprisingly, sT-induced δ -4E-BP1 hyperphosphorylation is not dependent on mTOR activity (170). The sT LSD region is known to bind the Fbw7 E3 ligase to promote cell proliferation but Fbw7 targeting is not sufficient to explain either cell transformation or 4E-BP1 hyperphosphorylation (338).

We show here that MCV sT, through its LSD domain, also promotes mitogenesis and 4E-BP1 hyperphosphorylation by functioning as a promiscuous E3 ligase inhibitor that also targets cellular anaphase-promoting complex/cyclosome (APC/C) E3 ligase activity. During sT-induced mitosis, sT-induced CDK1/CYCB1 rather than mTOR

directly phosphorylates 4E-BP1 to the mitosis-specific δ isoform. Using a flow cytometry-based method to directly measure mitotic cap-dependent protein synthesis for the first time, we do not detect a general shift from cap-dependent to cap-independent protein translation in mitotic cells compared to interphase cells. Mitotic cells actually show higher saturation levels of p4E-BP1^{T37/T46+}, consistent with 4E-BP1 inactivation, than interphase cells. Consistent with this, and in contrast to previous studies, we find that δ -4E-BP1 positive mitotic cells show high levels of cap-dependent protein translation that is reduced by the cap translation inhibitor 4E1RCat. When accentuated or sustained high levels of mitotic cap-dependent protein translation may play a role in cancer cell transformation and contribute to mTOR-inhibitor resistance in subsets of cancers.

2.2 MATERIALS AND METHODS

2.2.1 Cell Culture and Transfection/Transduction

293, 293FT, U2OS, HeLa and BJ-tert (BJ-T) cells were maintained in DMEM (Corning Cellgro) supplemented with 10% FBS. 293 and 293FT cells were transfected using Lipofectamine 2000 (Invitrogen) and harvested after 48 h.

2.2.2 Kinase Inhibitors

The following active-site kinase inhibitors were dissolved in DMSO and used for kinase inhibition and in vitro phosphorylation experiments: mTOR kinase inhibitor PP242 (Selleckchem), CDK1 kinase inhibitor RO-3306 (Calbiochem) and pan Aurora kinase inhibitor VX-680 (Selleckchem).

2.2.3 Plasmids and Transfections

Plasmids pcDNA6.sTco (wild-type MCV sT, codon optimized) and pcDNA6.sTmLSD that were used for transient transfection experiments are previously described (170, 338). To efficiently express SV40 sT, codon-optimized SV40 sT (GenBank accession number KM359729 (336)) was generated by overlapping PCR.

2.2.4 Immunoblotting and Antibodies

Cells were lysed in lysis buffer (50 mM Tris-HCl pH 7.4, 0.15 M NaCl, 1% Triton X-100, 2 mM Na₃VO₄, 2 mM NaF and 0.1% SDS) containing protease inhibitors (Roche). Lysates were resolved by 12% SDS-PAGE and transferred to nitrocellulose. Membranes were blocked with 5% milk in 1X TBS and incubated with primary antibodies overnight at 4 °C. Blots were subsequently incubated with IRDye-labeled anti-rabbit or anti-mouse secondary antibodies and analyzed on the Odyssey infrared scanner (LI-COR Biosciences). The following primary antibodies were used in this study: total 4E-BP1, phospho-4E-BP1^{T37/T46}, phospho-4E-BP1^{T70}, phospho-4E-BP1^{S65}, eIF4E, eIF4G, phospho-S6^{S242/S244}, total S6, phospho-Histone H3^{S10}, total Histone H3, cdc25C, phospho-Aurora A/B/C, total Aurora A, total Aurora B, Skp2, Cdc20, Plk1, Claspin (Cell Signaling), total Aurora C, phospho-MPM2 (Millipore), Cdh1 (Calbiochem), cyclin A, cyclin D1, cMyc (Santa Cruz Biotechnology), HA (Covance), FLAG (Sigma Aldrich), 800CW goat polyclonal anti-rabbit IgG and 680CW goat polyclonal anti-mouse IgG (LI-COR Biosciences). Previously described CM8E6 (338) and CM5E1 (170) were used to detect MCV sT. For cycloheximide (CHX) chase assays, BJ-T cells were treated with 100 µg/mL CHX and harvested at different time points for immunoblotting.

2.2.5 Immunoprecipitation

293 cells co-transfected with sT constructs and myc-cdh1, HA-cdc20 or pcDNA6 empty vector were harvested after 48 h and lysed in IP lysis buffer (50 mM Tris-HCl pH 7.4, 0.15 M NaCl, 1% Triton X-100, 2 mM Na₃VO₄ and 2 mM NaF) supplemented with

protease inhibitors (Roche). Pre-cleared lysates were incubated with either anti-myc tag or anti-HA antibodies overnight at 4 °C. Immune complexes were precipitated with protein A/G sepharose beads (Santa Cruz) for 1 h at 4 °C. Beads were collected, washed with lysis buffer and boiled in 1X SDS loading buffer. Samples were subjected to SDS-PAGE and immunoblotting.

2.2.6 Two-Dimensional Electrophoresis

293 cells were lysed using lysis buffer (50 mM Tris-HCl, pH 7.4, 0.15 M NaCl, 1% Triton X-100, 2 mM Na₃VO₄, 2 mM NaF) supplemented with protease inhibitors (Roche). Clarified lysates were focused using immobilized pH 3-6 gradient strips (Bio-Rad) with linear voltage ramping for 2 h at 200 V, 2 h at 500 V and 16 h at 800 V. Focused proteins were then subjected to SDS-PAGE for two-dimensional resolution and detected by immunoblotting.

2.2.7 Flow Cytometry

293 and BJ-T cells were trypsinized and fixed in 70% ethanol for DNA staining or in 10% buffered formalin for AHA incorporation assays. Fixed cells were washed with PBS containing 1% FBS and permeabilized with 0.25% Triton X-100 for 30 min on ice. For cell cycle analysis, cells were resuspended in PI/RNase staining solution (0.05 mg/mL propidium iodide, 0.1 mg/mL RNase A in 1X PBS) and incubated for 30 min at room temperature. For phospho-histone H3^{S10}, phospho-MPM2, and phospho-4E-BP1^{T37/T46}

analysis, cells were incubated with the corresponding fluorophore-conjugated antibodies for 2 h at room temperature.

2.2.8 Cell Cycle Synchronization and Mitotic Cell Enrichment

293 cells were treated with medium containing 0.5 μ M nocodazole or 0.5 mM L-mimosine for 16 h to induce mitotic arrest or G1 arrest, respectively. Mitotic cells were enriched by double-thymidine block (2 mM) and release using 293 and U2OS cells or by mitotic shake-off (344) using BJ-T cells stably expressing wild-type MCV sT. To block cell cycle at late G2, HeLa and U2OS cells were incubated in medium containing CDK1 inhibitor RO-3306 (10 μ M) for 24 h. Cell cycle entry from G2 to mitosis was induced by RO-3306 washout. Cells arrested by nocodazole and released from RO-3306 arrest were treated with 10 μ M of proteasome inhibitor MG132 for 30 min prior to kinase inhibitor treatment to retain cells in mitosis.

2.2.9 In vitro Phosphorylation Assays

Recombinant GST-4E-BP1 (0.2 μ g) (SignalChem) was incubated in a 24- μ L reaction containing 1X protein kinase buffer (NEB) and 20 units of recombinant CDK1/CYCB1 (NEB) or 10 μ g of mitotic HeLa cell lysate, supplemented with 200 μ M ATP and/or 5 μ M active site kinase inhibitors, for 30 min at 30 °C. HeLa cells were arrested in mitosis by treatment with 0.5 μ M nocodazole for 16 h and enriched by mechanical shake-off for lysis in non-denaturing lysis buffer (50 mM Tris-HCl pH 7.4, 0.15 M NaCl, 1% Triton X-100, 2 mM Na_3VO_4 and 2 mM NaF). The reactions were stopped by adding 5X SDS

sample buffer to 1X concentration and boiling for 5 min. Reaction samples were then subjected to SDS-PAGE and immunoblotting. For in vitro protein dephosphorylation, 293 cell extracts were incubated with lambda phosphatase in protein metallophosphatase reaction buffer (NEB) supplemented with 2 mM MnCl_2 for 30 min at 37 °C. Reactions were stopped by adding 2X SDS sample buffer and then subjected to SDS-PAGE and immunoblotting.

2.2.10 m7GTP Cap Binding Assay

Shake-off (mitosis-enriched) and adherent cells (mitotic-depleted) from MCV sT-transduced BJ-T cells or asynchronous BJ-T cells were lysed in buffer (50 mM Tris-HCl, pH 7.4, 0.15 M NaCl, 1% Triton X-100, 2 mM Na_3VO_4 and 2mM NaF) supplemented with protease inhibitors (Roche). Lysates (30 μg of total protein) were incubated with 5.0 μL m7GTP sepharose beads (GE Healthcare) for overnight at 4 °C. Beads were collected, washed with lysis buffer, and subjected to SDS-PAGE and immunoblotting. 25 μg of total protein was loaded as input control (83%).

2.2.11 In vitro mRNA Synthesis and Translation

Capped FLuc reporter mRNA was synthesized by the MessageMAX T7 ARCA-Capped message transcription kit (Cell Script) using 1 μg pCD-V5-FLuc linearized by MscI as template. Purified RNA was polyadenylated using the A-Plus Poly (A) polymerase tailing kit (Cell Script). Translation reactions were performed in a final volume of 10 μL consisting of 7 μL of nuclease treated rabbit reticulocyte lysate (RRL) (Promega), 0.8

pmol of capped and polyadenylated reporter mRNAs and amino acids mixture (50 μ M each). GST-4E-BP1 was incubated with either CDK1 or 1 μ g/mL BSA in the presence of DMSO or 10 μ M RO-3306 (see reaction setup for previous section). As a control, PBS alone was incubated with the same amount of either DMSO or 10 μ M RO-3306. Either buffer or pre-treated GST-4E-BP1 (12.4 μ L) was added to the rabbit reticulocyte lysate reaction mixture. The prepared RRL mixture was incubated for 15 min at 30 °C. The reaction was then stopped by adding 10 μ L of luciferase lysis buffer to the mixture. Translation was measured as firefly luciferase activity.

2.2.12 Nascent Protein Synthesis Analysis

BJ-T sT stable cells were labeled with an azide-linked methionine analog, L-azidohomoalanine (AHA) (Life Technologies) at 25 μ M for 45 min in the presence or absence of PP242 (5 μ M), followed by mitotic shake-off to separate mitotic cells and interphase cells. To analyze mitotic cap-dependent translation in U2OS and HeLa cells, cells were arrested G2/M boundary by 10 μ M RO-3306 treatment for 24 h (345). After 30 min of RO-3306 removal, cells were labeled with AHA (25 μ M) for 90 min in methionine-depleted DMEM medium (Corning Cellgro) after optimization of pre-experiments. Translation inhibitors (4E1RCat (50 μ M) or cycloheximide (100 μ g/ml)) or DMSO (0.1%) were added to cells with AHA. Cells were trypsinized and fixed in 10% formalin for 5 min. Fixed cells were permeabilized in PBS containing 0.1% saponin and 1% FBS for 30 min at room temperature. Cells were harvested and labeled with the Alexa Fluor 488 alkyne using the Click-iT cell reaction buffer kit (Life Technologies).

AHA incorporation in cells was analyzed by flow cytometry as a measure for nascent protein synthesis in interphase and mitotic cells.

2.2.13 Statistical Analysis

One-sided t-test was performed for densitometric analysis of m7GTP pull-down assays and two-sided t-test (unequal variances) for in vitro translation assays. A p-value less than 0.05 was considered to be significant.

2.3 RESULTS

2.3.1 MCV sT increases mitogenesis by targeting the cellular anaphase promoting complex E3 ligase.

To search for factors contributing to MCV sT-induced transformation, the viral oncoprotein was expressed in primary immortalized BJ-tert (BJ-T) fibroblasts. These cells displayed a rounded phenotype in culture with increased phospho-histone H3 serine 10 (pH3^{S10}) phosphorylation, characteristic for mitosis (**Figure 12A**). Increased pH3S10 and increased expression of mitotic markers (including cyclin B1 (CYCB1) and phospho-aurora kinase B (pAURKB)) were also observed in 293 cells expressing MCV sT (**Figure 13**). Immunoprecipitation of sT revealed an in vivo complex with the APC/C substrate recognition subunit, Cdc20 that was dependent on an intact LSD (**Figure 12B**). MCV sT also interacted with another APC/C substrate recognition subunit, Cdh1, but substantial Cdh1-binding occurred with sT^{mLSD} having alanine substitutions at residues 91-95, suggesting that sT may bind Cdh1 at other sites in addition to the LSD. In line with these results, known APC/C E3 targets, including aurora kinase A (AURKA) and AURKB, Skp2, polo-like kinase 1 (Plk1) and CYC A2, showed markedly reduced turnover in the presence of sT on cycloheximide (CHX) chase immunoblotting (**Figure 12C**). These APC/C E3 targets retained rapid turnover in the presence of empty vector or sTmLSD expression. CYCD1, which is not directly regulated by APC/C (346) was unaffected by MCV sT or sT^{mLSD} expression. Similarly, MCV sT expression stabilized FLAG-tagged AURKA and endogenous CYCB1, but not CYCD1, after nocodazole-release of 293 cells whereas MCV sT^{mLSD} expression did not (**Figure 14**).

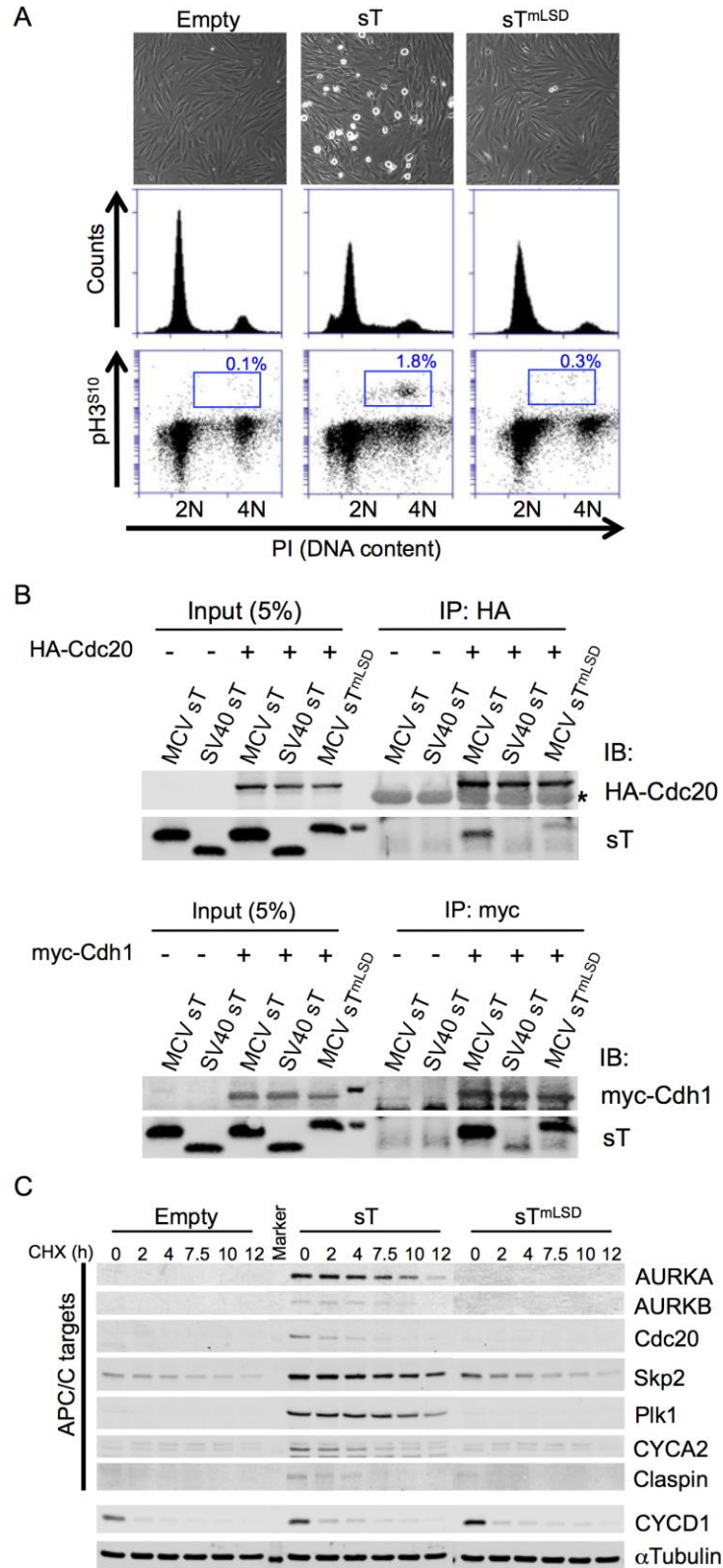


Figure 12. MCV sT increases mitotic entry by targeting APC/C E3-ubiquitin ligases.

Figure 12 (continued)

(A) MCV sT induces cellular mitogenesis. BJ-tert (BJ-T) cells stably transduced with MCV sT have increased mitotic rounding and a 6 to 18-fold increase in pH3^{S10+} mitotic cells compared to empty vector or sT^{mLSD} transduced cells. (B) MCV sT interacts with APC/C E3 ligase substrate recognition subunit Cdc20 and Cdh1 proteins. HA-tagged Cdc20 or myc-tagged Cdh1 expression plasmids were co-transfected with MCV sT, MCV sT^{mLSD}, or SV40 sT expression plasmids into 293 cells, and immunoprecipitated 48 h later with anti-HA or anti-myc antibodies, followed by immunoblotting using mixed anti-MCV sT (CM8E6) and anti-SV40 sT (PAb419) antibodies. Cdc20 interaction with MCV sT was nearly eliminated in the sT^{mLSD} mutant protein while partial interaction was retained between MCV sT^{mLSD} and myc-Cdh1 proteins. Weak interaction between SV40 sT and myc-Cdh1 only was detected. Asterisk indicates immunoglobulin heavy chain. (C) APC/C target proteins (AURKA/B, Cdc20, Skp2, Plk1, cyclin A, and claspin) are stabilized by MCV sT expression. BJ-T cells were treated with cycloheximide (100 µg/mL) to inhibit new protein synthesis and harvested at the indicated time points. The half-lives of proteins regulated by APC/C are extended by expression of MCV sT but not empty vector or MCV sT^{mLSD} controls. Cyclin D is not directly regulated by Cdh1 and its half-life was unchanged by MCV sT expression. A representative α-tubulin loading control is shown. Representative results are shown from three independent experiments.

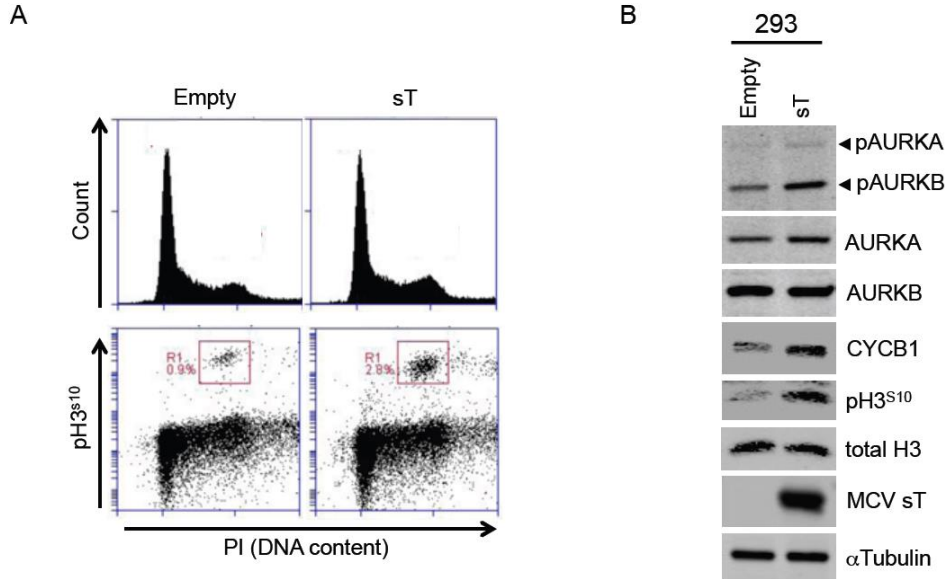


Figure 13. MCV sT increases mitogenesis in 293 cells.

(A) MCV sT expression increases phospho-histone H3^{S10} (pH3^{S10}) positive mitotic cells. (B) MCV sT expression in 293 cells increases mitotic marker expression including pAURKA, pAURKB, CYCB1, and pH3^{S10}. Transfected 293 cells were split into two fractions for cell cycle profile (A) and mitosis marker immunoblotting (B).

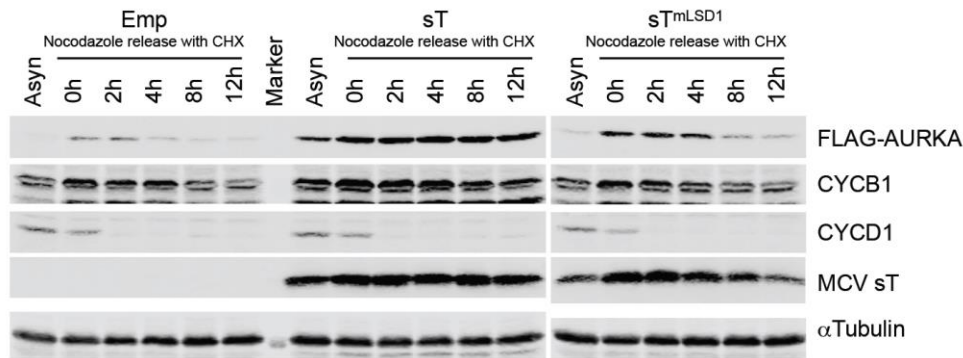


Figure 14. MCV sT stabilizes APC/C targets (AURKA and CYCB1) in nocodazole-arrested 293 cells.

293 cells co-transfected with FLAG-tagged AURKA and MCV sT, sT^{mLSD}, or empty vector, were arrested with nocodazole (0.5 μM) for 15 h, and then treated with CHX after nocodazole washout and harvested at different time points for immunoblotting. Asynchronous cells for each transfection were used as a control for nocodazole arrest. MCV sT, but not sT^{mLSD} or empty vector stabilizes AURKA and CYCB1 proteins in metaphase-arrested 293 cells. MCV sT increased FLAG-AURKA and CYCB1 expression in asynchronous cells, consistent with sT induction of increased mitogenesis.

2.3.2 MCV sT induces mTOR-independent 4E-BP1 phosphorylation.

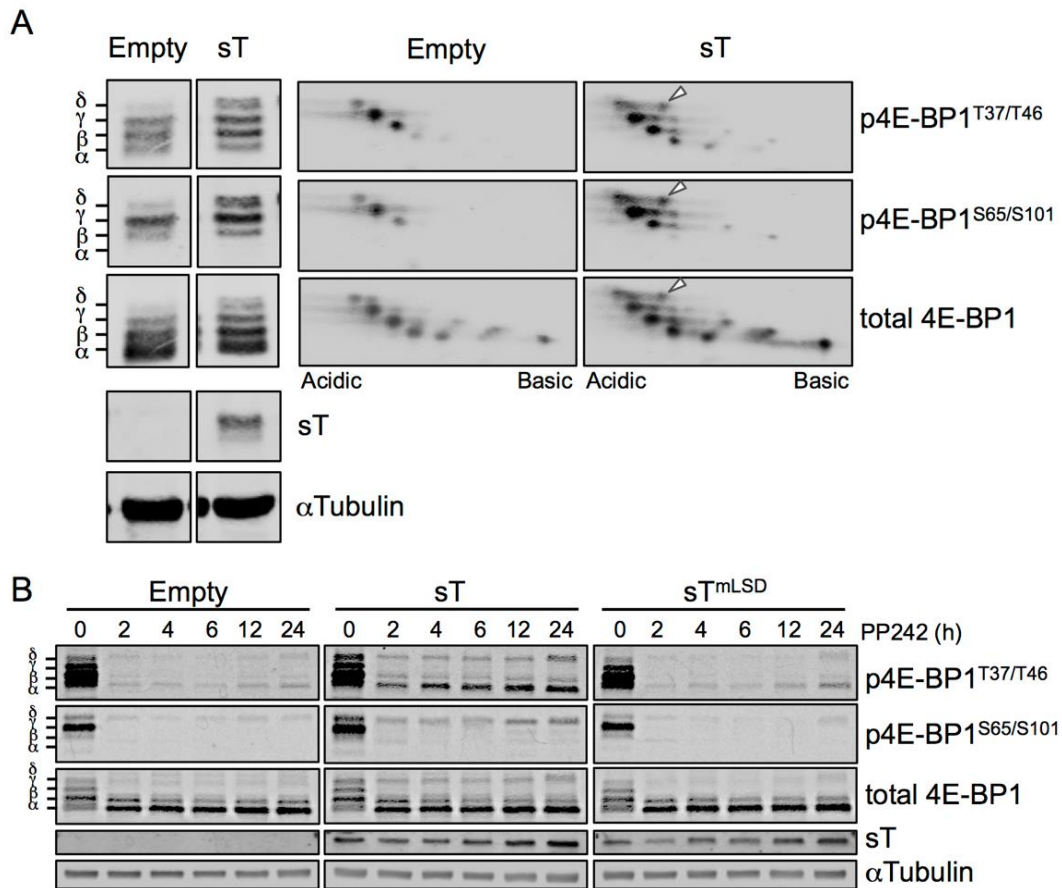


Figure 15. MCV sT induces cellular 4E-BP1 hyperphosphorylation.

(A) MCV sT induces p4E-BP1^{T37/T46} and p4E-BP1^{S65/S101} phosphorylation. 4E-BP1 phosphospecies are named α through δ according to molecular mass. Higher molecular mass isoforms, particularly β , γ , and δ were increased following sT expression in 293 cells and include authentic phosphorylation sites as detected by phospho-specific antibodies. A 2D gel fractionation of these same lysates (pH 3-6 isoelectric focusing/SDS-PAGE) were aligned to the 1D gel. Arrow heads indicate new 4E-BP1 isoelectric focusing spots after sT expression detected by p4E-BP1^{T37/T46}, p4E-BP1^{S65/S101}, and total 4E-BP1 antibodies. (B) MCV sT-induced 4E-BP1 phosphorylation is partially resistant to mTOR inhibition. 293 cells were transfected with MCV sT, sT^{mLSD}, or empty vector expression plasmids for 48 h, treated with the mTOR-inhibitor PP242 and harvested at the indicated time points. MCV sT depends on an intact LSD region to maintain PP242-resistant 4E-BP1 phosphorylation. Representative results are shown from three independent experiments.

We next examined the role of MCV sT in 4E-BP1 hyperphosphorylation. 4E-BP1 hyperphosphorylation isoforms are named α through δ according to ascending molecular mass (**Figure 15A**) (157). Most notable was the appearance of the highest molecular mass form, δ , containing phosphorylation marks at T37/T46 and S65/S101, after transfection of the sT expression vector into 293 cells, as previously described (170). A two-dimensional (2D) gel immunoblot (**Figure 15A**, right panel) aligned to the corresponding 1D SDS PAGE immunoblot shows that during MCV sT expression, a new phospho-isoform appears at the δ position (arrows) staining for p4E-BP1^{T37/T46} and p4E-BP1^{S65/S101}. MCV sT expression prolonged 4E-BP1 phosphorylation (**Figure 15B**) in the presence of the mTOR inhibitor PP242 (347) compared to empty vector control and sT^{mLSD} transfected cells, indicating that δ -4E-BP1 phosphorylation may be independent of mTOR kinase activity.

2.3.3 CDK1/CYCB1 directly phosphorylates 4E-BP1, in the presence and absence of sT, to the δ isoform during mitosis.

4E-BP1 phosphorylation is induced by microtubule assembly inhibitors such as nocodazole and paclitaxel that arrest cells in mitosis (208, 243). To assess the role of various kinases on mitotic 4E-BP1 phosphorylation, nocodazole-treated HeLa mitotic cell lysates were reacted with recombinant GST-4E-BP1 and kinase inhibitors, including PP242 (mTORC1 and mTORC2), RO-3306 (CDK1), and VX-680 (pan AURK) (**Figure 16A**). GST-4E-BP1 was robustly phosphorylated at authentic sites by mitotic HeLa lysates, and this was reversed by inhibition of CDK1 but not by mTOR or AURK inhibition.

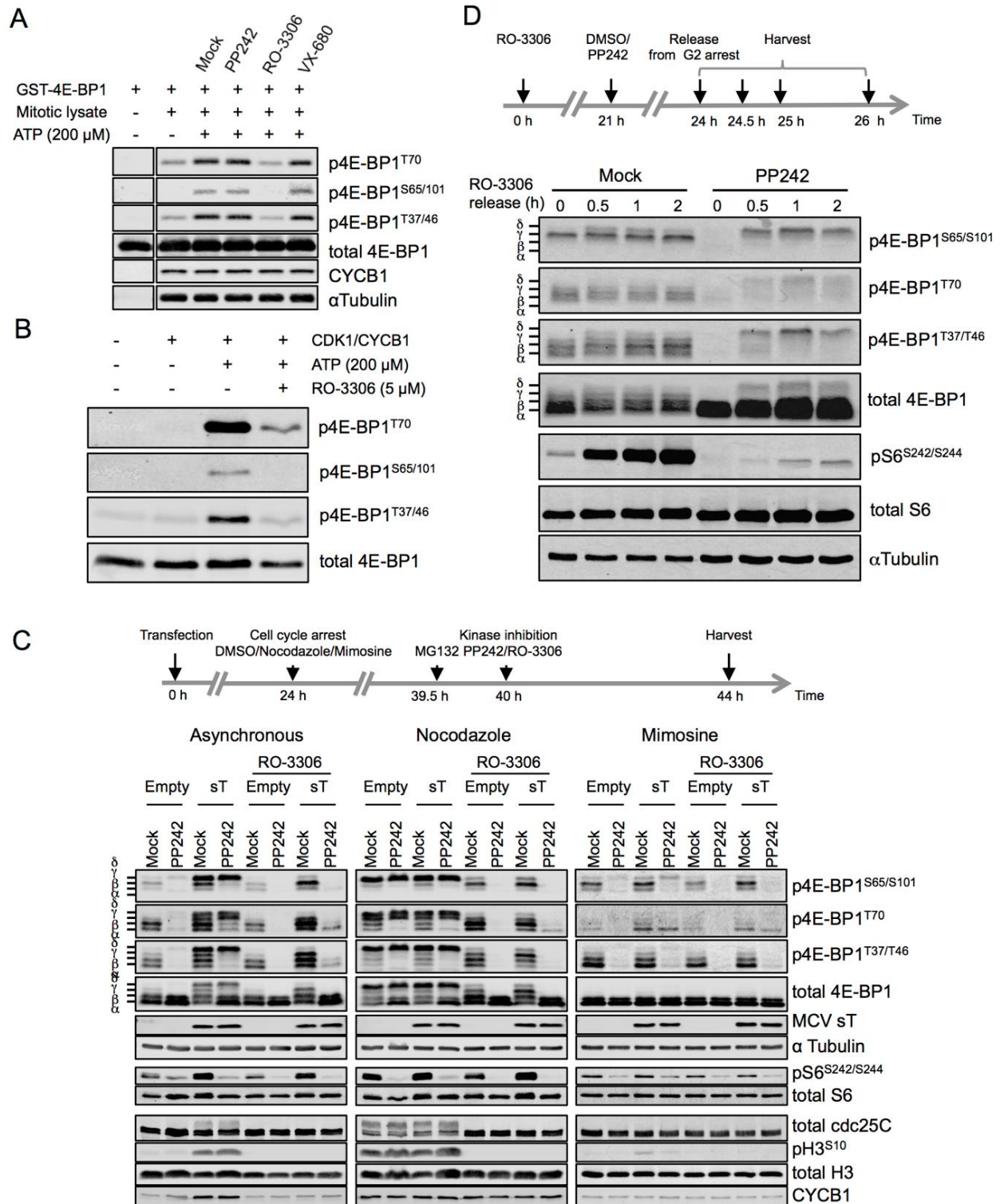


Figure 16. CDK1/CYCB1 phosphorylates 4E-BP1 during mitosis.

Figure 16 (continued)

(A) CDK1 inhibition in mitotic lysates reduces 4E-BP1 phosphorylation. Mitotic HeLa cell lysates (10 μ g) enriched by nocodazole arrest, were mixed with 0.2 μ g GST-4E-BP1, reacted for 30 min at 30 °C in the presence or absence of 5 μ M mTOR (PP242), CDK1 (RO-3306), or AURK (VX-680) kinase inhibitors and then immunoblotted with antibodies as shown. ATP-dependent 4E-BP1 phosphorylation was sensitive to CDK1 inhibitor but resistant to mTOR and AURK inhibitors. Equal loading of total 4E-BP1, CYCB1, and α -tubulin is shown. Representative results are shown from three independent experiments. (B) Recombinant CDK1/CYCB1 kinase phosphorylates GST-4E-BP1 at the known regulatory residues T37/T46, S65/S101, and T70. CDK1/CYCB1 (20 units) was mixed with bacterial expressed GST-4E-BP1 in kinase reaction buffer for 30 min at 30 °C, and immunoblotted with phospho-specific antibodies. ATP-dependent 4E-BP1 phosphorylation by CDK1/CYCB1 occurred at phospho-specific sites and was sensitive to the CDK1 active site inhibitor RO-3306. Representative results shown from two independent experiments. (C) δ -4E-BP1 is induced during mitosis and inhibited by a CDK1 inhibitor. 293 cells were transfected with empty vector or MCV sT, and arrested for 20 h with DMSO (asynchronous), nocodazole (prometaphase), and mimosine (late G1). Cells treated were treated at 16 h with kinase inhibitors (5 μ M PP242 or 10 μ M RO-3306 + 10 μ M MG132) as indicated. MCV sT induces δ -4E-BP1 in asynchronous cells sensitive to RO-3306 but not PP242. Nocodazole-arrest induces similarly RO-3306 sensitive and PP242 resistant δ -4E-BP1 even in the absence of sT, whereas δ -4E-BP1 is only weakly induced by sT in mimosine-arrested cells. Markers for mitosis (pH3^{S10} , CYCB1), a CDK1 substrate (*cdc25C*), and an mTORC1 downstream substrate ($\text{pS6}^{\text{S242/S244}}$) showed active drug treatments. Representative results are shown from two independent experiments. (D) δ -4E-BP1 phosphorylation during mitosis occurs in the absence of active mTOR. U2OS cells were arrested at G2/M boundary with 10 μ M RO-3306 for 24 h, released by washing and harvested at the time points shown. Cells were treated for 3 h pre-release with DMSO or 5 μ M PP242. In the absence of mTOR inhibition, no δ -4E-BP1 is found at 0 h but accumulates, together with β and γ isoforms, during mitotic transit. During PP242 inhibition, δ -4E-BP1 still accumulates during mitosis but lower molecular mass (β and γ) isoforms are reduced. Results shown from a single experiment.

Evidence that CDK1 is responsible for δ -4E-BP1 mitotic phosphorylation was also obtained by treatment of nocodazole-arrested HeLa cells with the CDK1 inhibitor RO-3306 (**Figure 17A**). δ -4E-BP1 hyperphosphorylation could not be fully restored by RO-3306/MG132 co-treatment. A technical issue in using mitotic kinase inhibitors to assess 4E-BP1 phosphorylation is the occurrence of mitotic slippage, a side effect of kinase inhibition concurrently causing enforced exit from mitosis with general loss of mitotic kinase activities (345, 348). Mitotic slippage can be prevented by simultaneous inhibition of APC/C-mediated protein degradation with the proteasome inhibitor MG132, which in effect “freezes” the mitotic phenotype. Like RO-3306, treatment of nocodazole-arrested HeLa cells with the AURK inhibitor VX-680 also eliminated δ -4E-BP1 phosphorylation (**Figure 17B**). Unlike RO-3306, however, this was completely reversed by co-treatment with VX-680/MG132, suggesting that AURK inhibition effects on 4E-BP1 phosphorylation are due to mitotic slippage. Extensive in vitro phosphorylation studies also failed to reveal evidence for direct 4E-BP1 phosphorylation by purified AURKB (pers. comm., SMA Lens and RCC Hengeveld, UMC-Utrecht). To confirm direct 4E-BP1 phosphorylation by CDK1/CYCB1, we generated an in vitro phosphorylation reaction using purified CDK1/CYCB1 and GST-4E-BP1 (**Figure 16B**). CDK1 phosphorylation of 4E-BP1 was ATP-dependent and inhibitable by RO-3306. CDK1 phosphorylation occurred at the previously-described T70 residue (207) as well as at authentic 4E-BP1 phosphorylation sites, including T37/T46, S65/S101 that are known to regulate 4E-BP1 binding to eIF4E.

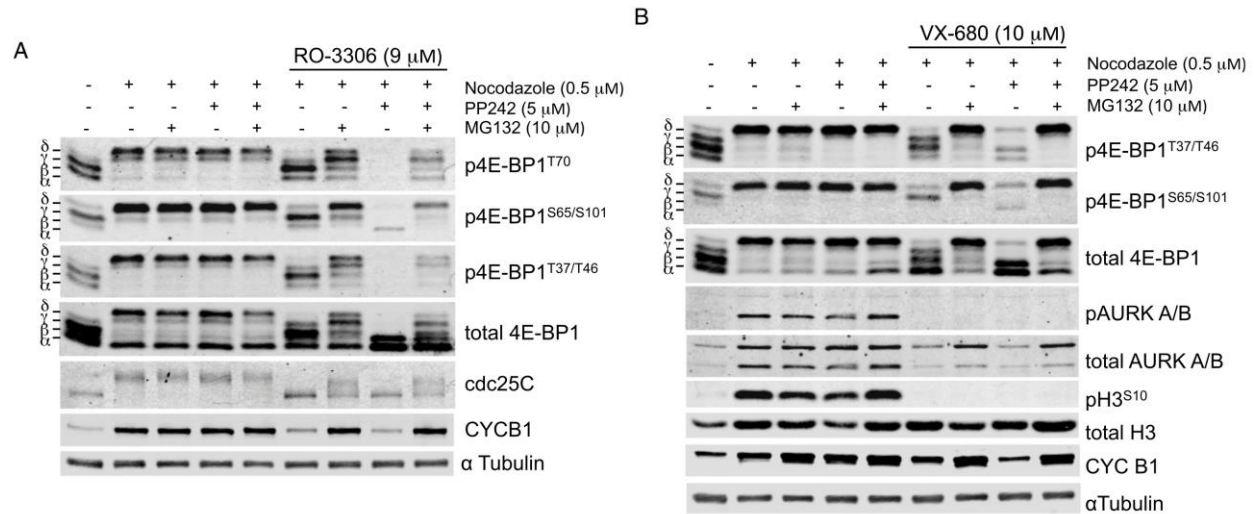


Figure 17. Mitotic slippage with mitotic kinase inhibition.

(A) CDK1 inhibition during nocodazole/MG132 treatment fails to fully restore δ -4E-BP1 hyperphosphorylation. Notably, residual 4E-BP1 phosphorylation during RO-3306 treatment is further reduced by PP242 treatment suggesting that mTOR phosphorylation may partially restore 4E-BP1 phosphorylation under conditions of CDK1 inhibition. Cdc25C is a direct phosphorylation target for CDK1. (B) The same experiment as in (A) was repeated using the pan-AURK inhibitor VX-680. Treatment with VX-680 reduces 4E-BP1 hyperphosphorylation in nocodazole-arrested HeLa cells by inducing mitotic exit. When HeLa cells were arrested with nocodazole (0.5 μ M) for 16 h and treated with the proteasome inhibitor MG132 (10 μ M) to prevent APC/C-mediated mitotic exit, VX-680 no longer prevents 4E-BP1 hyperphosphorylation but does inhibit AURKB-mediated phosphorylation of H3^{S10}.

Mitotic δ -4E-BP1 phosphorylation was also examined in nocodazole-arrested 293 cells in the presence of CDK1 and mTOR inhibitors (**Figure 16C**). MG132 was added to nocodazole-arrested cells 30 min before RO-3306 treatment to prevent CDK1 inhibition-induced mitotic slippage (348). In this experiment, pH3^{S10+} mitotic cells comprised ~0.9% of the total asynchronous (no cell cycle arrest) cell population (**Figure 16C**, left panel and **Figure 13**). MCV sT expression promotes formation of PP242-resistant δ -4E-BP1 that is lost after treatment with RO-3306. Notably, S6^{S242/244} phosphorylation, a known phosphorylation mark for mTORC1 kinase activity (349, 350),

is nearly ablated by PP242 but not by RO-3306. These results are consistent with sT induction of δ -4E-BP1 through CDK1 rather than mTOR kinase activity.

Distinctive 4E-BP1 phosphorylation patterns were seen during nocodazole (prometaphase) and mimosine (late G1) cell cycle arrest (**Figure 16C**). During nocodazole arrest, the δ -4E-BP1 isoforms became prominent even in the absence of MCV sT expression. In contrast, δ -4E-BP1 isoforms were nearly absent under all conditions for cells arrested in G1 by mimosine. Whereas δ -4E-BP1 was resistant to mTOR inhibition, CDK1 inhibition during nocodazole mitotic arrest ablated δ -4E-BP1. These results were confirmed in HeLa cells treated with nocodazole and kinase inhibitors (**Figure 17**).

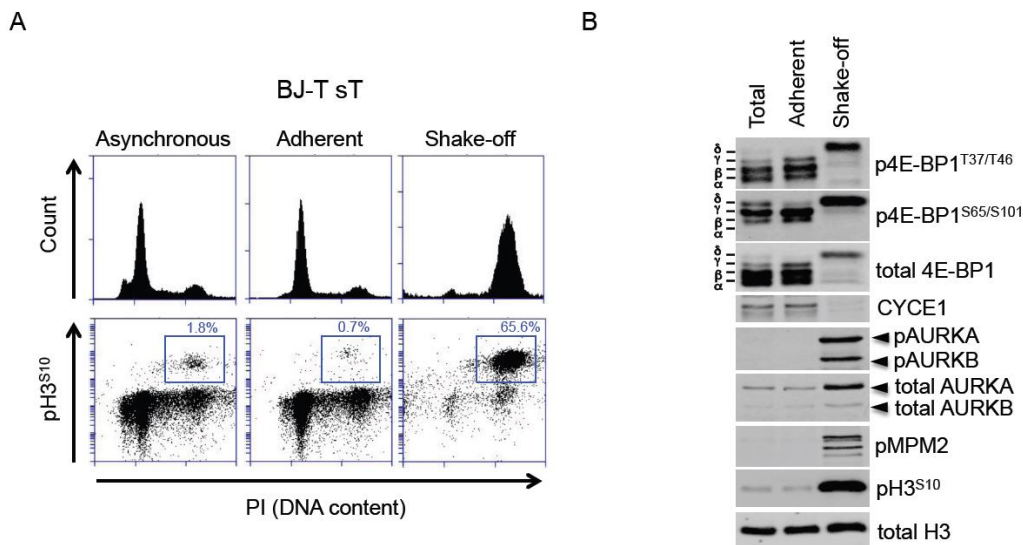


Figure 18. δ -4E-BP1 phospho-isoform expression in sT-expressing mitotic cells.

(A) BJ-T cells transduced with MCV sT can be enriched for mitotic and non-mitotic cell populations by mechanical shake-off. Non-adherent cells are enriched for pH3^{S10} positivity from 1.8% to 66% after shake-off, while remaining pH3^{S10} positivity was reduced to less than 1% for adherent cells. (B) Immunoblotting for δ -4E-BP1 reveals that δ -4E-BP1 is present only in the mitotic fraction, confirmed by mitotic markers pAURKA, pAURKB, pH3^{S10}, and pMPM2. Adherent cells, positive for CYCE1, are negative for δ -4E-BP1. Representative result is shown of three independent experiments.

To confirm these findings in the absence of chemical inhibitors, we used mechanical shake-off to isolate mitotic cells from sT-expressing BJ-T cells (**Figure 18**). This maneuver enriched the mitotic cell fraction from ~2% to ~66% as determined by flow cytometry with propidium iodide (PI) and pH3^{S10} staining (**Figure 18A**). Shake-off cells exclusively expressed the δ isoform whereas adherent cells expressed only α , β , and γ isoforms of 4E-BP1 (**Figure 18B**). In vitro lambda phosphatase treatment of sT-expressing and nocodazole-arrested 293 cell lysates showed that the high molecular mass 4E-BP1 isoforms, including the α , β , γ , and δ isoforms, are formed as a result of phosphorylation rather than another type of post-translational modification (**Figure 19**).

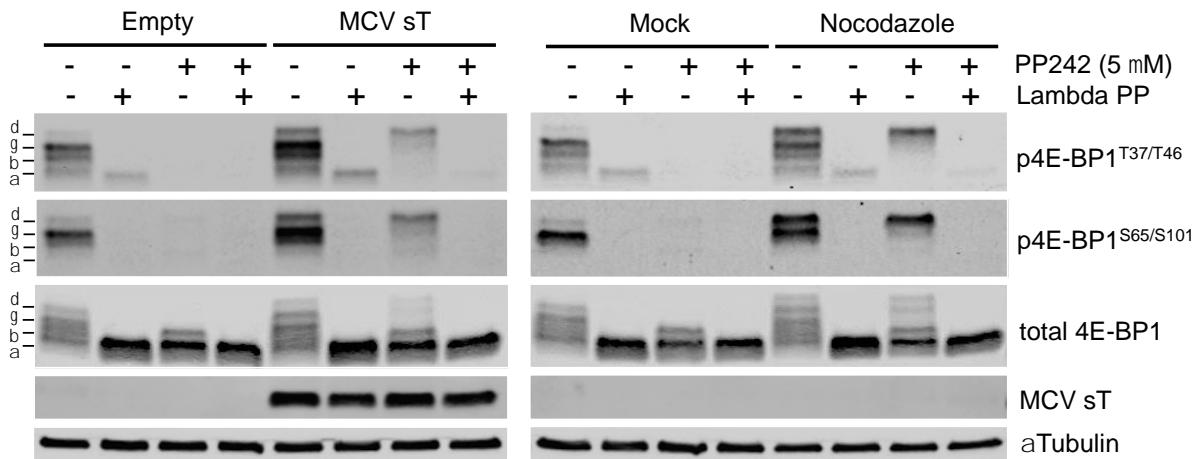


Figure 19. 4E-BP1 β , γ , and δ isoforms are completely lost after lambda phosphatase treatment.

Although PP242-inhibitable mTOR kinase activity contributes to mitotic 4E-BP1 phosphorylation, particularly for lower molecular mass α and β forms (**Figure 16C**), mTOR may be dispensable for mitotic 4E-BP1 hyperphosphorylation under some conditions. U2OS cells were arrested at the G2/M boundary for 24 h using 10 μ M RO-3306 (345, 351) (**Figure 16D**). After RO-3306 removal, cells progressed through mitosis

with most exiting mitosis 3 h after RO-3306 release. PP242 pre-treatment markedly reduced pS6^{S242/244} but not δ -4E-BP1, consistent with mTOR-independent phosphorylation of 4E-BP1 during mitosis. Similar results were seen with HeLa cells (data not shown) while 293 cells failed to arrest in G2 with RO-3306 and could not be examined.

2.3.4 δ 4E-BP1 is induced in mitosis during normal cell cycling.

Nocodazole-arrest experiments suggest that δ -4E-BP1 accumulates during mitosis even in the absence of MCV sT expression. To confirm this in the absence of drug treatment, 293 cells were synchronized by double-thymidine block and release, harvested at sequential time points and immunostained for pH3^{S10} and p4E-BP1^{T37/T46} (**Figure 20A**). For each time point after release, cells were pre-treated with PP242 or DMSO vehicle control 1 h prior to harvesting.

Flow cytometry showed peak pH3^{S10+} mitotic entry occurring reproducibly at 10 h, which began to diminish by 12 h after release (**Figure 20A** and **Figure 21**). This same pattern occurred with PP242 pre-treatment, although mitotic entry was more abundant at 8 h post-release. Unexpectedly, pH3^{S10+} mitotic 293 cells formed an orthogonal population with the highest per cell saturation levels of p4E-BP1^{T37/T46} compared to any other stage of the cell cycle. PP242 pre-treatment reduced p4E-BP1^{T37/T46+} staining for interphase cells at 2-8 h (note leftward shift for p4E-BP1^{T37/T46+} staining among pH3^{S10-} cells) consistent with mTOR regulation of 4E-BP1. At peak mitotic entry (8-10 h post release), however, pH3^{S10+} cells were resistant to loss of p4E-BP1^{T37/T46+} staining with PP242 treatment.

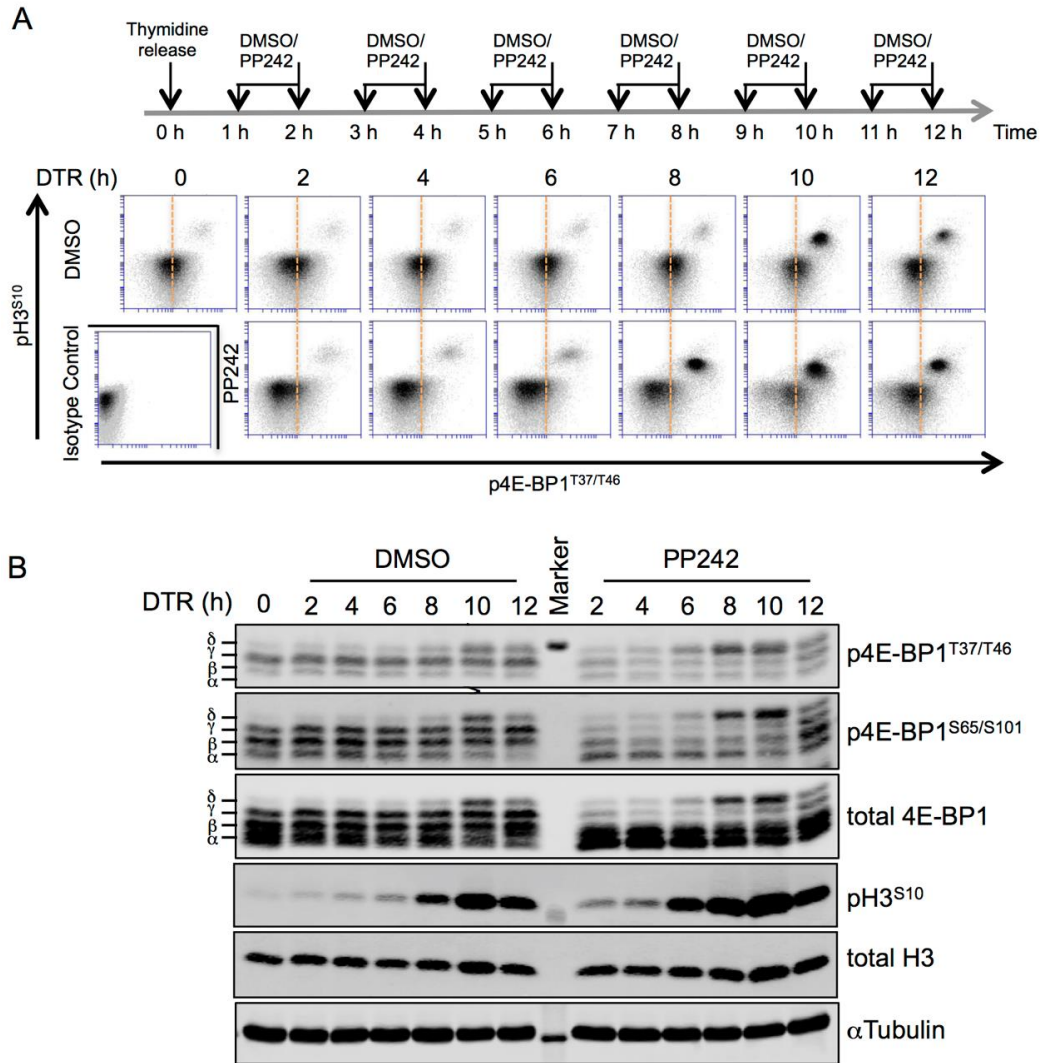


Figure 20. 4E-BP1 is hyperphosphorylated to the δ isoform during mitosis.

(A) $\text{pH3}^{\text{S10+}}$ mitotic 293 cells have higher levels of $\text{p4E-BP1}^{\text{T37/T46+}}$ saturation than cells in other portions of the cell cycle. Dual flow cytometry staining for pH3^{S10} and $\text{p4E-BP1}^{\text{T37/T46}}$ was performed on 293 cells synchronized by double-thymidine block and release, which show peak mitotic entry at 10 h post-release. Vertical bar represents the centroid for $\text{p4E-BP1}^{\text{T37/T46+}}$ fluorescence staining at time 0 h. To determine if 4E-BP1 phosphorylation depends on mTOR activity, cells were also treated 1 h prior to harvesting with 5 μM PP242. Mitotic cells formed an orthogonal $\text{pH3}^{\text{S10+}}/\text{p4E-BP1}^{\text{T37/T46+}}$ population having high levels of inactivated (phosphorylated) 4E-BP1 that were not dependent on mTOR activity. In contrast, interphase $\text{pH3}^{\text{S10-}}$ cells were largely mTOR-inhibition sensitive. PP242 treatment increases mitotic entry at 8 h post-release. (B) PP242-resistant δ -4E-BP1 is formed during peak mitotic entry. Protein lysates were collected from cells in (A) and immunoblotted for phospho-4E-BP1 and phospho- H3^{S10} . Representative results are shown from three independent experiments.

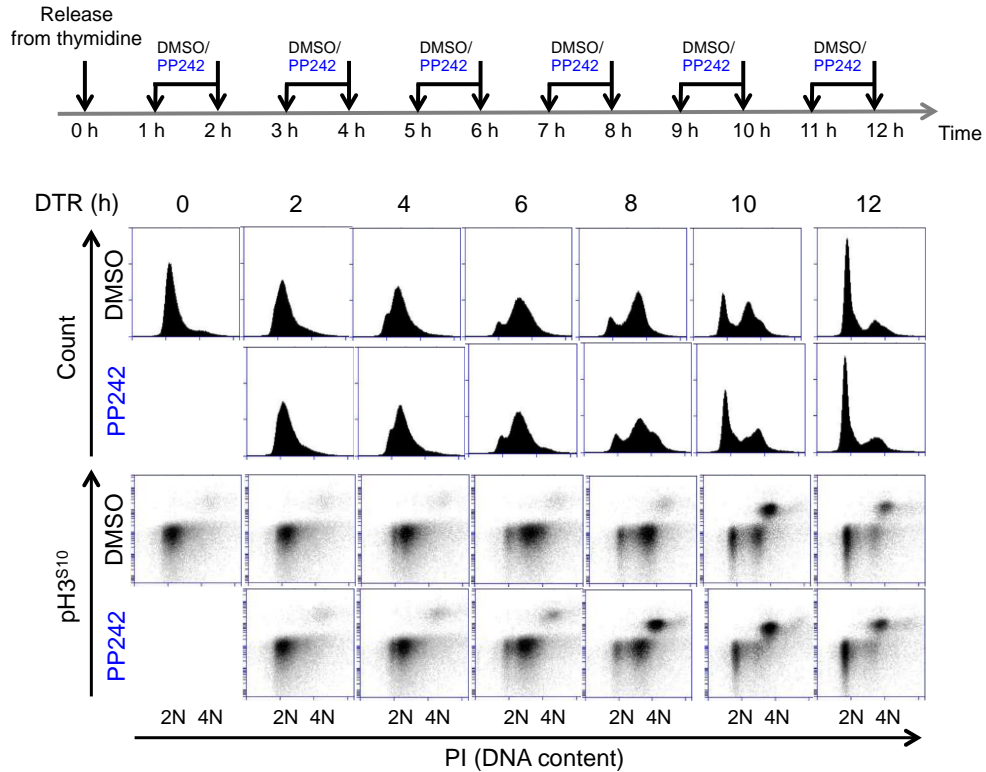


Figure 21. Flow cytometry, with PI and phospho-H3^{S10} staining, of 293 cells synchronized by double-thymidine release.

Immunoblots performed on these same cell fractions at each time point (**Figure 20B**) showed prominent α - γ 4E-BP1 phosphorylation at early time points (0-6 h), which was sensitive to mTOR inhibition. The δ isoform emerged 8-12 h after release, corresponding to maximum pH3^{S10+} and p4E-BP1^{T37/T46+} staining, and was resistant to PP242 inhibition. Similar results, but with a less abundant orthogonal pH3^{S10+}/p4E-BP1^{T37/T46+} cell population, were seen in U2OS cells (**Figure 22**).

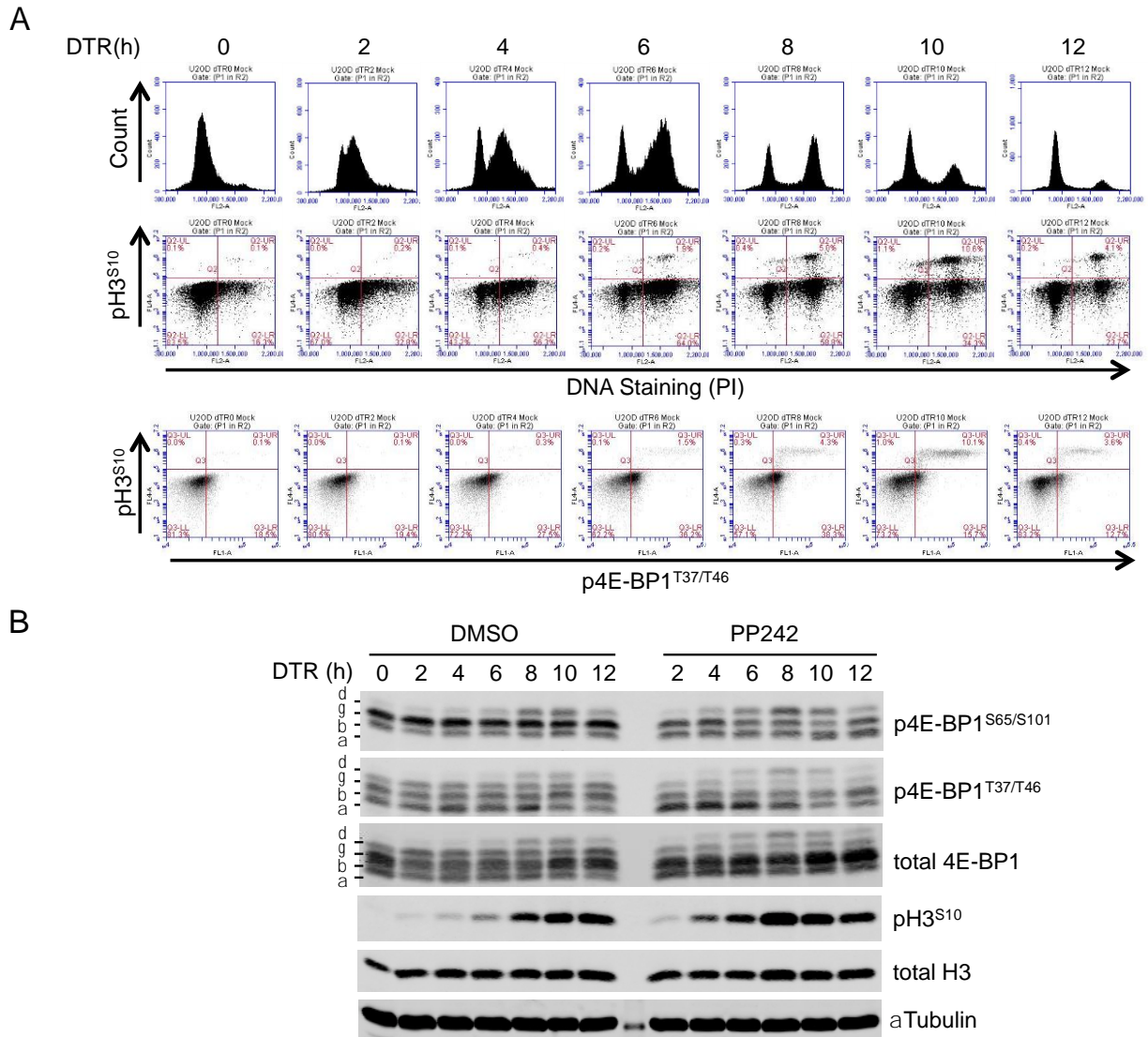


Figure 22. δ -4E-BP1 induction during mitosis in synchronized U2OS cells.

(A) Flow cytometry, with PI and phospho-H3^{S10} staining, of U2OS cells synchronized by double-thymidine release indicates maximum mitotic entry 10 h post-release, in the presence and absence of mTOR inhibition by PP242. Dual phospho-H3^{S10} and phospho-4E-BP1^{T37/T46} positive mitotic cells form an orthogonal cell population that peaks at 10 h and is reduced by 12 h post-release. (B) Protein lysates from (A) were immunoblotted for phospho-4E-BP1 and phospho-H3^{S10}. The δ -4E-BP1 isoform is apparent 6-12 hours after release, corresponding to pH3^{S10} positivity. This 4E-BP1 isoform is resistant to PP242 in U2OS cells.

2.3.5 CDK1 activates cap-dependent translation during mitosis.

According to the existing model for 4E-BP1-regulated protein synthesis, high levels of p4E-BP1^{T37/T46} are predicted to promote cap-dependent translation during pH3^{S10+} mitosis (30). We directly examined this by using cap-binding assays for mitosis-enriched and -depleted cells and by employing a new flow cytometry method designed to directly measure single-cell cap-dependent protein synthesis.

We performed m7GTP cap resin pulldown assays to assess the functional correlates of our flow cytometry and western blot findings. Highly-enriched mitotic BJ-T cells expressing MCV sT, isolated by shake-off (non-adherent), showed m7GTP cap binding to eIF4G that was unaffected by PP242 treatment (**Figure 23A**). In contrast, although interphase-enriched BJ-T cells (adherent), had comparable levels of eIF4G, eIF4G cap binding remained sensitive to PP242. Input 4E-BP1 protein from mitosis-enriched cells was almost exclusively in the δ -4E-BP1 isoform. This is consistent with mTOR-independent cap-binding during mitosis and mTOR-dependent cap-binding during interphase. Qualitatively similar results were found for HeLa cells using G2/M arrest enrichment and shake-off (**Figure 24**). For mitosis-enriched HeLa cells, modest but reproducible reduction in eIF4G-m7GTP cap association was present with RO-3306 treatment alone but not PP242 treatment alone. Combined RO-3306 and PP242 treatment nearly eliminated eIF4G association to m7GTP. These results were confirmed by metabolic labeling using the Click-IT methionine analog L-azidohomoalanine (AHA) to measure nascent protein synthesis (**Figure 23B**). In this assay, cells were incubated with AHA for 90 min (352), in the absence or presence of PP242, in methionine-depleted medium, and then subjected to mitotic shake-off. Newly synthesized protein

was then labeled with Alexa Fluor 488-alkyne by the copper(I)-catalyzed azide-alkyne [3 + 2] cycloaddition (Click-iT) reaction (353)) and measured by flow cytometry. Co-staining for pH3^{S10} allowed segregation of individual cells into “mitotic” (pH3^{S10+}) and “interphase” (pH3^{S10-}) populations. Up to 74% of DMSO-treated mitotic cells were AHA positive in comparison to 91% of DMSO-treated interphase cells with AHA positivity. PP242 treatment reduced new protein synthesis for pH3^{S10-} interphase BJ-T cells but had no effect on protein synthesis for pH3^{S10+} mitotic BJ-T cells (**Figure 23B**). Similar analyses using double thymidine block and release synchronization of 293 cells, however, revealed that PP242 reduced new protein synthesis for both mitotic and interphase cells (**Figure 25**), suggesting that PP242 resistance may be cell line specific.

We next generated capped, polyadenylated luciferase reporter mRNA using T7 polymerase (354, 355) and performed in vitro translation in commercial rabbit reticulocyte lysates to measure cap-dependent translation (**Figure 23C**). Addition of 4E1RCat (356), a cap-dependent translation inhibitor that prevents eIF4F formation, virtually abolished translation. Addition of recombinant GST-4E-BP1 reduced cap-dependent translation in the reticulocyte lysates to ~20% of buffer control (**Figure 23C**). This inhibition was reduced to 45% of buffer control when GST-4E-BP1 was phosphorylated (p4E-BP1) by a CDK1/CYCB1 kinase reaction. This reversal of inhibition was antagonized by the CDK1 inhibitor RO-3306.

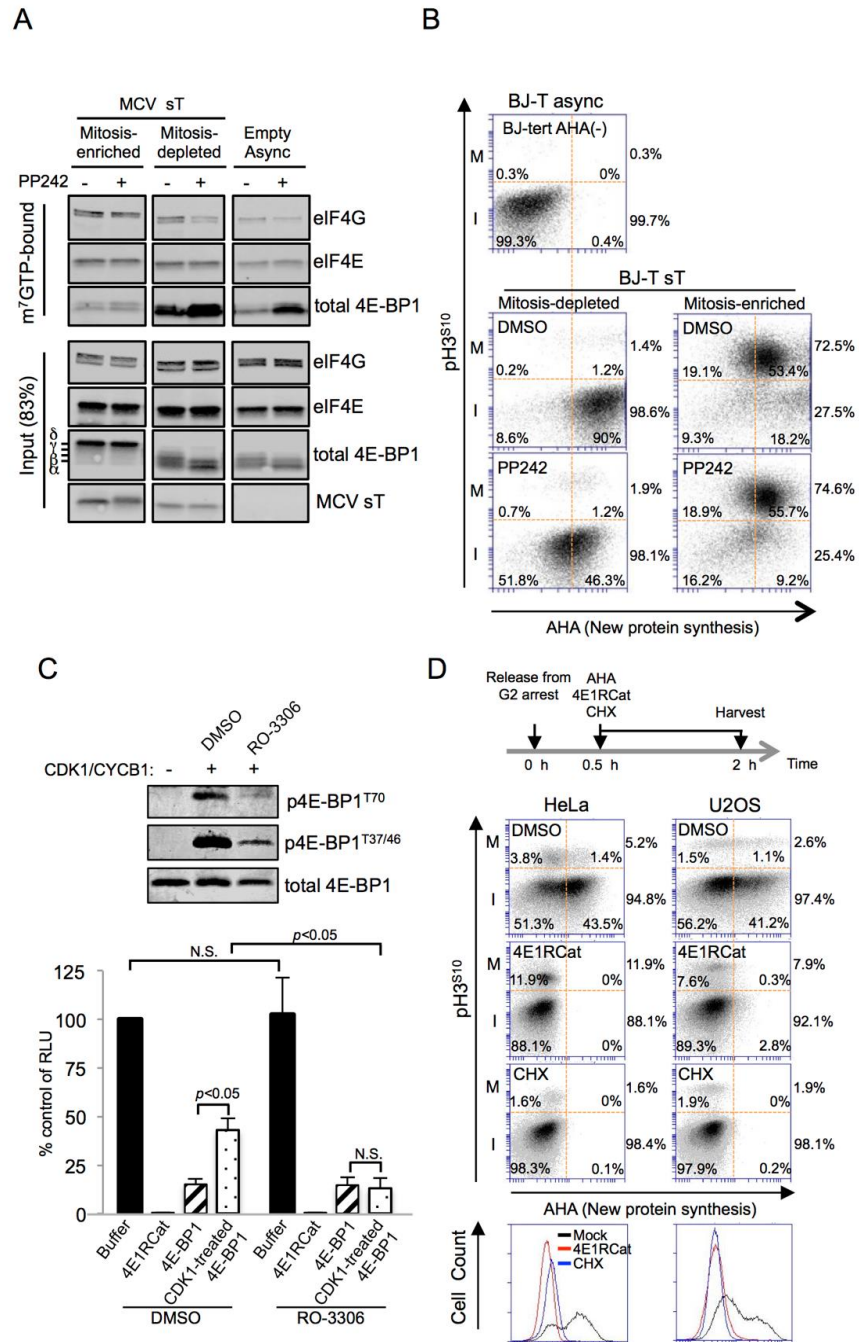


Figure 23. eIF4F formation on the m⁷GTP cap and direct measurement of cap-dependent protein translation during mitosis (M) and interphase (I).

(A) eIF4F formation on the m⁷GTP cap is PP242 independent for mitosis-enriched cells but PP242 sensitive for mitosis-depleted cells. BJ-T cells expressing MCV sT were harvested by mitotic shake-off to enrich for mitotic (non-adherent) and non-mitotic (adherent) populations, and compared to asynchronous empty vector BJ-T cells without shake-off. Lysates were bound to m⁷GTP-resin, precipitated and immunoblotted.

Figure 23 (continued)

Mitosis-enriched cell eIF4G-binding, as well as 4E-BP1-binding, to the eIF4E/cap complex was unaffected by mTOR inhibition. For mitosis-depleted cells, eIF4G-binding was reduced and 4E-BP1-binding was increased by mTOR inhibition. Representative results from two independent experiments are shown. (B) Nascent protein synthesis during mitosis is resistant to mTOR inhibition in BJ-T cells. BJ-T cells stably expressing sT were labeled with azido-homoalanine (AHA) for 45 min in methionine-depleted media, separated by mitotic shake-off as in (A), reacted with Click-iT Alexa Fluor 488 alkyne after permeabilization, and new protein synthesis measured by flow cytometry. Relative mitotic protein synthesis was determined by dividing percentage of pH3^{S10+}-AHA+ cells by percentage of total pH3^{S10+} cells. Likewise, interphase protein synthesis was determined by dividing percentage of pH3^{S10-}-AHA+ cells by percentage of total pH3^{S10-} cells. Approximately 91% of pH3^{S10-} adherent interphase cells showed AHA incorporation that was sensitive to mTOR inhibition. Only 74% of pH3^{S10+} positive mitotic cells were positive for AHA uptake but this new protein synthesis was resistant to PP242 treatment. Baseline fluorescence was determined in asynchronous BJ-T cells without AHA incubation. (C) In vitro capped mRNA translation is inhibited by 4E1RCat and activated by CDK1/CYCB1. Capped and polyadenylated luciferase mRNA was generated in a T7 polymerase reaction and used to generate luciferase protein in a rabbit reticulocyte lysate. 4E1RCat abolished luciferase translation while addition of GST-4E-BP1 reduced translation to 15% of buffer control (averages for three independent experiments with SEM shown). When GST-4E-BP1 was phosphorylated by CDK1/CYCB1 in kinase reaction buffer, translation increased to 43% of buffer control. This effect was eliminated by RO-3306 pre-treatment. Insert shows GST-4E-BP1 phosphorylation immunoblot. (D) Mitotic translation is primarily cap-dependent for HeLa and U2OS. HeLa or U2OS cells were synchronized for 24 h at the G2/M boundary, released by washing and incubated with the 25 μ M of AHA for 90 min in methionine-depleted media, and then harvested 2 h after release. Harvested cells were permeabilized and reacted with Alexa Fluor-488 alkyne to measure AHA incorporation into protein. DMSO vehicle control, CHX (100 μ g/ml) or 4E1RCat (50 μ M) were added together with AHA 30 min after release. M: mitotic pH3^{S10+} cells; I: interphase pH3^{S10-} cells. Vertical bar represents maximum AHA incorporation after CHX translation inhibition. Fewer mitotic (26%) than interphase (42%) HeLa cells were positive for new protein synthesis but all cells were sensitive to 4E1RCat inhibition of cap-dependent translation. For U2OS, cell numbers positive for total mitotic and interphase translation were identical (42%) and cap-dependent translation represented 73% and 85% of mitotic and interphase translation, respectively. Bottom panel shows 4N gated AHA positivity for treated cells shows that 4E1RCat inhibition (cap-dependent) is similar to CHX (total) translation inhibition. Representative results are shown for one of three repeated experiments.

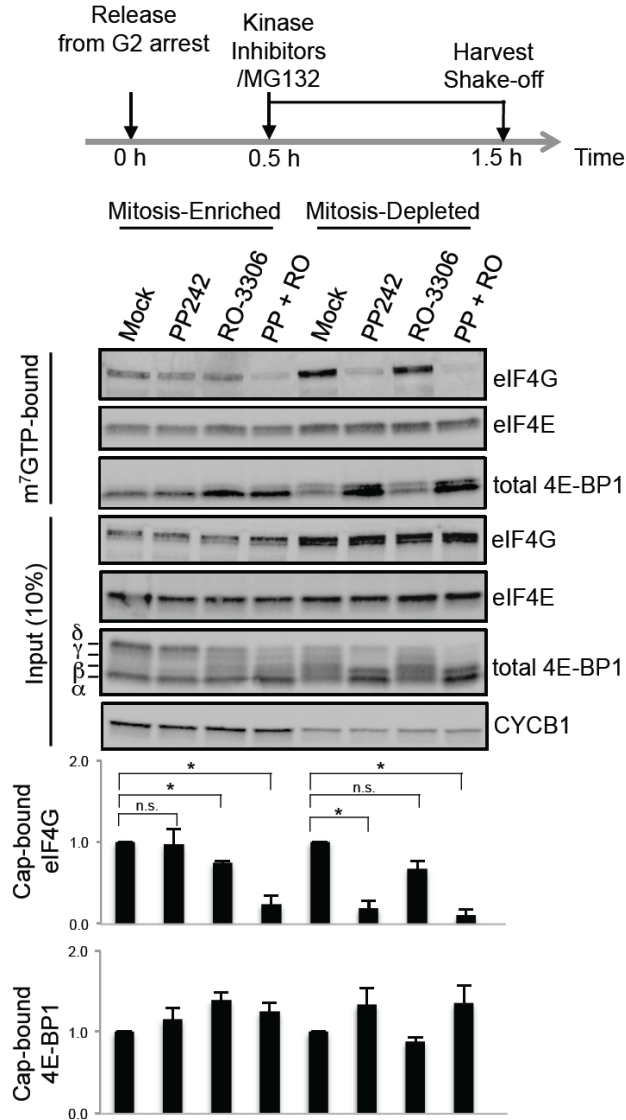


Figure 24. eIF4F formation on the m7GTP cap is inhibited by CDK1 inhibition in mitosis-enriched HeLa cells.

HeLa cells were enriched or depleted for mitosis by G2/M boundary arrest synchronization and shake-off. For mitosis-enriched cells, 4E-BP1 binding to the m7GTP resin was increased by RO-3306 treatment alone. RO-3306 but not PP242 significantly inhibits eIF4G pull-down by m7GTP resin in HeLa cells. Near-complete inhibition, however, was present with combined PP242 and RO-3306 (PP+RO), suggesting cooperativity for mTOR and CDK1 in mitosis-enriched cells. For mitosis-depleted HeLa, PP242 alone inhibits eIF4G binding and activates 4E-BP1 binding to the m7GTP resin. Error bars are SEM, asterisks denote significant comparisons by one-sided t test with $p < 0.05$ while n.s. denotes non-significant change. Quantitative LICOR immunoblotting shown is representative for one of three independent experiments used to generate average and SEM values for cap-binding.

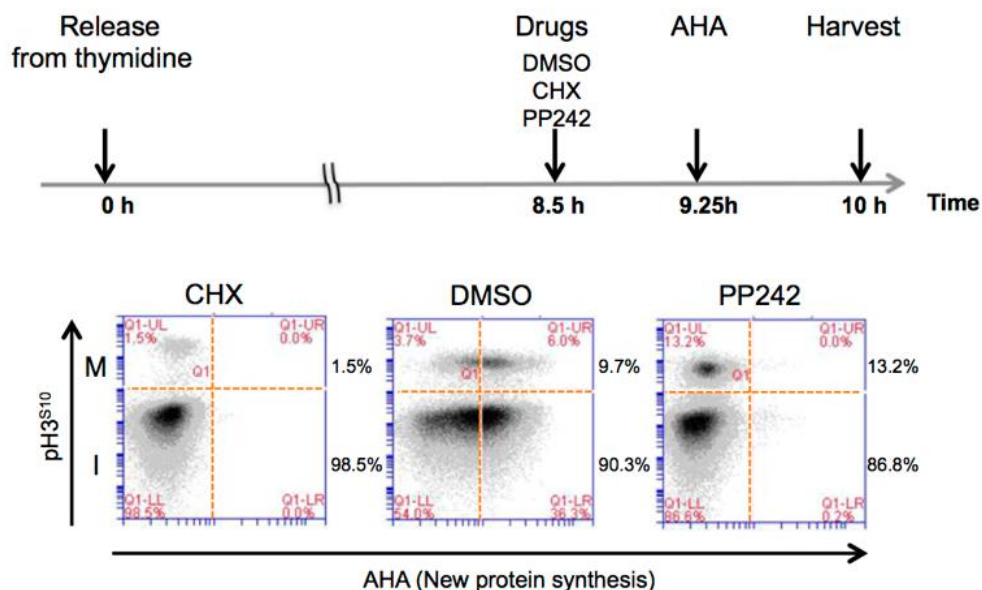


Figure 25. The 293 cell-nascent protein synthesis is sensitive to PP242.

Double-thymidine release was performed for 293 cells. Drug treatment (PP242 at 5 μ M and CHX at 100 μ g/mL) was given at 8.5 h and AHA (25 μ M) at 9 h, 15 min post-release, and then cells were harvested at 10 h. The protein synthesis inhibitor CHX served as a negative control for AHA incorporation, and pH3^{S10} was used to measure mitotic activity. New protein synthesis is similar for both phospho-pH3^{S10}-positive and phospho-pH3^{S10}-negative mock-treated cells, indicating that protein synthesis is not inhibited during mitosis for 293 cells. Unlike BJ-T, PP242 reduced AHA incorporation for both mitotic and non-mitotic populations.

Measurement of cap-dependent protein synthesis during mitosis was directly determined for HeLa and U2OS cells after G2 release and synchronization using our AHA assay in cells treated with 4E1RCat (**Figure 23D**). Co-staining for pH3^{S10} allowed segregation of cells into mitotic (pH3^{S10}+) and interphase (pH3^{S10}-) populations. Nonspecific AHA incorporation was determined using the ribosome translation elongation inhibitor CHX (**Figure 23D**, vertical lines) and new protein synthesis was reflected by AHA fluorescence above this baseline.

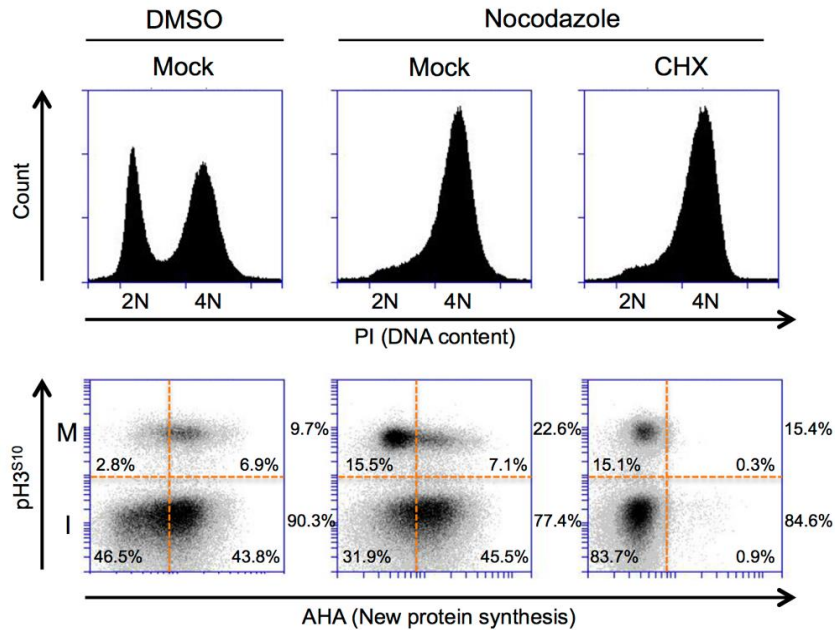


Figure 26. Nocodazole inhibits mitotic protein translation.

AHA incorporation is present for both mitotic (pH3^{S10+}) and interphase (pH3^{S10-}) 293 cells but is markedly reduced when pH3^{S10+} cells are treated with 0.5 μ M nocodazole. No significant change in AHA incorporation was noted for pH3^{S10-} cells with nocodazole treatment. Dotted lines represent threshold between pH3^{S10+} and pH3^{S10-} cells, with active or inhibited new protein synthesis. M: mitotic pH3^{S10+} cells; I: interphase pH3^{S10-} cells.

Like BJ-T cells, fewer (27%) mitotic HeLa cells were positive for new protein synthesis compared to interphase (46%) HeLa cells (**Figure 23D**). In contrast, percentages of mitotic and interphase U2OS cells with new protein synthesis were identical (42% of mitotic and interphase cells). For both cell lines, however, nearly all new protein synthesis in both mitosis and interphase was cap-dependent and sensitive to 4E1RCat treatment. Preliminary analyses revealed that MG132 treatment nonspecifically inhibited protein synthesis as previously reported (357), preventing us from accurately measuring the effects of CDK1 inhibition on mitotic translation under conditions that inhibit mitotic slippage. Using direct AHA uptake, however, we could confirm that nocodazole treatment inhibits mitotic protein synthesis (**Figure 26**).

2.4 DISCUSSION

Tumor viruses have been central to cell biology because their oncogenes allow interrogation of specific cell proliferation and survival pathways. Among many critical findings, viral oncoproteins have been essential to the discovery of cellular oncogenes (358) and the tumor suppressor p53 (287, 311, 359); the characterization of the G1/S checkpoint (312) and the Akt-mTOR pathway (360); and identification of common innate immune and tumor suppressor signaling networks (361). MCV sT, an oncoprotein for MCC, induces mTOR-resistant 4E-BP1 hyperphosphorylation and cell transformation (170), which led us to investigate mTOR-independent 4E-BP1 signaling and cap-dependent translation in mitosis.

In addition to targeting Fbw7 (338), MCV sT inhibits APC/C E3 ligases, as well as other specific E3 ligases (unpublished), and induces mitogenesis in sT-expressing cells. One consequence of this is increased mitotic CDK1/CYCB1 activity that is responsible for 4E-BP1 phosphorylation and δ -4E-BP1 formation. Caution is appropriate in interpreting our data since mitotic kinase inhibition can cause mitotic slippage and exit from the mitotic phenotype. Considerable effort by our group was devoted to evaluating AURKA and AURKB as potential 4E-BP1 mitotic kinases since AURK inhibitors (e.g. VX-680, MK-5108 and AZD-1152) also reduce 4E-BP1 hyperphosphorylation during mitosis. This was reversible, however, by co-treatment with MG132 to prevent APC/C-mediated mitotic egress and we have no evidence that AURKs are directly responsible for 4E-BP1 phosphorylation. In contrast, there is considerable evidence from this study and others (207, 208) to indicate that CDK1/CYCB1 is a bona fide kinase for 4E-BP1.

This study suggests an alternative pathway for CDK1/CYCB1 regulated cap-dependent translation during mitosis (**Figure 27**). We find that mitotic 4E-BP1 is highly phosphorylated at the priming residues T37 and T46 in pH3^{S10+} cells, which runs counter to what would be predicted if cap-dependent translation is reduced during mitosis through an mTOR-related mechanism. The high molecular mass δ -4E-BP1 isoform is specific to mitosis and our data indicates that this results from CDK1-mediated phosphorylation. While δ -4E-BP1 can form under mitotic conditions in which mTOR is inhibited, it seems likely that mTOR cooperates with CDK1/CYCB1 to generate the mitotic δ -4E-BP1 by phosphorylating lower molecular mass α , β , and γ isoforms that may be precursors to the δ -4E-BP1 isoform. Another limitation to our study is that we measure only 4E-BP1 phosphorylation but not δ -4E-BP1 dephosphorylation or turnover. These are likely to affect steady-state p4E-BP1 levels as well.

Our findings contrast with studies suggesting that loss of mTOR activity leads to inhibition of mitotic eIF4G cap-association and cap-dependent translation. We see that cap-dependent protein translation is sustained during mitosis using a pulse flow cytometry approach. Pharmacological (4E1RCat) cap-dependent translation inhibitor used on three cell lines under two different mitotic-enrichment conditions provide evidence that this effect is generalizable. To our knowledge, our AHA incorporation assays are the first time that cap-dependent translation has been directly measured in mitotic and interphase cells. Like [35S]-methionine incorporation studies, AHA incorporation measurements required incubation of cells in low methionine media. While

most mitotic translation is cap-dependent in all of the cell lines tested, differences in relative mitotic and interphase translation were present between cell lines.

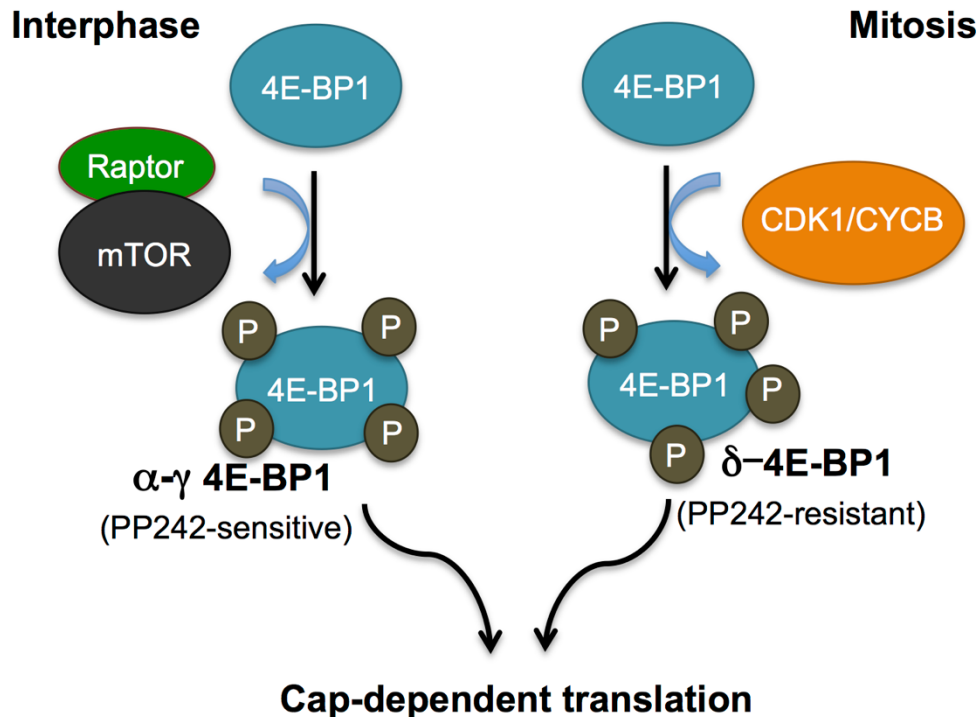


Figure 27. Model for cell cycle dependent 4E-BP1 regulation of cap-dependent mRNA translation.

Interphase 4E-BP1 is inhibited by mTORC1 kinase, whereas CDK1/CYCB1 is primarily responsible for δ -4E-BP1 inactivation during mitosis.

We suspect that technical issues, that have only recently been resolved, explain differences between our studies and those of others. Measurement of mitotic protein translation (both cap-dependent and independent) has relied on separation of mitotic and interphase cells in bulk culture, often using nocodazole-induced mitotic enrichment. We confirm that nocodazole inhibits mitotic translation for synchronized 293 cells. This has been ascribed by Coldwell et al. (243) to inhibitory phosphorylation of eIF2 and eIF4GII by nocodazole downstream to 4E-BP1 regulation. This is consistent with our

findings that nocodazole both promotes δ -4E-BP1 and inhibits mitotic translation. We have not tested other mitotic-arrest compounds (e.g., paclitaxel) to determine if they have similar limitations. A second technical challenge is that mitotic cells represent a small fraction of the total cell population. Contamination with interphase cells is nearly inevitable in mitotic enrichment protocols and will dramatically alter conclusions such as the role of mTOR in regulating 4E-BP1 during mitosis. In our experience, flow cytometry can help to resolve this dilemma by directly measuring mitotic status (pH3^{S10} or pMPM2 status) in cells while simultaneously determining translation regulator status, such as p4E-BP1^{T37/T46}. Finally, newly-developed classes of cap-dependent translation inhibitors, such as 4E1RCat, now allow direct determination of cap-dependent translation. When used in combination with AHA incorporation, direct measurement of mitotic cap-dependent translation can be determined.

Both nocodazole and PP242 are nonetheless important inhibitors to measure 4E-BP1 phosphorylation and translation during mitosis. As indicated, nocodazole does not interfere with δ -4E-BP1 formation and is useful for accentuating mitotic regulation of 4E-BP1. mTOR regulates translation through ribosomal biosynthesis as well as direct phosphorylation of translation machinery components downstream from 4E-BP1, such as eIF4B (362) and eEF2 elongation factor (363). Further, eIF4B regulation by 14-3-3 σ may also play a role in later stages of mitotic protein translation and may be missed in our study of early mitosis (241). Thus, PP242 may affect mitotic translation by acting downstream to 4E-BP1. We also find evidence that in most cells mTOR typically acts in concert with CDK1/CYCB1 to promote mitotic cap-dependent translation.

Cap-dependent translation of preformed mRNAs provides rapid regulation of gene expression that may be required for rapid cellular responses, such as transit through mitosis. These changes generally cannot be accurately measured by standard mRNA expression techniques. Mounting evidence suggests that dysregulated cap-dependent translation from aberrant PI3K-Akt-mTOR and MEF-RAF-MEK-ERK signaling contributes to cancer cell transformation (223, 271). Regardless of the contribution of activated cap-dependent translation to cancer cell transformation, such as in MCV-positive MCC, our findings point towards the possibility that combined mTOR and CDK1/CYCB1 inhibition may prove useful for cancer treatment, particularly for mTOR-inhibitor resistant cancers.

3.0 MITOTIC PROTEIN KINASE CDK1 PHOSPHORYLATION OF MESSENGER RNA TRANSLATION REGULATOR 4E-BP1 SER83 MAY CONTRIBUTE TO CELL TRANSFORMATION

Work described in this chapter was published in the Proceedings of the Academy of
Sciences

Proc Natl Acad Sci U S A. 2016 Jul 26;113(30):8466-71

**with authors Celestino Velásquez, Erdong Cheng, Masahiro Shuda, Paula J.
Lee-Oesterreich, Lisa Pogge von Strandmann, Marina A. Gritsenko, Jon M.
Jacobs, Patrick S. Moore, and Yuan Chang**

Celestino Velásquez, Erdong Cheng, Masahiro Shuda, Paula J. Lee-Oesterreich, Lisa Pogge von Strandmann, Marina A. Gritsenko, and Jon M. Jacobs performed experiments and analyzed the data. Celestino Velásquez, Erdong Cheng, Masahiro Shuda, Jon M. Jacobs, Patrick S. Moore, and Yuan Chang designed experiments. Celestino Velásquez, Erdong Cheng, Masahiro Shuda, Jon M. Jacobs, Patrick S. Moore, and Yuan Chang wrote the manuscript.

This chapter demonstrates that 4E-BP1 hyperphosphorylation is a generalizable phenomenon in mitotic cells and describes the novel phosphorylation of 4E-BP1 Ser83 by the mitotic CDK1 kinase and its potential contribution to cell transformation. mTOR-directed 4E-BP1 phosphorylation promotes cap-dependent translation and tumorigenesis. During mitosis, CDK1 substitutes for mTOR and fully phosphorylates 4E-BP1 at canonical sites (T37, T46, S65, and T70) as well the non-canonical S83 site resulting in a mitosis-specific hyperphosphorylated δ isoform. Colocalization studies with a phospho-S83 specific antibody indicate that 4E-BP1 S83 phosphorylation accumulates at centrosomes during prophase, peaks at metaphase, and decreases through telophase. While S83 phosphorylation of 4E-BP1 does not affect general cap-dependent translation, expression of an alanine substitution mutant 4E-BP1.S83A partially reverses rodent cell transformation induced by Merkel cell polyomavirus (MCV) small T (sT) antigen viral oncoprotein. In contrast to inhibitory mTOR 4E-BP1 phosphorylation, these findings suggest that mitotic CDK1-directed phosphorylation of δ -4E-BP1 may yield a gain-of-function, distinct from translation regulation, that may be important in tumorigenesis and mitotic centrosome function.

3.1 INTRODUCTION

Eukaryotic cells synthesize proteins primarily through cap-dependent mRNA translation. This process is mediated by a complex of eukaryotic translation initiation factors, eIF4F, which assemble on the 7-methyl-guanosine cap of mRNA (3). eIF4E occupation of the 5' cap of mRNA results in the recruitment of eIF4F complex members—mainly eIF4G, eIF4A, and eIF3—which in turn attract the 40S ribosome and the rest of the translation machinery (3). A set of small binding proteins called eIF4E-binding proteins (4E-BPs)—4E-BP1, 4E-BP2, and 4E-BP3—inhibit cap-dependent translation by interacting with the cap-bound eIF4E (144). The best-characterized and predominant eIF4E binding protein is 4E-BP1, which has a molecular weight of 15 kDa and is expressed in most tissues (144). 4E-BP1 competes with the complex scaffold protein eIF4G for the same binding site on eIF4E and prevents eIF4F cap complex assembly and ribosome recruitment (144).

The PI3K-AKT pathway regulates the translation repressor function of 4E-BP1 by activating the mammalian target of rapamycin (mTOR) kinase (144). Stimulated by metabolic and growth-related signals, mTOR phosphorylates 4E-BP1 and decreases its affinity for eIF4E in favor of translation (143). Priming phosphorylations at Thr(T)37 and T46 are required for subsequent phosphorylations at T70 and Ser(S)65 (143). Double alanine substitutions of the critical T37 and T46 priming sites render a constitutively active protein that strongly binds eIF4E and is insensitive to mTOR inhibition (153). Three additional potential phosphorylation sites have been identified—S83, S101, and S112—whose regulation mechanisms remain unclear (154, 175, 176).

Accumulating evidence indicates that dysregulation of cap-dependent translation through 4E-BP1 inactivation contributes to malignant transformation (143, 144). Frequently activated in cancers, the PI3K-AKT-mTOR pathway leads to enhanced 4E-BP1 phosphorylation and, thus, diminished translation repression activity (159, 246, 340); and multiple reports have found expression of high levels of phosphorylated 4E-BP1 in tumors (143). Overexpression of eIF4E transforms cells by enhancing translation of oncogenic mRNA, which can be reversed by ectopic expression of a non-phosphorylatable 4E-BP1 priming site mutant (254, 257, 268). Resistance of various cancers to mTOR inhibitor treatment indicates that other pathways are implicated in 4E-BP1 inactivation (364). Several serine/threonine kinases have been shown to phosphorylate 4E-BP1, such as p38 MAPK, ERK, PIM2, ATM, CDK1, PLK1, LRRK2, GSK3 β , and CK1 ϵ (163, 207, 210, 211, 215, 217-219, 222). We recently demonstrated that CDK1 phosphorylates 4E-BP1 at canonical sites T37, T46, S65, and T70 during mitosis and generates a high molecular weight phospho-isoform called δ -4E-BP1, even in the absence of mTOR activity (209). Although we have observed active cap-dependent translation during mitosis, the function of hyperphosphorylated δ -4E-BP1 and its contribution to tumorigenesis remain unknown.

Here we identify a CDK1 phosphorylation site, S83, that is unique to mitotic δ -4E-BP1. 4E-BP1 S83 phosphorylation does not participate in regulation of general cap-dependent translation or eIF4F complex formation. Instead, S83-phosphorylated δ -4E-BP1 preferentially localizes to mitotic centrosomes and peaks during metaphase. When S83 is substituted with alanine, 4E-BP1.S83A, to prevent δ -4E-BP1 formation, the

mutant 4E-BP1 partially inhibits cell transformation induced by the viral oncoprotein
Merkel cell polyomavirus (MCV) small T (sT) antigen.

3.2 MATERIALS AND METHODS

3.2.1 Cell Culture and Transfection/Transduction

293, 293FT, HeLa, U2OS, U87, U251, and Rat-1 cells (ATCC) were maintained in DMEM (Corning Cellgro) supplemented with 10% FBS. HCT116 cells (ATCC) were maintained in McCoy's medium (Sigma) supplemented with 10% FBS. 293 and 293FT cells were transfected using Lipofectamine 2000 (Invitrogen) and harvested after 48 h. Rat-1 cells were transduced by lentiviral infection and harvested after 5-10 days.

3.2.2 Plasmids

FLAG-HA-HA tagged 4E-BP1 open reading frame was excised from pBabe HA-4E-BP1 (170) and cloned into pCMVtag2B vector to generate pCMVtag2B.HA-4EBP1. HA-4E-BP1 mutants (T37A/T46A, S83A, S83D, S83E, S65A/S101A, T70A, I15A/F114, and T37E/T46E/S65E/T70E) were generated from pCMVtag2B.HA-4EBP1 wild type construct by the QuikChange Lightning site-directed mutagenesis kit (Agilent Technologies). pLVX EF.puro was modified from pLVX-puro vector (Clontech) by replacing CMV promoter with elongation factor-1alpha (EF) promoter (170). Codon-optimized MCV sT and HA-4E-BP1 sequences were inserted into pLVX EF.puro using AfeI and SbfI sites. The primers used for each site-directed mutagenesis are listed on **Table 1**, and the plasmids constructs are listed on **Table 2**.

Table 1. Primers used for in vitro site-directed mutagenesis of HA-tagged 4E-BP1.

Primer name	Sequence (5' to 3')
4E-BP1 T37A for	GGGGACTACAGCACGGCACCCGGCGGC
4E-BP1 T37A rev	GCCGCCGGGTGCCGTGCTGTAGTCCCC
4E-BP1 T37D for	GGGGACTACAGCACGGACCCCGGCGGCACG
4E-BP1 T37D rev	CGTGCCGCCGGGTCCGTGCTGTAGTCCCC
4E-BP1 T37E for	GGGGACTACAGCACGGAACCCGGCGGCACG
4E-BP1 T37E rev	CGTGCCGCCGGGTCCGTGCTGTAGTCCCC
4E-BP1 T46A for	ACGCTCTTCAGCACCGCACCCGGGAGGT
4E-BP1 T46A rev	ACCTCCCGGTGCGGTGCTGAAGAGCGT
4E-BP1 T46D for	ACGCTCTTCAGCACCGACCCGGGAGGTACCAGG
4E-BP1 T46D rev	CCTGGTACCTCCCGGGTTCGGTGCTGAAGAGCGT
4E-BP1 T46E for	ACGCTCTTCAGCACCGAACCCGGGAGGTACCAGG
4E-BP1 T46E rev	CCTGGTACCTCCCGGGTTCGGTGCTGAAGAGCGT
4E-BP1 S65A for	GAGTGTCGGAACGCACCTGTGACCAAAACACCC
4E-BP1 S65A rev	GGGTGTTTTGGTCACAGGTGCGTTCGGACACTC
4E-BP1 S65D for	GAGTGTCGGAACGACCCTGTGACCAAAACACCC
4E-BP1 S65D rev	GGGTGTTTTGGTCACAGGGTCGTTCCGACACTC
4E-BP1 S65E for	GAGTGTCGGAACGAACCTGTGACCAAAACACCC
4E-BP1 S65E rev	GGGTGTTTTGGTCACAGGTTCGTTCCGACACTC
4E-BP1 T70A for	CCTGTGACCAAAGCACCCCAAGGG
4E-BP1 T70A rev	CCCTTGGGGGTGCTTTGGTCACAGG
4E-BP1 T70D for	CCTGTGACCAAAGACCCCAAGGGATCTGCCC
4E-BP1 T70D rev	GGGCAGATCCCTTGGGGGTCTTTGGTCACAGG
4E-BP1 T70E for	CCTGTGACCAAAGAACCCCAAGGGATCTGCCC
4E-BP1 T70E rev	GGGCAGATCCCTTGGGGGTCTTTGGTCACAGG
4E-BP1 S83A for	GGGGTCACCGCACCTTCCAGT
4E-BP1 S83A rev	ACTGGAAGGTGCGGTGACCCC
4E-BP1 S83D for	GGGGTCACCGACCCCTCCAGT
4E-BP1 S83D rev	ACTGGAAGGGTCGGTGACCCC
4E-BP1 S83E for	GGGGTCACCGAACCTTCCAGT
4E-BP1 S83E rev	ACTGGAAGGTTCGGTGACCCC
4E-BP1 S101A for	CTGCGCAATGCCCCAGAAGATAAG
4E-BP1 S101A rev	CTTATCTTCTGGGGCATTGCGCAG
4E-BP1 I15A for	CCAAGCCGGGCCGCCCCGCCACTCGC
4E-BP1 I15A rev	GCGAGTGGCGGGGGCGGCCCGGCTTGG
4E-BP1 F114A for	GAGTCACAGGCAGAGATGGAC
4E-BP1 F114A rev	GTCCATCTCTGCCTGTGACTC

Table 2. Plasmids constructs used for HA-tagged 4E-BP1 and MCV sT expression.

Plasmid number	Name of construct	Gene
3144	pCMVtag2B.4EBP1.wt	Human 4E-BP1 WT
3146	pCMVtag2B.4EBP1.T37A/T46A	Human 4E-BP1 T37A and T46A mutant
3576	pCMVtag2B.4EBP1.I15A/F114A	Human 4E-BP1 I15A and F114A mutant
3662	pCMVtag2B.4EBP1.S83A	Human 4E-BP1 S83A mutant
3804	pCMVtag2B.4EBP1.S83D	Human 4E-BP1 S83D mutant
3803	pCMVtag2B.4EBP1.S83E	Human 4E-BP1 S83E mutant
3224	pCMVtag2B.4EBP1.EEEE	Human 4E-BP1 T37E, T46E, S65E, and T70E mutant
3780	pCMVtag2B.4EBP1.S65A/S101A	Human 4E-BP1 S65A and S101A mutant
3487	pCMVtag2B.4EBP1.T70A	Human 4E-BP1 T70A mutant
2989	pLVX EF MCS Puro	Empty lentiviral vector
2990	pLVX EF sT.co WT Puro	codon-optimized MCV sT antigen
3984	pLVX EF HA-4E-BP1.wt	Human 4E-BP1 WT
3985	pLVX EF HA-4E-BP1.T37A/T46A	Human 4E-BP1 T37A and T46A mutant
3986	pLVX EF HA-4E-BP1.I15A/F114A	Human 4E-BP1 I15A and F114A mutant
3681	pLVX EF HA-4E-BP1.S83A	Human 4E-BP1 S83A mutant
2504	psPAX2	HIV Gag
2505	pMD2.G	VSV-G envelope protein

3.2.3 Fluorescence Quantification

Single channel image generated by fluorescence microscope was opened in ImageJ. Each fluorescent cell was selected by in a 45-pixel diameter circle, and the intensity value of each circle was measured. Background subtraction was done by subtracting the value measured with the same size circle placed on the background of the image.

3.2.4 In vitro Translation Assay

TNT quick coupled transcription/translation system was used for in vitro protein synthesis per manufacturer instructions (Promega). DNA template for the TNT was generated from plasmid pFR_CrVP_xb (Addgene) by primers with a 5' flanking T7 promoter sequence as described in the previous chapter (209). Reaction was performed

in a 20- μ l volume containing 0.5 μ g of bicistronic reporter DNA template in the presence of varying concentrations of either untreated or CDK1-treated GST or GST-4E-BP1 or in the presence of 0.5 μ M m7GTP cap-analog (Promega). GST-4E-BP1 or GST alone (2 μ g) was pre-incubated with either 10 units of CDK1/Cyclin B1 (NEB) or 1 μ g/mL BSA for 1 h at 30 °C. Reaction mix was incubated at 30 °C for 1 h. Luciferase assay was performed by dual luciferase assay kit (Promega).

3.2.5 Lentiviral Transduction

Codon-optimized MCV sT and HA-4E-BP1 sequences were inserted into pLVX EF.puro using AfeI and SbfI sites. For lentivirus production, 293FT (Invitrogen) cells were transfected with the pLVX lentivirus vector and the two psPAX2 and pMD2.G packaging vectors. Lentivirus infection was performed in the presence of 6 μ g/ml polybrene. Infected cells were selected with puromycin (2 μ g/ml).

3.2.6 Immunoblotting and Antibodies

Cells were lysed in buffer (50 mM Tris-HCl, pH 7.4; 0.15 M NaCl; 1% Triton X-100; 2 mM Na_3VO_4 ; 2 mM NaF; 0.1% SDS) containing protease inhibitors (Roche). Lysates were resolved by 12% (5-20% for cap-binding assay) SDS-PAGE and transferred to nitrocellulose. Membranes were blocked with 5% milk in 1X TBS and incubated with primary antibodies overnight at 4 °C. Blots were subsequently incubated with IRDye-labeled anti-rabbit or anti-mouse secondary antibodies and analyzed on the Odyssey infrared scanner (LI-COR Biosciences). The following primary antibodies were used in

this study: phospho-4E-BP1^{S83} antiserum, phospho-4E-BP1^{T70}, phospho-4E-BP1^{S65/S101}, phospho-4E-BP1^{T37/T46}, total 4E-BP1, phospho-Histone H3^{S10}, eIF4E, eIF4G, eIF4A, γ -tubulin (Cell Signaling), α tubulin (DSHB), HA (Covance), 800CW goat polyclonal anti-rabbit IgG, and 680CW goat polyclonal anti-mouse IgG (LI-COR Biosciences).

3.2.7 Cell Cycle Synchronization

HeLa, HCT116, U87, U251, U2OS, and 293 cells (ATCC) were synchronized as described in the previous chapter (209).

3.2.8 Kinase Inhibitors

Active site kinase inhibitors were used in cell culture as follows: 5 μ M PP242 (mTOR) and 9 μ M RO-3306 (CDK1). Proteasome inhibitor MG132 (10 μ M) was co-incubated with RO-3306 for in vivo CDK1 inhibition. PP242, RO-3306, VX-680 (AURK), and BI-6727 (PLK1) kinase inhibitors were used at 5 μ M for in vitro phosphorylation assays.

Phospho-Ser83 4E-BP1 Polyclonal Antibody Production. Rabbits were immunized with 4E-BP1 synthetic phospho-peptide ⁷⁷TIPGVT(pS)PSSDEP⁸⁹. Antiserum was periodically collected after multiple immunization boosts.

3.2.9 Flow Cytometry

Asynchronous U2OS, U87, HeLa, and 293 cells were trypsinized, fixed in 10% buffered formalin, and permeabilized with 0.1% saponin in 1% FBS/PBS for 15 min at RT. Cells

were stained with p4E-BP1T37/T46 antibody or rabbit IgG control antibody for 3 h at RT. After washing three times with 1% FBS/PBS, cells were reacted with anti-rabbit Alexa 488-labeled IgG (Invitrogen) for 1 h at RT. For phospho-histone H3^{S10} staining, cells were permeabilized with 1% FBS/PBS containing 0.25% Triton X-100 for 3 min at RT. Alexa 647-labeled pH3S10 antibody (Cell Signaling) or control Alexa 647-labeled rabbit IgG (Cell Signaling) were reacted with cells for 1 h at RT. After washing three times with 1% FBS/PBS, DNA was stained with 1% FBS/PBS containing 50 µg/mL propidium iodide (PI) and 40 µg/mL RNase A (Sigma) for 30 min. For p4E-BP1^{S83} flow cytometry analysis, U2OS and HeLa cells were treated with growth medium containing 0.5 µM nocodazole or DMSO for 20 h. p4E-BP1S83 antiserum or pre-immune serum in 1% FBS/PBS were used. Cells were analyzed by the BD Accuri C6™ cell analyzer (BD Biosciences).

3.2.10 Mass Spectrometry

HeLa cells were disrupted, proteins tryptically digested, phosphopeptide enriched, TMT10-labeled, and high mass accuracy LC-MS/MS analyzed as previously described (365). Variations include use of TMT10 instead of iTRAQ labeling, cell lysate versus tissue disruption, and use of Q Exactive Orbitrap MS. 293 cell LC-MS/MS analyses were performed identically, except for quantitation which used label-free approaches as previously described (366).

3.2.11 Two-Dimensional Electrophoresis

HeLa cells were lysed in non-denaturing lysis buffer supplemented with protease inhibitors (Roche). Lysates were isoelectrically focused as described in the previous chapter (209).

3.2.12 In Vitro Protein Phosphorylation Assay

Recombinant GST-4E-BP1 was incubated in a reaction containing 1X protein kinase buffer (NEB) and mitotic HeLa cell lysate as described in the previous chapter (209).

3.2.13 Immunofluorescence

293, HeLa, U2OS, or U87 cells (0.3×10^6) were seeded onto poly-L-lysine treated glass coverslips. The next day, cells were washed with ice-cold 1X PBS and fixed with 2% paraformaldehyde for 15 min at RT, followed by permeabilization with cold MeOH for 10 min at $-20\text{ }^{\circ}\text{C}$. Cells were blocked with 10% normal goat serum (Cell Signaling) for 1 h at RT and then stained with p4E-BP1^{S83} antiserum pre-absorbed with unphosphorylated ⁷⁷TIPGVTSPSSDEP⁸⁹, together with γ -tubulin or phospho-histone H3S10 antibodies (Cell Signaling) for 2 h at RT. Cells were then washed with cold 1X PBS three times for 5 min each and incubated with Alexa 488-labeled anti-rabbit secondary antibody and Alexa 568-labeled anti-mouse antibody (Invitrogen) at RT for 1 h. Cells were examined by fluorescence microscopy (Olympus). Confocal microscopy

was performed with Leica TCS SP2 upright confocal microscope. Intensity of fluorescence staining was measured by ImageJ.

3.2.14 m7GTP Cap Binding Assay

293 were lysed in non-denaturing lysis buffer supplemented with protease inhibitors (Roche). Lysates were incubated with m7GTP sepharose beads (Jena Bioscience) as described in the previous chapter (209).

3.2.15 Foci Formation Assays

Rat-1 cells were infected with recombinant lentiviruses and grown for two weeks in 6-well plates for foci formation assay. To determine viral titer and establish stable cell lines, cells were selected with puromycin (2 µg/ml) for pLVX EF vectors. After two weeks, foci were stained with crystal violet (0.025% in 1X PBS), and plates were photographed and scanned with Odyssey scanner (LI-COR) for quantification.

3.3 RESULTS

3.3.1 δ -4E-BP1 hyperphosphorylation is a feature of mitosis across multiple cancer cell lines.

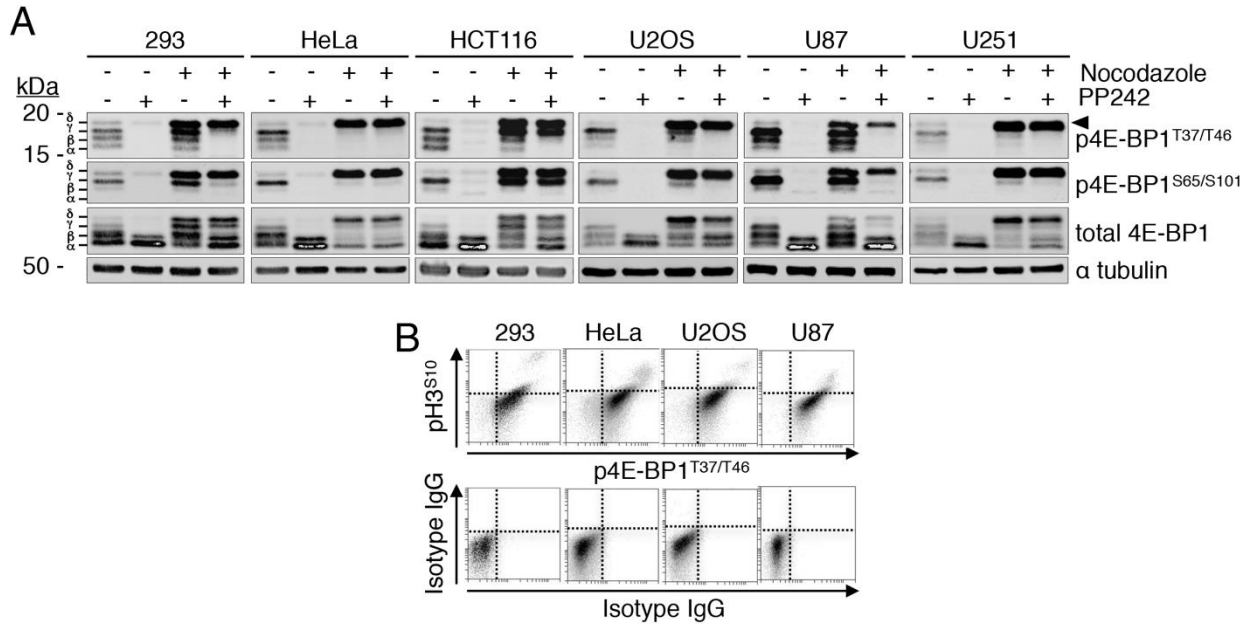


Figure 28. δ -4E-BP1 hyperphosphorylation is a common feature of mitosis across multiple cancer cell lines.

(A) Mitotic arrest of various cancer cell lines induces δ -4E-BP1. 293, HeLa, HCT116, U2OS, U87, and U251 cells were arrested for 20 h with DMSO or nocodazole (prometaphase). Cells were treated at 16 h with mTOR kinase active-site inhibitor PP242 (5 μ M). Nocodazole arrest induces PP242-resistant δ -4E-BP1 (black arrowhead) in all cell lines tested. (B) pH3^{S10} mitotic cells have higher levels of 4E-BP1^{T37/T46} phosphorylation than interphase cells. Dual flow cytometry staining for pH3^{S10} and p4E-BP1^{T37/T46} was performed on asynchronous 293, HeLa, U2OS, and U87 cells. Increased pH3^{S10} fluorescence was correlated to increased p4E-BP1^{T37/T46} fluorescence for all cell lines.

4E-BP1 has four discernible gel isoforms named α , β , γ , and δ based on ascending molecular weight and phosphorylation (157). To determine the generalizability of δ -4E-BP1 expression during mitosis, six cell lines—293, HeLa, HCT116, U2OS, U87, and

U251—were arrested in prometaphase with nocodazole and examined for 4E-BP1 phosphorylation. Hyperphosphorylated δ -4E-BP1 was the predominant isoform in mitotic cells from all cell lines and is resistant to the mTOR inhibitor PP242 (**Figure 28A**). Asynchronous cells expressed mainly α , β , and γ 4E-BP1 isoforms that were sensitive to mTOR inhibition. Expression of α , β , and γ forms was variably detectable and sensitive to PP242 in nocodazole-arrested cells, which is consistent with non-mitotic cell contamination. In addition, flow cytometry revealed a correlation between phospho-4E-BP1^{T37/T46} (p4E-BP1^{T37/T46}) and mitotic marker phospho-histone H3^{S10} (pH3^{S10}), indicating that mitotic cells tend to have a high level of 4E-BP1 phosphorylation (**Figure 28B**).

3.3.2 S83 phosphorylation is a component of δ -4E-BP1 and is mediated by CDK1/CYCB.

The phosphorylation of 4E-BP1 is hierarchical, with mTOR-directed priming phosphorylations at T37 and T46 being essential for additional phosphorylations at T70 and S65 (172). S65 phosphorylation is abundant in the γ -isoform in asynchronous cells as well as the higher molecular weight δ -isoform during mitosis (**Figure 28A**). Lambda phosphatase treatment collapses all 4E-BP1 isoforms to the unphosphorylated form (209). These data are consistent with the δ -isoform having a unique phosphorylation site in addition to phosphorylations at other known sites. To identify additional phosphorylation sites responsible for the slower migration of the δ -isoform, HeLa and 293 cells arrested in mitosis, compared to asynchronous populations, were examined by liquid chromatography-tandem mass spectrometry (LC-MS/MS) based quantitative

phosphoproteome analysis. The phospho-S83 site represented by the digested peptide, $^{74}\text{DLPTIPGVT}(\text{pS})\text{PSSDEPPMEASQSHLR}^{99}$, was quantitatively identified only in mitotic cells (**Figure 29**).

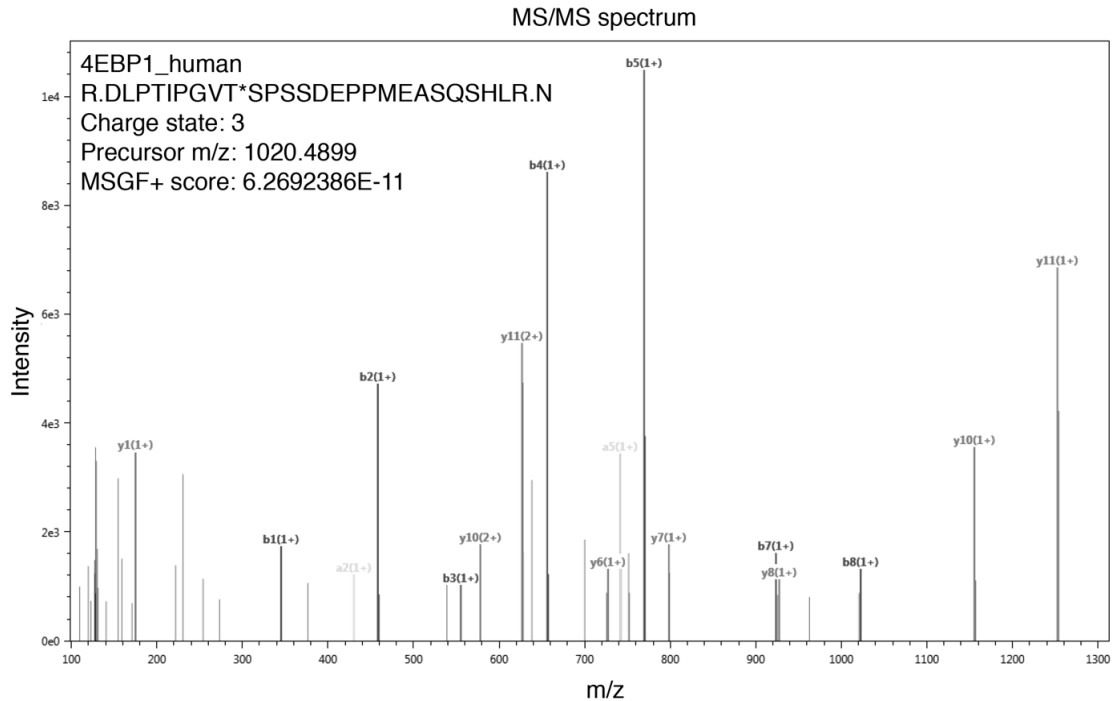


Figure 29. LC-MS/MS spectrum for phospho-S83 4E-BP1 peptide identified only in mitotic HeLa cells.

HeLa cells were disrupted, proteins tryptically digested, phosphopeptide enriched, TMT10-labeled, and high mass accuracy LC-MS/MS analyzed as previously described (365). Variations include use of TMT10 instead of iTRAQ labeling, cell lysate versus tissue disruption, and use of Q Exactive Orbitrap MS.

To confirm that phosphorylation at S83 is a bona fide component of the δ -4E-BP1 isoform, a phospho-specific antibody was raised in rabbits by immunizing with a synthetic 4E-BP1 peptide having S83 phosphorylated ($^{77}\text{TIPGVT}(\text{pS})\text{PSSDEP}^{89}$). This antiserum is specific for phospho-S83 but also has weak reactivity to non-phosphorylated 4E-BP1 that requires pre-absorption or peptide blocking to reduce. Rabbit antiserum was screened by immunoblotting against lysates from asynchronous

and mitotic 293 cells expressing HA-tagged 4E-BP1 variants—wild-type, T37A/T46A, S65A/S101A, T70A, and S83A. Immunoblotting showed loss of reactivity against only 4E-BP1.S83A expressed in mitotic cells, confirming the specificity of the antibody (**Figure 30**). Phosphorylation of endogenous 4E-BP1 at T37, T46, S65, and T70 was present in α , β , and γ isoforms in asynchronous HeLa cells but not at S83 (**Figure 31A**). S83 phosphorylation, however, was abundant only in the δ -4E-BP1 isoform of HeLa cells arrested with nocodazole. Reactivity of the δ -isoform with the other 4E-BP1 phospho-specific antibodies in the presence and absence of PP242 indicated that S83 phosphorylation occurs in addition to phosphorylation at other sites in δ -4E-BP1, and is resistant to mTOR inhibition. Asynchronous and mitotic HeLa cell lysates from Figure 31A were also fractionated by two-dimensional electrophoresis (**Figure 31B**). S83 phosphorylation of 4E-BP1 was detected on the slowest-migrating isoelectric focusing spot corresponding to δ -4E-BP1 (white arrowheads) and a second spot (black arrowheads) below it that is absent in p4E-BP1^{T37/T46} staining. In addition, a 4E-BP1.T37A/T46A priming-site mutant protein was phosphorylated at S83 but not at S65 in mitotic cells, indicating that phosphorylation at S83, in contrast to S65, may not be dependent on T37/T46 phosphorylation (**Figure 31C**). Furthermore, S83 phosphorylation of 4E-BP1 in mitotic cells was confirmed by flow cytometry staining with pH3^{S10} and p4E-BP1^{S83} antiserum. U2OS (**Figure 31D**) and HeLa (**Figure 32**) cells showed p4E-BP1^{S83} positivity exclusively for pH3^{S10+} mitotic cells. When U2OS cells were arrested with nocodazole (**Figure 31D**), mitotic cells formed a discrete p4E-BP1^{S83+}/pH3^{S10+} population indicating that nearly all mitotic cells express the δ -4E-BP1 isoform.

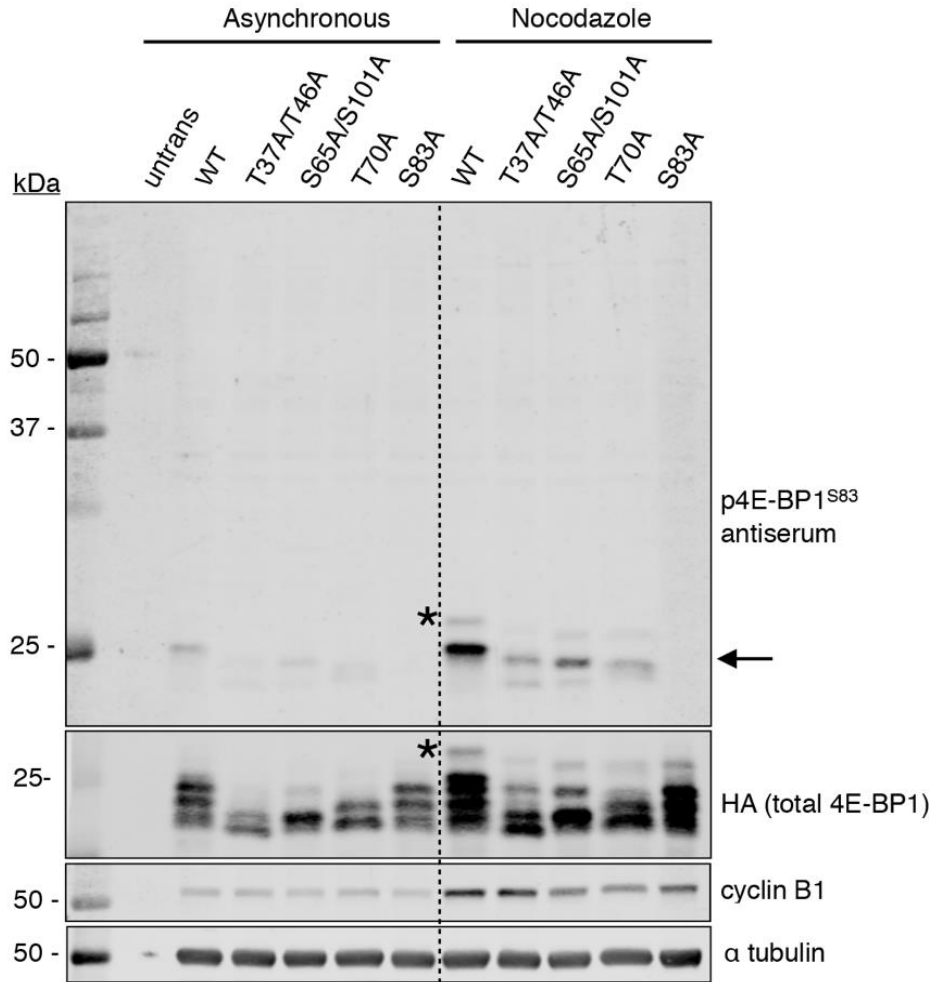


Figure 30. p4E-BP1^{S83} rabbit antiserum specificity screen against 4E-BP1 phosphorylation mutants.

293 cells were transfected with wild-type HA-4E-BP1 and phospho-defective mutants T37A/T46A, S65A/S101A, T70A, and S83A and were arrested with nocodazole (0.5 μ M) for 16h and harvested for immunoblotting with p4E-BP1^{S83} rabbit antiserum. Mutation of S83 to alanine eliminated the p4E-BP1^{S83} signal from nocodazole-arrested 293 cells (arrow). However, mutations at canonical phosphorylation sites still showed the S83 phosphorylation mark despite the relatively faster migration of mutant proteins due to the loss of phosphorylation at mutated sites. Slow migrating bands (asterisks) may represent minor protein population from triple-tagged vector FLAG-HA-HA-4E-BP1. Increased cyclin B1 in nocodazole-treated conditions confirms mitotic arrest with nocodazole treatment.

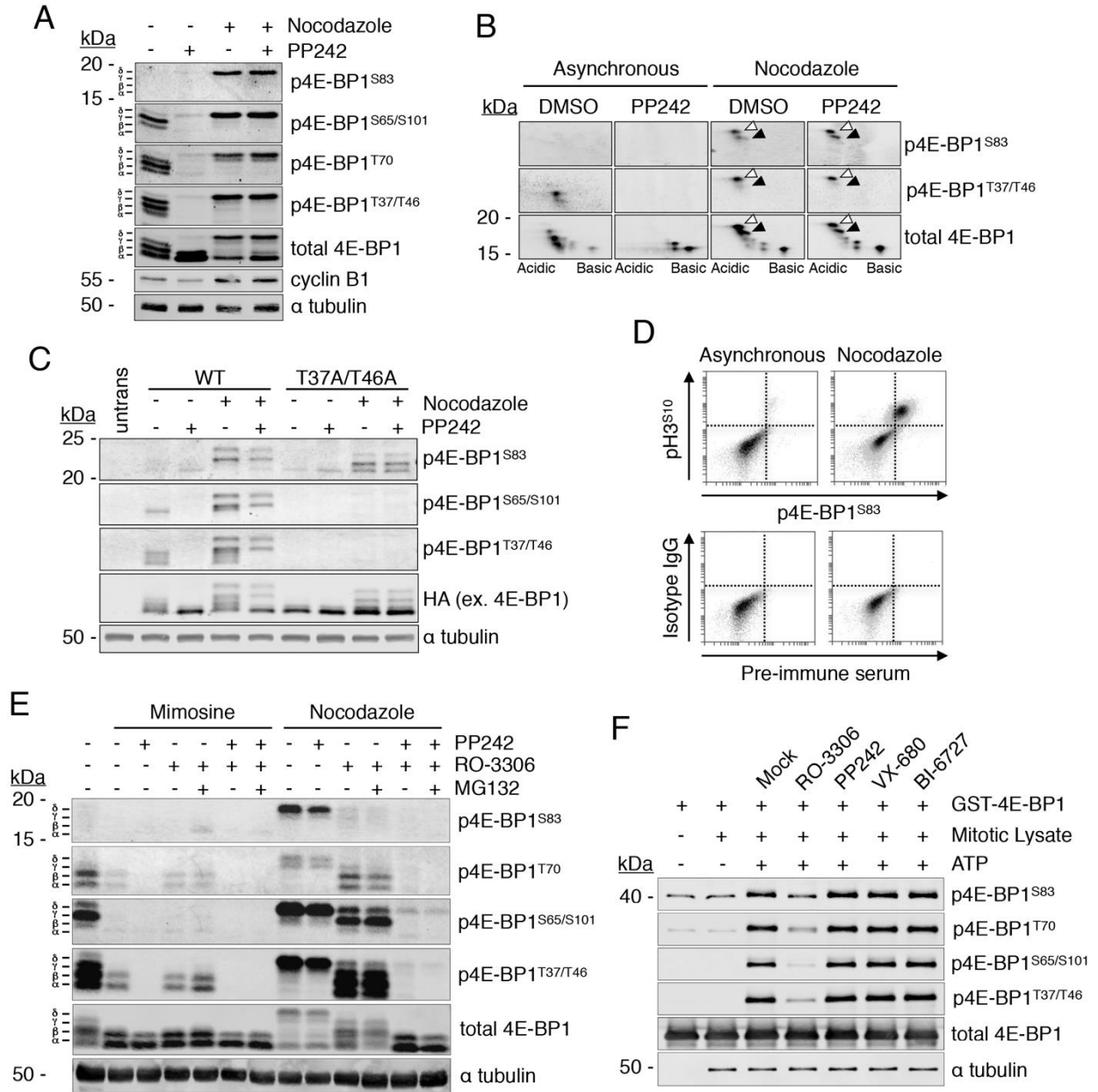


Figure 31. S83 phosphorylation is a component of δ -4E-BP1 and is mediated by CDK1/CYCB.

(A) Polyclonal anti-p4E-BP1^{S83} rabbit antiserum detects S83 phosphorylation in mitotic δ -4E-BP1. HeLa lysates from asynchronous and nocodazole arrest conditions were immunoblotted with p4E-BP1^{S83} antiserum. p4E-BP1^{S83} was found only in the δ -4E-BP1 isoform in mitotic cells and was resistant to mTOR inhibition by PP242. (B) HeLa cell lysates from (A) were fractionated by isoelectric focusing (pH 3-6), followed by immunoblotting with phospho-specific and total 4E-BP1 antibodies. White arrowheads

Figure 31 (continued)

indicate the isoelectric focusing spot corresponding to δ -4E-BP1, and black arrowheads indicate a second spot revealed by p4E-BP1^{S83} staining. (C) Priming-site mutation of T37/T46 to alanine does not inhibit S83 phosphorylation during mitosis. Wild-type and T37A/T46A mutant HA-4E-BP1 expression plasmids were transfected into 293 cells. Cells were arrested for 20 h with DMSO or nocodazole 48 h post-transfection. Cells were treated at 16 h with mTOR kinase active-site inhibitor PP242 (5 μ M). Mutation of 4E-BP1 at T37/T46 blocked S65 phosphorylation but did not prevent S83 phosphorylation during mitosis. (D) pH3^{S10+} mitotic cells are positive for 4E-BP1^{S83} phosphorylation. Dual flow cytometry staining for pH3^{S10} and p4E-BP1^{S83} was performed on asynchronous and nocodazole-arrested U2OS cells. pH3^{S10} fluorescence was correlated to p4E-BP1^{S83}. (E) CDK1 inhibition by RO-3306 ablates S83 phosphorylation in mitotic cells. HeLa cells were arrested in G1 by L-mimosine treatment and mitosis by nocodazole treatment for 20 h. Cells were subsequently treated with kinase inhibitors PP242 (mTOR, 5 μ M) and RO-3306 (CDK1, 9 μ M) for 4 hours, supplemented with 10 μ M MG132 proteasome inhibitor to prevent mitotic exit/slippage. 4E-BP1^{S83} phosphorylation was abolished by RO-3306 treatment, along with δ -4E-BP1, in mitotic cells. Combined PP242 and RO-3306 erased most mitotic 4E-BP1 phosphorylation in these cells. S83 phosphorylation and δ -4E-BP1 were absent in G1-arrested cells, as expected. (F) Mitotic lysate phosphorylates GST-4E-BP1 at S83. Mitotic HeLa cell lysates enriched by nocodazole arrest were incubated with GST-4E-BP1 and reacted in buffer containing 200 μ M ATP for 30 min at 30 °C in the presence or absence of mTOR (PP242), RO-3306 (CDK1), VX-680 (AURK A/B/C), and BI-6727 (PLK1) kinase inhibitors (5 μ M). GST-4E-BP1 was phosphorylated at S83 and the other known regulatory sites. CDK1 inhibition by RO-3306 treatment reduces S83 phosphorylation, consistent with the other phosphorylation sites. Treatment with kinase inhibitors against other mitotic kinases AURK A/B/C and PLK1 did not inhibit S83 phosphorylation.

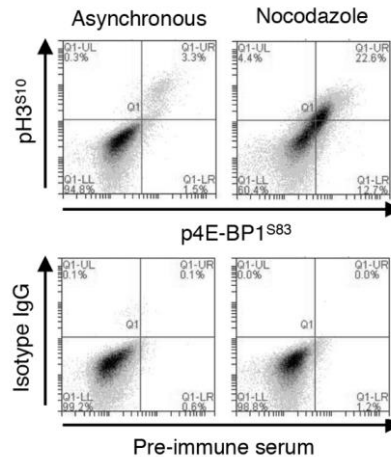


Figure 32. p4E-BP1^{S83} flow cytometry staining of HeLa cells.

Dual flow cytometry-stained p4E-BP1^{S83} mitotic HeLa cells are positive for p4E-BP1^{S83}.

We have previously shown that proline-directed, serine/threonine kinase CDK1/CYCB phosphorylates 4E-BP1 during mitosis at T37/T46, S65/S101, and T70, all which share the minimal consensus S/T-P sequence (209, 367). To determine whether CDK1 also phosphorylates S83, HeLa cells were arrested in G1 by L-mimosine treatment or in mitosis by nocodazole treatment and then treated with CDK1 active site inhibitor RO-3306, supplemented with MG132 proteasome inhibitor to prevent mitotic slippage (345, 368). CDK1 inhibition by RO-3306 abolished S83 phosphorylation and δ -4E-BP1 formation, in addition to reducing phosphorylation at the other phosphorylation sites (**Figure 31E**). G1-arrested cells had low levels of phosphorylated 4E-BP1 that was sensitive to mTOR inhibition by PP242 but insensitive to RO-3306 (347). To confirm whether CDK1 directly phosphorylates S83, recombinant GST-4E-BP1 was mixed with mitotic HeLa lysate in an in vitro phosphorylation assay. Mitotic lysate phosphorylated GST-4E-BP1 at S83, which was reversed by addition of RO-3306 but not of PP242, VX-680 (pan-AURK inhibitor), or BI-6727 (PLK1 inhibitor) (**Figure 31F**). Taken together, these findings demonstrate that CDK1 phosphorylates 4E-BP1 at S83 during mitosis.

3.3.3 S83-phosphorylated 4E-BP1 colocalizes with centrosomes during mitosis and peaks at metaphase.

S83 phosphorylation of 4E-BP1 in mitotic cells was also confirmed by immunofluorescence microscopy. Staining of 293 (**Figure 33A**), HeLa, U87, and U2OS (**Figure 34**) cells showed p4E-BP1^{S83} positivity in all mitotic cells, which are also positive for pH3^{S10}, with the exception of telophase cells whose chromosomes are decondensed and hence negative for pH3^{S10} (369). In addition to a diffuse staining pattern in mitotic cells, p4E-BP1^{S83} also formed two distinct puncta near condensed chromosomes, which colocalized with centrosomal marker γ -tubulin as detected by confocal microscopy (**Figure 33B**). To show that this binding is phospho-specific, we performed a phospho-peptide competition assay for the staining (**Figure 35A**). These data suggest that a portion of p4E-BP1^{S83} may colocalize with centrosomes during mitosis. To further dissect the kinetics of mitotic 4E-BP1 S83 phosphorylation, asynchronous 293 cells were counted in each of the phases of mitosis (pH3^{S10+}) and in interphase (pH3^{S10-}) based on their morphology and chromosome condensation. pH3^{S10} is present throughout mitosis but declines in telophase due to chromosome decondensation (369), and p4E-BP1^{S83} is low in prophase, peaks at metaphase, and also declines in telophase (**Figure 33C**). Cells were also stained for p4E-BP1^{T37/T46} and did not exhibit substantial differences across most phases (**Figure 36**). Altogether, these data demonstrate that the phosphorylation of 4E-BP1 at S83 is regulated throughout mitosis.

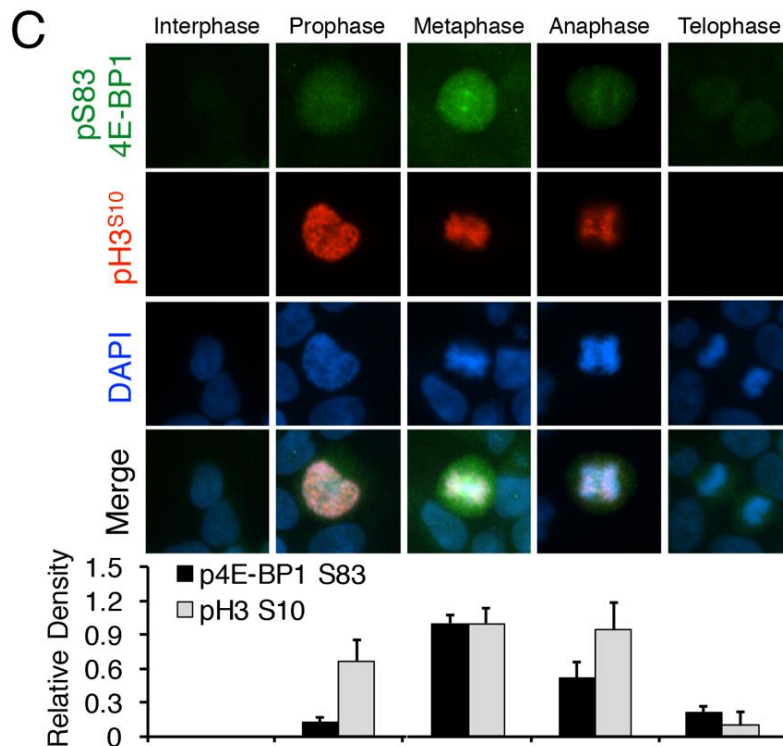
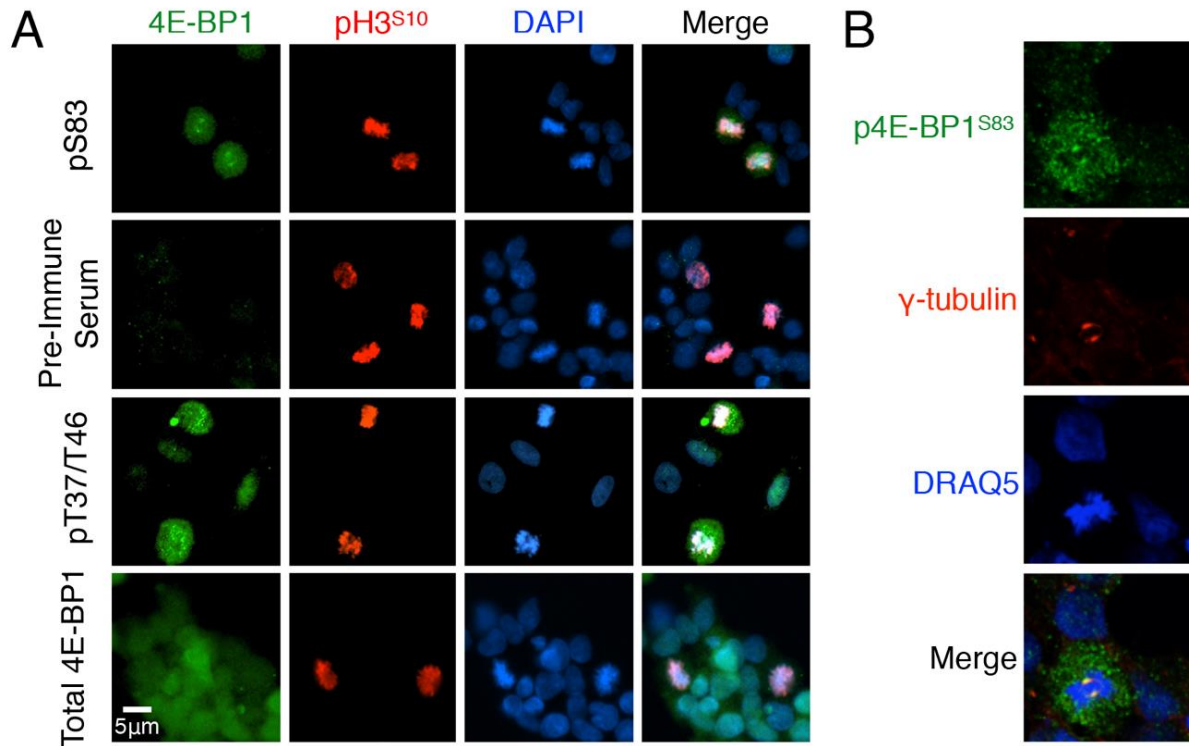


Figure 33. S83-phosphorylated 4E-BP1 colocalizes with centrosomes during mitosis and peaks at metaphase.

Figure 33 (continued)

(A) Immunofluorescence staining shows the presence of p4E-BP1^{S83} only in mitotic cells. Asynchronous 293 cells were fixed, and dual-stained with p4E-BP1^{S83} antiserum (green) and pH3^{S10} (red) antibodies. Nuclear DAPI stain is shown in blue. (B) p4E-BP1^{S83} staining colocalizes with γ -tubulin staining to centrosomes in mitotic nuclei of 293 cells. Asynchronous 293 cells were fixed and dual-stained with p4E-BP1^{S83} antiserum (green) and γ -tubulin (red) antibodies. Nuclear DRAQ5 stain is shown in blue. Stained cells were observed by confocal microscopy for colocalization studies. (C) 4E-BP1 S83 phosphorylation peaks at metaphase and declines in telophase. Asynchronous 293 cells were fixed and dual-stained with p4E-BP1^{S83} antiserum (green) and pH3^{S10} (red) antibodies. Nuclear DAPI stain is shown in blue. Cells in interphase and in different phases of mitosis (prophase, metaphase, anaphase, and telophase) were identified by morphology and chromosome condensation. Intensity of p4E-BP1^{S83} staining for cells in each phase was quantified by ImageJ. Thirty cells for each phase were quantified, and plot and error bars were obtained from three independent experiments.

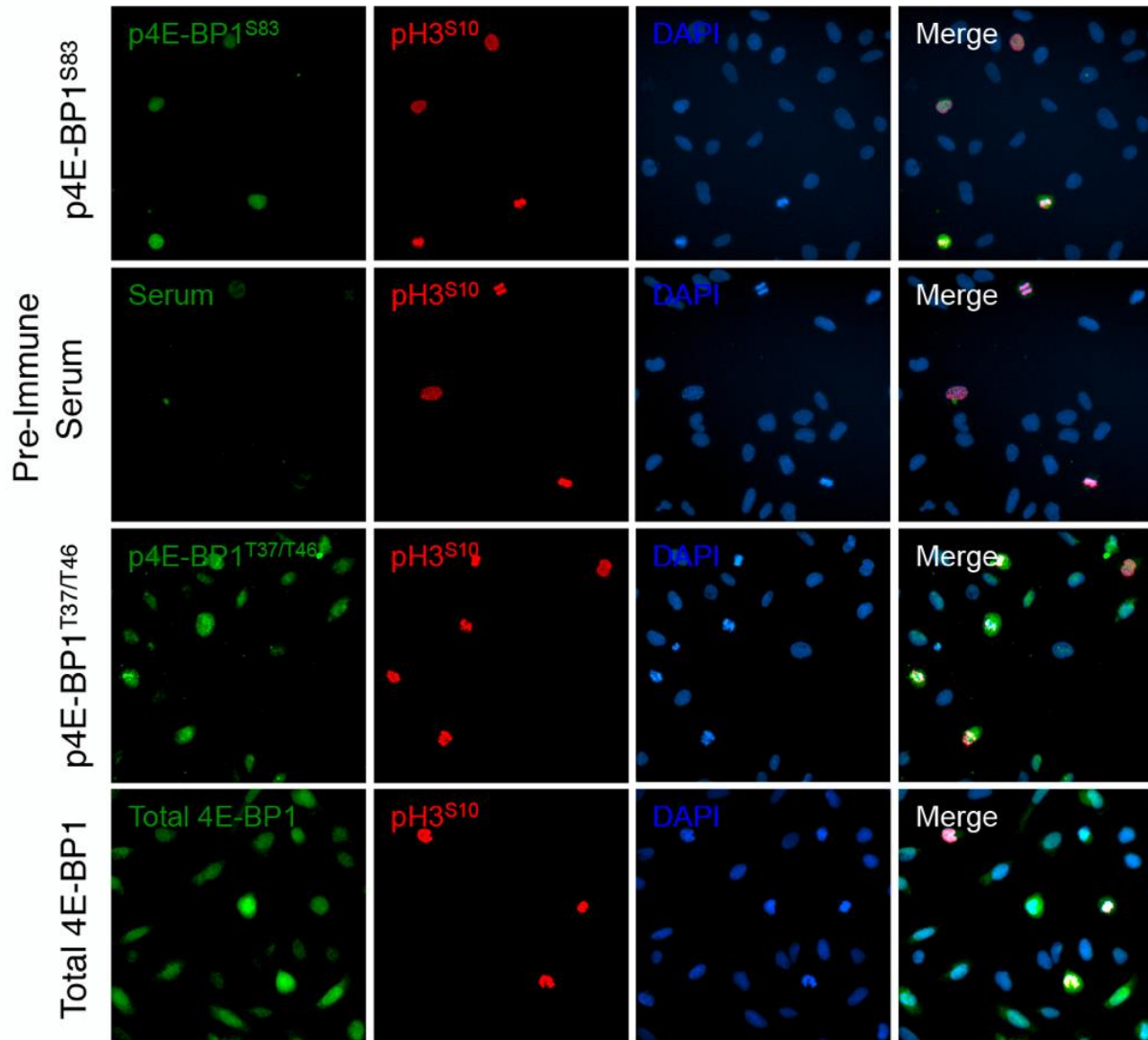


Figure 34. p4E-BP1^{S83} immunofluorescence staining of U2OS cells.

U2OS cells were arrested and released as in Figure 30, fixed, and dual-stained with p4E-BP1^{S83} antiserum (green) and pH3^{S10} (red) antibodies. Nuclear DAPI stain is shown in blue. Immunofluorescence staining shows the presence of p4E-BP1^{S83} only in pH3^{S10+} mitotic cells. Similar results were obtained with HeLa and U87 cells. p4E-BP1^{S83} was pre-absorbed with control non-phosphorylated peptide antigen ⁷⁷TIPGVTSPSSDEP⁸⁹.

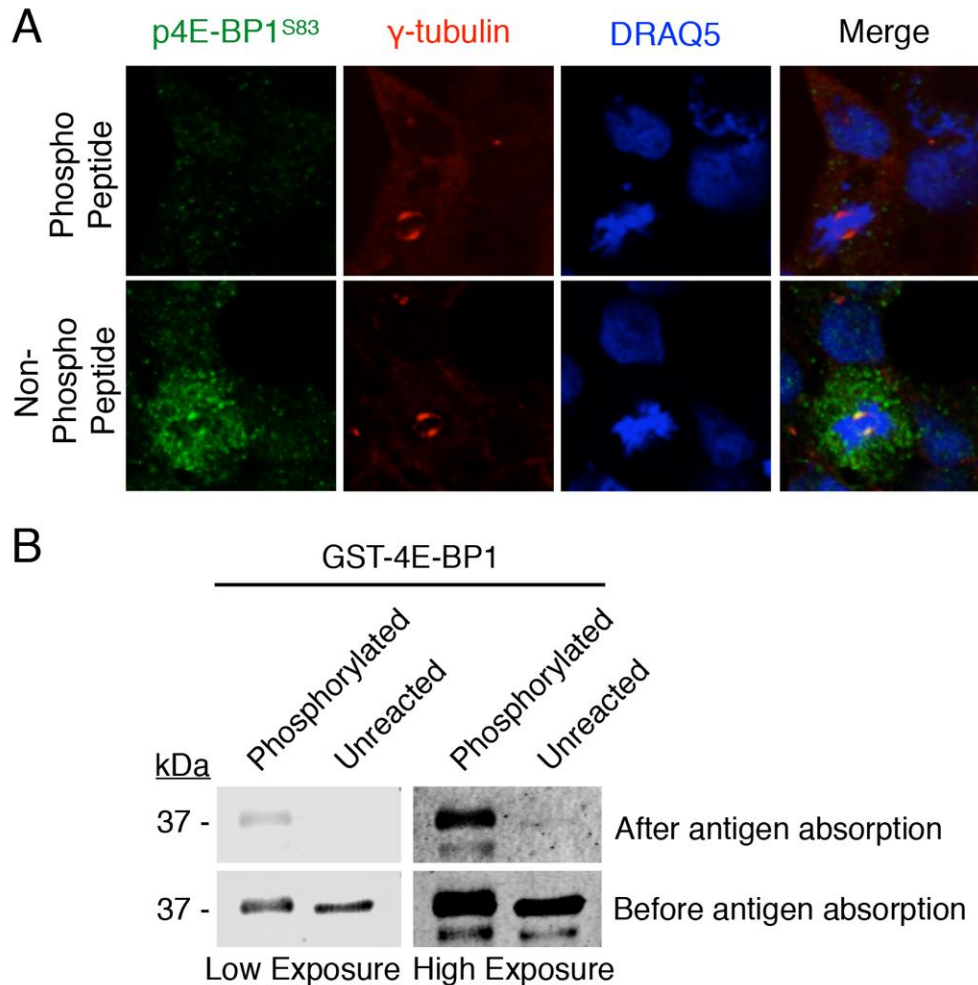


Figure 35. Epitope competition assays with antigen pre-absorbed p4E-BP1^{S83} antiserum.

(A) Confocal microscopy staining of 293 cells with phosphorylated peptide and non-phosphorylated peptide pre-absorbed p4E-BP1^{S83} antiserum. p4E-BP1^{S83} antiserum was incubated with non-phosphorylated (non-phospho) or phosphorylated (phospho) 4E-BP1 S83 peptide (⁷⁷TIPGVTSPSSDEP⁸⁹) prior to immunofluorescence staining and confocal microscopy. Asynchronous 293 cells were fixed and dual-stained with p4E-BP1^{S83} antiserum (green) and γ -tubulin (red) antibodies. Nuclear DRAQ5 stain is shown in blue. Non-phosphorylated peptide pre-absorbed p4E-BP1^{S83} staining colocalizes with γ -tubulin staining to centrosomes, which is ablated with phosphorylated peptide preabsorption. (B) Immunoblotting staining of unreacted and phosphorylated GST-4E-BP1 with dephosphorylated GST-4E-BP1 pre-absorbed p4E-BP1^{S83} antiserum. p4E-BP1^{S83} antiserum was incubated with lambda phosphatase-treated GST-4E-BP1 and purified with glutathione sepharose beads prior to immunoblotting staining. Dephosphorylated GST-4E-BP1 pre-absorbed p4E-BP1^{S83} antiserum stains only GST-4E-BP1 phosphorylated by mitotic HeLa cell lysate.

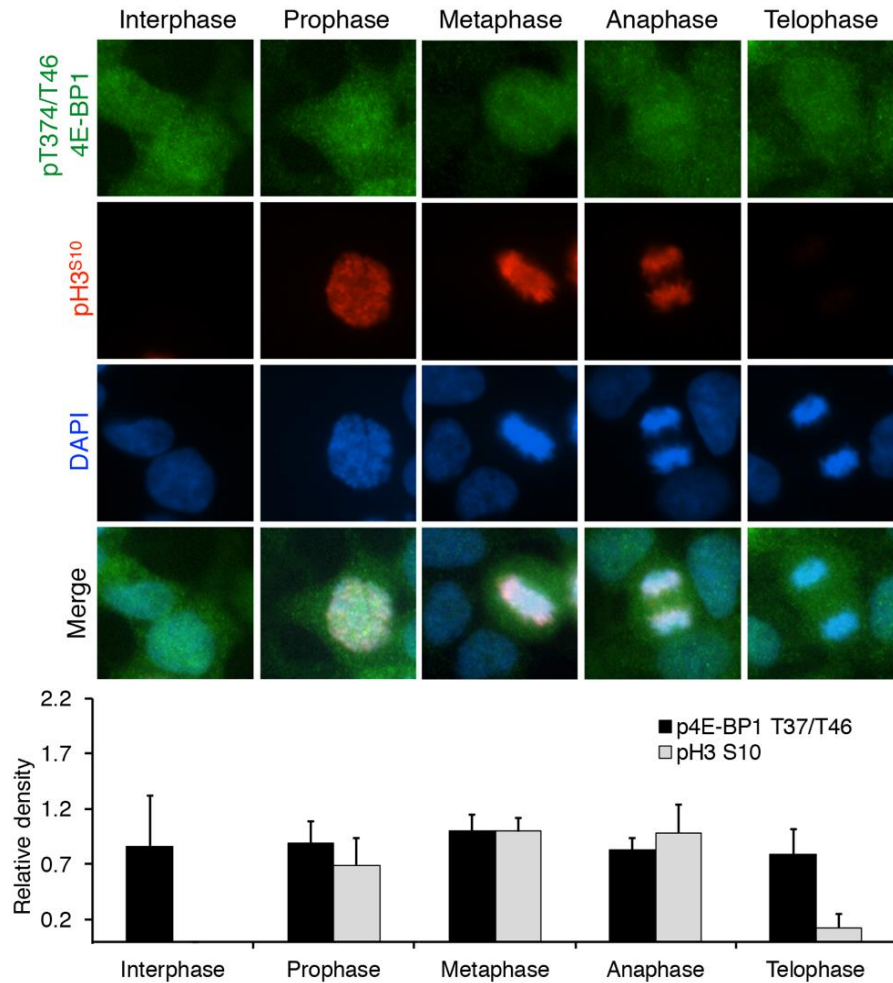


Figure 36. p4E-BP1^{T37/T46} phosphorylation is maintained during interphase and mitosis.

Asynchronous 293 cells were fixed and dual-stained with p4E-BP1^{T37/T46} (green) and pH3^{S10} (red) antibodies. Nuclear DAPI stain is shown in blue. Cells in interphase and in different phases of mitosis were identified by morphology and chromosome condensation. Thirty cells for each phase were counted from three experiments.

3.3.4 Mutation of 4E-BP1 at S83 does not affect general cap-dependent translation but partially reverses MCV sT-induced Rat-1 cell transformation.

4E-BP1 possesses an amino acid motif necessary for interaction with eIF4E, containing the sequence ⁵⁴YDRKFLM⁶⁰ (100). The consensus binding motif Y(X)₄LΦ (where X is any amino acid residue and Φ is a hydrophobic residue) is shared by other 4E-BPs and translation initiation factor eIF4G. Recently, a C-terminal loop region of 4E-BP1, ⁷⁹PGVTS⁸³, was reported to also play an auxiliary role in binding eIF4E at a hydrophobic pocket separate from the canonical ⁵⁴YDRKFLM⁶⁰ binding pocket (105, 106, 370, 371). If S83 phosphorylation destabilizes this auxiliary domain, it may affect 4E-BP1:eIF4E interaction and cap-dependent initiation and translation.

To assess this, *in vitro* translation reactions were performed using using TNT transcription/translation coupled system using a bicistronic reporter with a firefly luciferase gene driven by cap-dependent translation followed by a renilla luciferase gene driven by cricket paralysis virus (CrPV) IRES-mediated translation. Recombinant GST-tagged 4E-BP1.S83A decreased cap-dependent translation to similar levels as wild-type GST-tagged 4E-BP1, and CDK1 phosphorylation of this protein rescued translation (**Figure 37A**). GST-4E-BP1.T37A/T46A having substitutions at priming sites inhibited translation despite CDK1 treatment. IRES-mediated translation, however, was unaffected by GST-4E-BP1 as expected (**Figure 37B**). Similarly, 4E-BP1.S83A had no detectable effect on m7GTP cap resin pull-down assays compared to wild-type 4E-BP1 protein (372). Compared to wild-type 4E-BP1, S83A, (or phosphomimetic mutants S83D and S83E) did not differ significantly in binding cap-bound eIF4E and did not significantly affect cap-complex formation, as measured by eIF4G and eIF4A pull-down

(Figure 38A). Unlike 4E-BP1.S83A, phosphorylation-defective and mTORC1 binding mutants (T37A/T46A and I15A/F114A) efficiently inhibited eIF4G binding to eIF4E and in vitro cap-dependent translation (100, 164, 165, 167), suggesting that S83 phosphorylation does not play a significant role in general cap-dependent translation regulation.

MCV sT transforms Rat-1 and NIH3T3 cells through a novel mechanism requiring 4E-BP1 phosphorylation that can be reversed by expression of a constitutively active 4E-BP1.T37A/T46A mutant (170, 209). To determine whether S83 phosphorylation is required for the transformation activity of this viral oncoprotein, we performed foci formation assays with Rat-1 co-expressing MCV sT and 4E-BP1 variants. Cells were first stably transduced with empty vector, wild-type 4E-BP1, 4E-BP1.T37A/T46A, 4E-BP1.I15A/F114A, or 4E-BP1.S83A, followed by transduction with empty vector or MCV sT. MCV sT transformed Rat-1 cells expressing either empty-vector control or wild-type 4E-BP1, and this was reversed by co-expression of non-phosphorylatable 4E-BP1.T37A/T46A and 4E-BP1.I15A/F114A mutant proteins (**Figure 38B**). 4E-BP1.S83A mutant expression partially but reproducibly decreased sT-induced transformation to ~51% of empty vector control and ~66% of wild-type 4E-BP1. Immunoblotting of lysates from these cells show comparable protein levels of wild-type 4E-BP1 and 4E-BP1.S83A; therefore, the negative effect on foci formation did not result from enhanced expression of the latter (**Figure 39**). Low protein levels were predictably observed for 4E-BP1.T37A/T46A and 4E-BP1.I15A/F114A mutants because they inhibit their own translation.

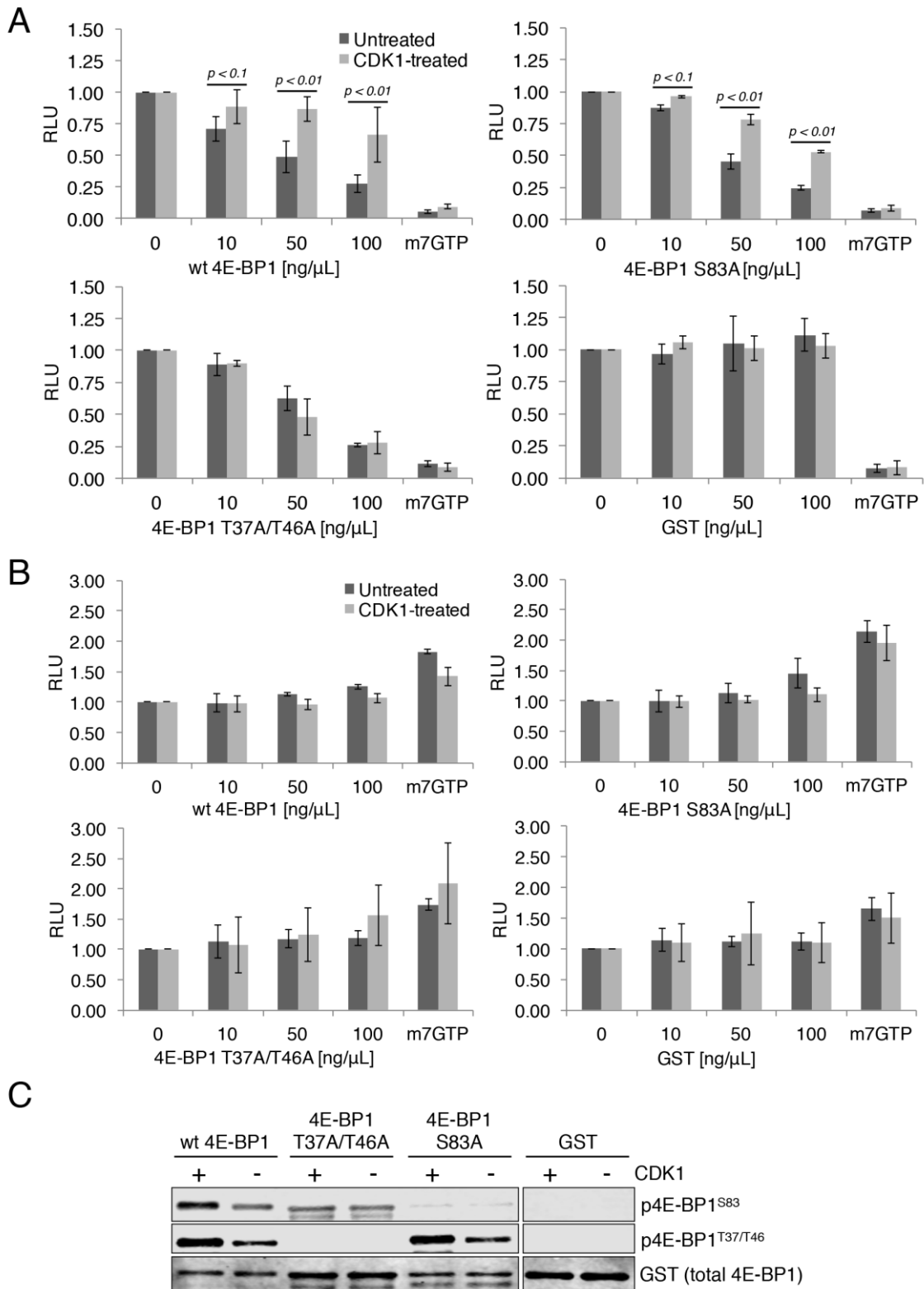


Figure 37. Mutation of 4E-BP1 at S83 does not affect general cap-dependent translation initiation complex formation.

Figure 37 (continued)

In vitro cap-dependent translation is not inhibited by blocking S83 phosphorylation. A bicistronic luciferase reporter was used in a TNT quick coupled transcription/translation system to produce firefly and renilla luciferase through cap-dependent and cricket paralysis virus (CrPV) IRES-mediated translation, respectively. (A) Addition of GST-4E-BP1 wild-type or S83A mutant decreased translation to similar levels; however, when these were phosphorylated by CDK1 in kinase buffer, translation was rescued. Addition of unphosphorylatable GST-4E-BP1 T37A/T46A inhibited translation even when reacted with CDK1. Translation was unaffected by GST protein alone. Cap-dependent translation specific inhibition by m7GTP cap analog incubation was used as a negative control. Luciferase activity was measured in relative light units (RLU). (B) IRES cap-independent translation using a CrPV IRES renilla luciferase reporter was unaffected by addition of GST-4E-BP1 as expected. (C) Recombinant GST-4E-BP1 and GST protein added in each translation reaction was immunoblotted with phospho-4E-BP1 antibodies.

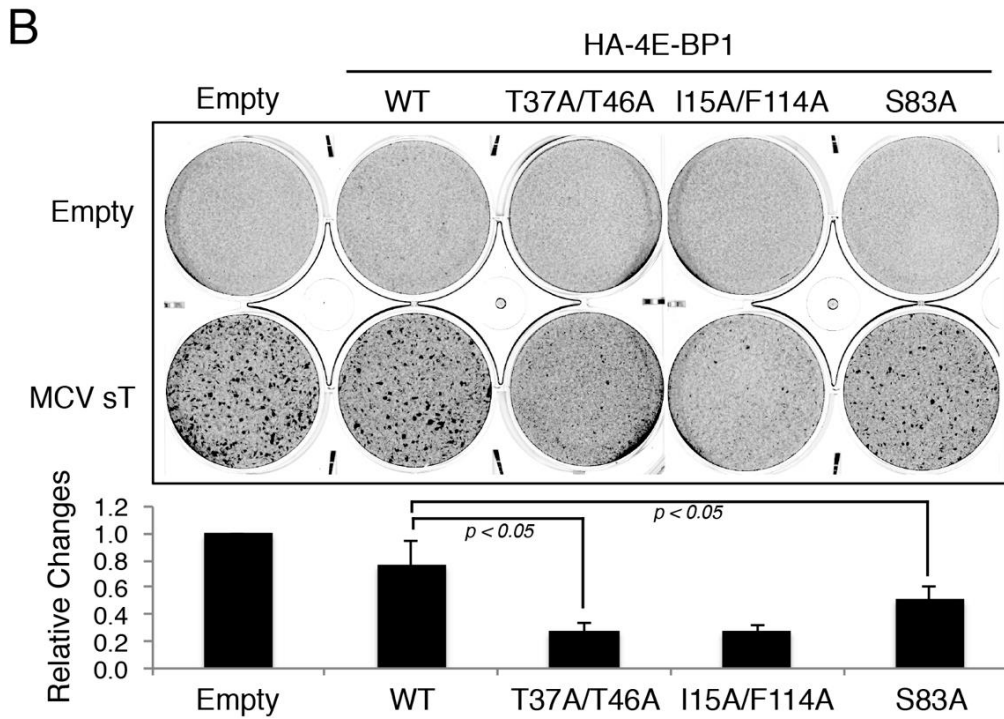
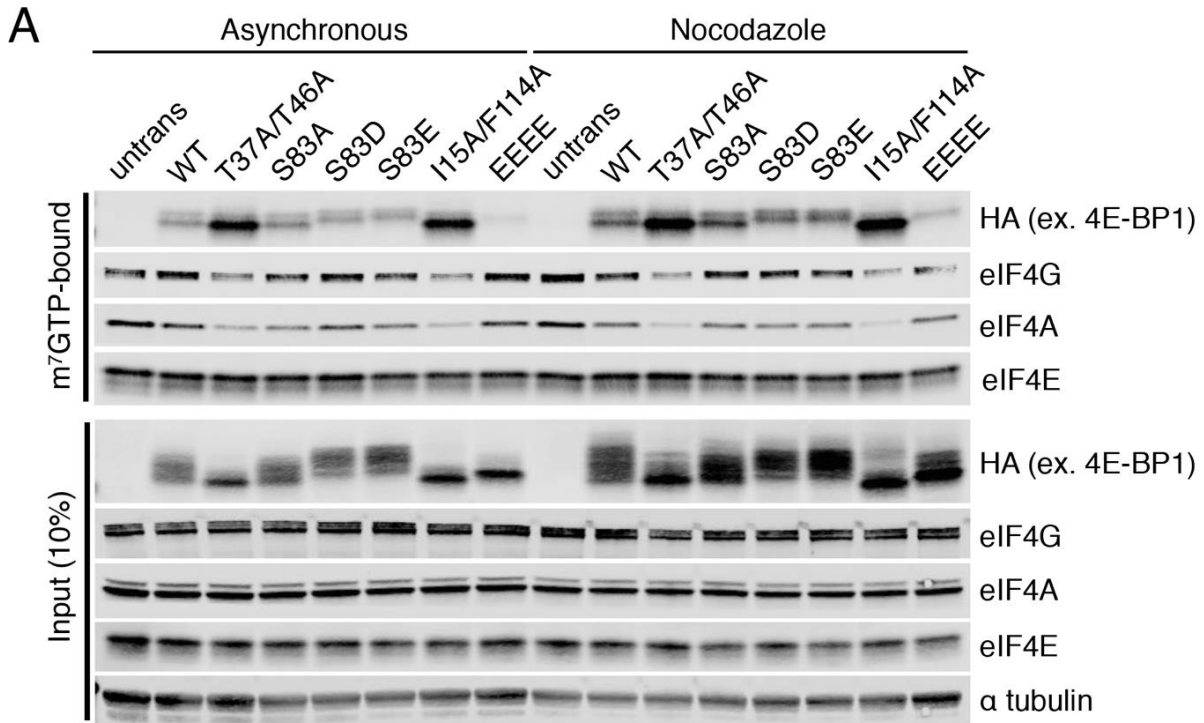


Figure 38. Mutation of 4E-BP1 at S83 does not affect general cap-dependent translation initiation complex formation but partially reverses MCV sT-induced Rat-1 cell transformation.

Figure 38 (continued)

(A) eIF4F cap-binding is not affected by S83 phosphorylation. 293 cells were transfected with wild-type HA-tagged 4E-BP1 and mutants T37A/T46A, S83A, S83D, S83E, I15A/F114A, and T37E/T46E/S65E/T70E (EEEE). After 48 h, cells were treated with DMSO or nocodazole for 20 h and harvested. Cell lysates were either directly immunoblotted (input) or mixed with m7GTP coupled sepharose beads, precipitated, and immunoblotted. S83A, S83D, and S83E mutants did not differ from wild-type 4E-BP1 in their binding to cap-bound eIF4E and did not affect eIF4G and eIF4A association to eIF4E. HA-4E-BP1 phosphorylation mutant T37A/T46A and mTORC1-binding mutant I15A/F114A reduced eIF4G and eIF4A binding, whereas the opposite pattern was found for negative control phosphomimetic mutant EEEE. Comparable amounts of eIF4G and eIF4A were pulled down with m7GTP beads for both asynchronous and mitotic cells. (B) A representative foci formation assay with the MCV sT viral oncoprotein in Rat-1 cells stably expressing HA-tagged 4E-BP1 wild type (WT), T37A/T46A, I15A/F114A, S83A mutants, and empty vector. Foci formed two weeks after MCV sT lentivirus transduction were stained with 0.5% crystal violet. Crystal violet staining intensity was measured using the LICOR infrared scanner. For each stable cell line, crystal violet staining intensity of empty vector-transduced cells was subtracted from that of sT-transduced cells, and relative intensity to empty vector control was determined for each HA-4E-BP1 mutant. Results are mean \pm SD from three-independent experiments.

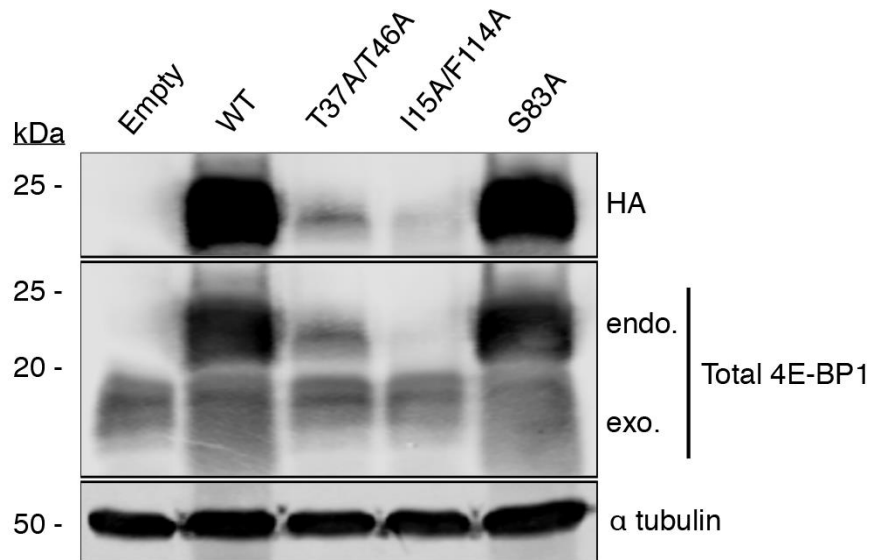


Figure 39. Expression of HA-tagged 4E-BP1 in Rat-1 cells used for transformation assays.

Rat-1 cells stably transduced with HA-tagged 4E-BP1 wild type (WT), T37A/T46A, I15A/F114A, S83A mutants, and empty vector were harvested prior to transformation assays and subjected to immunoblotting. Protein levels of WT and S83A-mutated 4E-BP1 were comparable, while expression of non-phosphorylatable mutants T37A/T46A and I15A/F114A was lower in comparison, as expected since they inhibit their own translation.

3.4 DISCUSSION

During mitosis, 4E-BP1 is hyperphosphorylated, rendering it inactive as a cap-dependent translation gate keeper (209). Our current studies show that S83-phosphorylated δ -4E-BP1 is specific to mitosis and is a result of CDK1 activity. When S83 is mutated to a non-phosphorylatable alanine, no changes in cap-binding or cap-dependent translation were detected. Instead, loss of this phosphorylation site partially reverses cell transformation caused by MCV small T oncoprotein. Unlike α - γ phosphorylated 4E-BP1 isoforms, δ -4E-BP1 preferentially accumulates at centrosomes during mitosis. Unlike 4E-BP1 phosphorylation by mTOR kinase at canonical sites, CDK1 phosphorylation of 4E-BP1 at S83 may lead to a gain-of-function for this hyperphosphorylated protein (**Figure 40**).

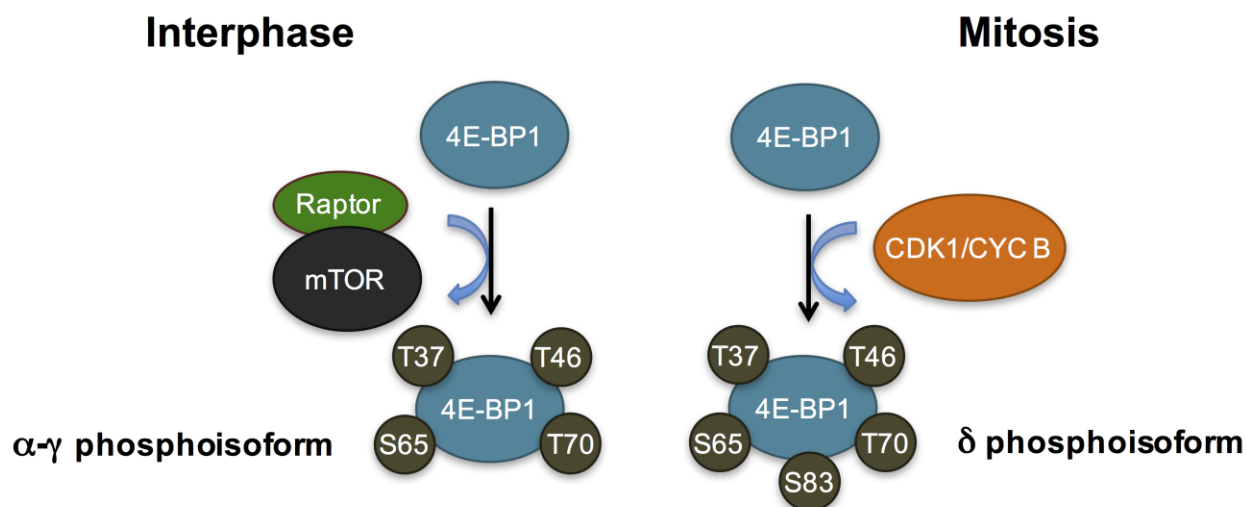


Figure 40. Novel mitosis-specific phosphorylation of 4E-BP1 Ser83 by CDK1.

Our findings confirm previous studies showing δ -4E-BP1 expression in multiple cell lines synchronized in mitosis by chemical or mechanical means (207, 208). Treatment with nocodazole, a microtubule-destabilizing drug, induced δ -4E-BP1 across

all cell lines. While mTOR inhibition by PP242 eliminates most phosphorylated 4E-BP1 isoforms in asynchronous cells, it does not affect δ -4E-BP1. The appearance of α , β , and γ forms of 4E-BP1 in nocodazole-arrested cells is likely due to interphase cell contamination resulting from differences in synchronization efficiency between cell lines. This would explain their sensitivity to PP242 treatment. As predicted by immunoblotting, flow cytometry analysis of all cell lines tested shows that pH3^{S10+} mitotic cells exhibit higher levels of p4E-BP1^{T37/T46+} than pH3^{S10-} interphase cells.

Because of its low abundance in asynchronous cells, S83 phosphorylation has not been thus far amenable to investigation in contrast to the canonical mTOR-regulated sites—T37, T46, S65, and T70 (154). We hypothesized that δ -4E-BP1 from mitotic cells has additional phosphorylation sites that have been missed in previous analyses where mitotic cells comprise less than 1% of all cells in bulk culture. We subjected interphase (mitosis-depleted) and mitotic (mitosis-enriched) HeLa and 293 cells for mass spectrometric analysis, and although our results were not quantitative, we identified S83 phosphorylation exclusively in mitotic cells. Mutation of mTOR priming sites T37A/T46A did not inhibit S83 phosphorylation in mitotic cells, suggesting that S83 targeting may not rely on mTOR activity as also evidenced by PP242-mediated mTOR inhibition. Our epitope-tagged 4E-BP1 construct does not migrate the same way as endogenous 4E-BP1 and makes it difficult to assess each phospho-isoform discretely. Nonetheless, we are confident that the highest molecular weight form of HA-tagged 4E-BP1 induced during mitosis represents δ -4E-BP1.

By generating a polyclonal antibody against p4E-BP1^{S83}, we were able to confirm that δ -4E-BP1 is phosphorylated at S83 and that this antibody can be used as a mitotic

marker for immunoblotting, immunofluorescence, and flow cytometry. We were also able to localize a portion of S83-phosphorylated 4E-BP1 at the centrosomes consistent with a previous report, which shows that 4E-BP1 knockdown leads to multipolar spindles and misaligned chromosomes (210). Further, S83 phosphorylation increased from prophase to metaphase and decreased thereafter, which is in agreement with nocodazole synchronization results and with the timing of CDK1 activity (367).

The p4E-BP1^{S83} antibody also enabled us to determine that CDK1 is the first kinase known to phosphorylate 4E-BP1 at the five phospho-residues (T37, T46, S65, T70, and S83) conserved in all three 4E-BPs—4E-BP1, 2, and 3 (144). The polyclonal p4E-BP1^{S83} antiserum has cross-reactivity against non-phosphorylated S83 that requires pre-absorption or peptide blocking, which would explain why unreacted GST-4E-BP1 can still be detected in our in vitro phosphorylation assays. However, the substantial increase in p4E-BP1^{S83} signal in ATP-supplemented reactions confirms our in vivo results. Epitope competition assay with dephosphorylated GST-4E-BP1 also shows that the antiserum is specific for S83-phosphorylated 4E-BP1 (**Figure 35B**). Nevertheless, all immunofluorescence colocalization studies were performed using antiserum pre-absorbed with non-phosphorylated peptide ⁷⁷TIPGVTSPSSDEP⁸⁹.

Others have reported and established modulation of cap-dependent translation through 4E-BP1 phosphorylation at mTOR-targeted sites. Using in vitro translation and m7GTP cap-affinity pulldown assays, we do not find general cap-dependent translation regulation by 4E-BP1 S83 phosphorylation. However, we cannot exclude the possibility that mRNA subpopulations might be regulated at the translational level by S83-phosphorylated 4E-BP1, such as terminal oligopyrimidine tract (TOP)-containing

mRNAs that are reported to be translationally active during mitosis (208). A recent study shows that the interaction between the C-terminal loop with eIF4E is required for eIF4F complex formation and translation repression in vivo using 4E-BP1 truncation mutants, which, in light of our results, prompts the examination of other loop residues (105). Expression of full-length 4E-BP1 constructs with mutations at canonical and non-canonical eIF4E binding motifs would provide robust evidence for this phenomenon in cells.

Overexpression of constitutively active 4E-BP1 or 4E-BP2 antagonizes cell transformation induced by eIF4E, v-Src, H-Ras, and MCV sT expression, indicating that 4E-BP1 acts as a tumor suppressor (170, 223, 373). Expression of S65A and T70A have also been reported to decrease CREF colony formation, but these results were not confirmed in the presence of an oncogene (374). Our work showing partial reversal of sT-mediated foci formation suggests that 4E-BP1 phosphorylation site S83 contributes to that MCV sT cell transformation activity. sT transformation is eliminated by a raptor-binding mutant of 4E-BP1 (164, 165, 167), suggesting that mTOR and CDK1 cooperatively promote sT-induced cell transformation. These findings hint at the possibility that this residue is also permissive for cell transformation induced by other oncoproteins.

Hyperphosphorylation of 4E-BP1 in various cancers has been strongly suggestive of uncontrolled protein synthesis. However, our study provokes a reassessment of the role of 4E-BP1 in cells, particularly during mitosis. It is possible that the S83-phosphorylated δ -4E-BP1 isoform has a previously undescribed gain-of-function role in mitosis.

4.0 CONCLUSION AND PERSPECTIVES

The work presented in this dissertation provokes a reexamination of mitotic cap-dependent translational control and raises the possibility for novel functions and regulation of the translation repressor protein 4E-BP1 (177, 209). mRNA translation has been assumed to be repressed during mitosis, until recent studies, including the ones in the previous chapters, have come to challenge this dogma (177, 207-209, 243). In previous studies, cells had been arrested in mitosis using microtubule destabilizers, which inadvertently inhibited cap-dependent translation. As the number of studies that use cell cycle synchronization methods that do not affect mRNA translation increases, the old paradigm will have to shift (243). This work also raises the hypothesis that cap-dependent mRNA translation is activated during mitosis to allow for the synthesis of proteins required for re-entry into the cell cycle. In tumorigenesis, it is feasible that the increased mitogenesis of cancer cells facilitates the translation of proto-oncogenes during mitosis, especially those encoded by tumor viruses like MCV. This work indicates that one of the principal events in this process is the hyperphosphorylation-inactivation of 4E-BP1 by the mitotic CDK1 kinase.

4.1 CDK1 REGULATION OF CAP-DEPENDENT TRANSLATION

Apart from challenging the mitotic translation dogma, this work identified a novel pathway that regulates cap-dependent mRNA translation through the mitotic CDK1 kinase. CDK1 takes over for mTOR kinase to activate cap-dependent mRNA translation by targeting 4E-BP1. CDK1 phosphorylates the canonical mTOR-regulated sites T37, T46, S65, and T70 of mitotic δ -4E-BP1 and also the novel S83 during mitosis. CDK1-inhibition by RO-3306 treatment in vivo and in vitro ablates δ -4E-BP1 phosphorylation at all sites. Interestingly, S83 phosphorylation is independent of priming T37/T46 phosphorylation, unlike S65 and T70, which indicates that CDK1 phosphorylates 4E-BP1 in a unique mode that is different from mTOR.

A recent report also indicates that cap-dependent translation is regulated in a similar manner during meiosis of human, mouse, and bovine oocytes (375). Although the authors claim that CDK1 activates mTOR to phosphorylate 4E-BP1 at S65 and T70 in this study, their data also suggest that CDK1 directly phosphorylates meiotic 4E-BP1, in line with our studies on mitotic 4E-BP1 and those of other groups (177, 207-209, 243). This is perhaps a common translation regulatory pathway in general cell division. Moreover, these results encourage further investigation to determine whether other CDKs regulate mRNA translation in other phases of the cell cycle. Identifying non-canonical, alternative pathways for cap-dependent mRNA translation regulation may explain resistance to mTOR-targeted therapies in cancer.

In addition, this work also hints at the existence of novel translational functions for 4E-BP1. Recent structural studies have shown that human eIF4E binds 4E-BP1 not only through its canonical dorsal surface, but also through its lateral surface. Both

human eIF4G and 4E-BP1 compete for dorsal eIF4E binding through their conserved YXXXXLΦ binding motif (103). 4E-BP1, however, has been shown to possess a secondary eIF4E-binding motif, ⁷⁹PGVTS⁸³, that forms a loop structure that contacts the lateral surface of eIF4E (**Figure 41**) (105-107, 370). S83 phosphorylation of 4E-BP1 may regulate the interaction of this loop with the lateral pocket of eIF4E, which may allosterically modulate the occupancy of eIF4G at the dorsal pocket. Whether eIF4G interacts with this non-canonical pocket on eIF4E remains unclear, as differences in protein solubilizing methods have yielded conflicting results (106, 107, 376).

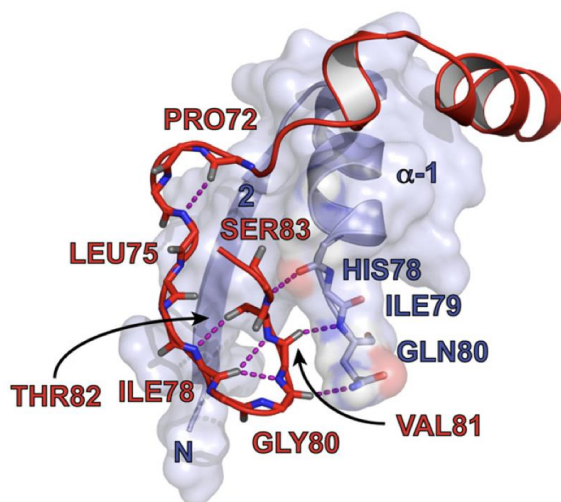


Figure 41. 4E-BP1 S83 is part of the loop binding the lateral pocket of eIF4E.

The secondary eIF4E binding site of 4E-BP1 (residues in red), composed of residues ⁷⁹PGVTS⁸³, makes hydrophobic contacts and hydrogen bonds with the eIF4E residues (in blue) within its lateral binding surface (Modified from Sekiyama et al. 2015 (105)).

Therefore, in this dissertation the effects of S83 phosphorylation on cap-dependent translation regulation by 4E-BP1 were also investigated. In vitro translation reactions with a recombinant GST-4E-BP1 S83A mutant did not affect cap-dependent translation compared to wild-type 4E-BP1. Cap-binding assays that measure translation initiation complex formation in cells did not show a significant difference between wild-type 4E-BP1 and the S83A mutant. This was unexpected in light of the presence of S83

on the secondary eIF4E binding motif recently identified on 4E-BP1. Interestingly, MCV sT-induced cell transformation of Rat1 cells was partially reversed by expression of the 4E-BP1 S83A mutant. Although no significant change in global cap-dependent mRNA translation was observed, these results suggest that S83 phosphorylation contributes to MCV sT-induced transformation.

It cannot be ruled out, however, that 4E-BP1 S83 phosphorylation modulates the translation of mRNA subpopulations with different 5' UTR compositions. Ribosomal profiling studies have identified that mRNAs that contain a terminal oligopyrimidine (TOP) tract in their 5' UTR are regulated by mTORC1 and are associated with increased 4E-BP1 phosphorylation (79, 80). Interestingly, TOP-containing mRNAs encoding ribosomal proteins and translation factors have also been reported to be actively translated during mitosis (244). It is possible that CDK1, instead of mTOR, activates the translation of these messages during mitosis. During mitosis, 4E-BP1 is phosphorylated by CDK1 near its canonical and non-canonical eIF4E binding motifs. In interphase, on the other hand, 4E-BP1 is not phosphorylated at the non-canonical loop containing S83, with which it could exert some inhibitory impact on eIF4E and mRNA translation that is absent during mitosis. Thus, 4E-BP1 S83 phosphorylation may regulate the translation of mRNA subpopulations, such as those containing TOP motifs, which can be distinguished from global mRNA translation using ribosomal profiling. Recent studies, however, have identified the La-related protein 1 (LARP1) as the main regulator of TOP mRNA translation in asynchronous cell populations (377). LARP1 binds the 5' cap of TOP messages and thus blocks eIF4F complex assembly (378). Activated mTORC1 sequesters LARP1 through its Raptor subunit to activate TOP

mRNA translation (379), which would explain the observed decreased translation of TOP mRNAs upon mTORC1 inhibition in the ribosomal profiling studies. Whether CDK1 or 4E-BP1 substitute for or work with LARP1 during mitosis remains to be explored.

4.2 S83-PHOSPHORYLATED 4E-BP1 AND MITOTIC TRANSIT

This work also demonstrates that δ -4E-BP1 is a common feature of mitotic cells. Multiple cancer cell lines that were arrested in mitosis expressed the δ -4E-BP1 phospho-isoform, which was unaffected by treatment with the mTOR inhibitor PP242. These mitotic cells had the highest level of 4E-BP1 phosphorylation as compared to corresponding interphase cells, supporting the notion that 4E-BP1 is fully inactivated during mitosis. Mass spectrometry analysis of 293 and HeLa cells identified a non-canonical phospho-S83 4E-BP1 peptide found only in mitotic cells, which led to the generation of a rabbit polyclonal antibody against this phospho-peptide. When tested by immunoblotting, the antibody recognized only δ -4E-BP1 in mitotic cell lysates, showing that S83 phosphorylation is a component of this phospho-species. Dual flow cytometry staining for mitotic marker phospho-S10 histone H3 and phospho-S83 4E-BP1 confirmed that only mitotic cells express S83-phosphorylated 4E-BP1.

Immunofluorescence assays also demonstrated that phospho-S83 4E-BP1 is a unique marker of mitotic cells by co-staining with phospho-S10 histone H3. S83 phosphorylation is low in prophase, peaks at metaphase, and declines in telophase, which is consistent with the timing of CDK1 activity (345) (**Figure 42**). Confocal microscopy showed that a fraction of phospho-S83 4E-BP1 colocalizes with

centrosomal protein γ -tubulin in mitotic cells. The presence of S83-phosphorylated 4E-BP1 at centrosomes provides clues on a potential novel function for δ -4E-BP1 during mitosis, such as regulating centrosome function. Sheng et al. also reported that 4E-BP1 localizes at centrosomes and plays a role in maintaining normal mitotic transit (210). Interestingly, abnormal spindle formation is observed when 4E-BP1 is depleted (210). The aforementioned study on mammalian oocytes shows that 4E-BP1 phosphorylated at S65 colocalizes with centrosomes and 4E-BP1 phosphorylated at T70 colocalizes with spindle fibers (375). Spindle defects are also observed in meiotic cells expressing a non-phosphorylatable 4E-BP1 mutant (375). These findings suggest that 4E-BP1 serves an important role in cell division of somatic and germ cells alike, where S83 phosphorylation might be a critical switch in this process.

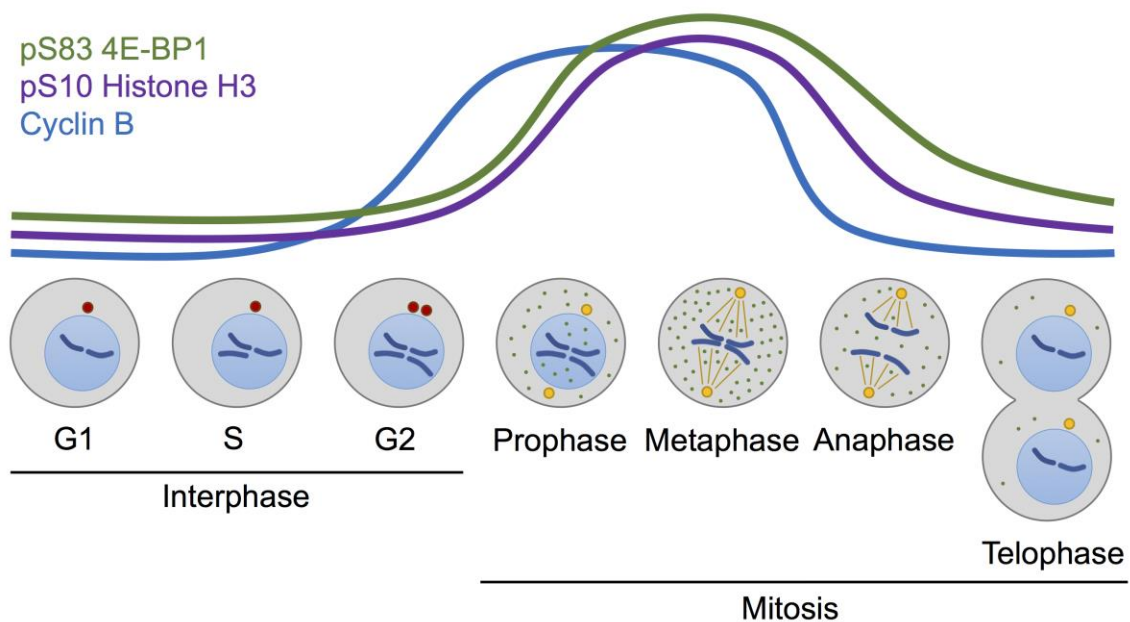


Figure 42. S83-phosphorylated 4E-BP1 is a novel mitotic marker.

This diagram shows the cell cycle timing of phospho-S83 4E-BP1 (green) compared to that of mitotic markers phospho-S10 histone H3 (purple) and cyclin B (blue). Phospho-S83 4E-BP1 is not present in interphase centrosomes (red dots) but colocalizes with mitotic centrosomes (yellow dots).

4.3 TUMOR VIRUS INDUCTION OF MITOTIC TRANSLATION

Human tumor viruses have been shown to manipulate the cell cycle by targeting mitotic E3 ligases in order to enhance the expression and stability of their own proteins. Four human tumor viruses—HBV, HTLV-1, HPV, and MCV—encode proteins that have no role in infection (Tax, X, E2, and sT, respectively) but target the mitotic anaphase-promoting complex/cyclosome (APC/C) checkpoint (380). The Merkel cell polyomavirus (MCV) viral oncoprotein small T antigen (sT) inhibits the APC/C cdc20 E3 ligase and promotes mitotic arrest, similar to the cellular APC/C inhibitor Emi1 (209, 245). In addition, MCV sT induces the hyperphosphorylation and inactivation of cap-dependent translation inhibitor 4E-BP1 during mitosis, which is required for the transforming activity of MCV sT (170). While mTOR regulates 4E-BP1 during interphase, MCV sT-activated mitotic kinase CDK1 hyperphosphorylates 4E-BP1 to generate the high molecular weight δ -4E-BP1 phospho-isoform. Studies with MCV sT revealed that cap-dependent translation is active during mitosis and suggest that mRNA translation is regulated at different phases of the cell cycle. In support of this notion, recent studies have shown that translation of APC/C inhibitor Emi1 is repressed during mitosis (245), while TOP-containing mRNAs are actively translated in this phase of the cell cycle (244).

This work opens up the possibility that the cell cycle is coupled to the regulation of translation, in addition to transcription. MCV appears to manipulate the cell cycle by targeting APC/C, possibly to promote a state where cap-dependent translation remains active even in mitosis. As a consequence, synthesis of viral proteins would proceed unhindered, yet this manipulation may also inadvertently lead to unscheduled, abnormal mitosis and tumorigenesis. S83-phosphorylated δ -4E-BP1 may be contributing to

malignant transformation during viral APC-targeting induced mitosis. Other viruses, such as adenovirus, orf virus, CAV, and HCMV, have also been reported to target APC (380). Just as some viruses induce S phase entry to replicate their DNA, some may also induce mitotic entry to translate their mRNA.

4.4 FUTURE DIRECTIONS

Collectively, the studies presented in this dissertation describe a novel regulatory mechanism for cap-dependent mRNA translation during mitosis. Future work to understand this mechanism will focus primarily on the following objectives: 1) identifying mRNAs that are preferentially translated during mitosis through CDK1 phosphorylation of 4E-BP1 and 2) determining whether 4E-BP1 S83 phosphorylation modulates its interaction with the lateral surface of eIF4E and affects mitotic spindle function.

To address the first research objective, RNA-immunoprecipitation-coupled sequencing (RIP-seq) and ribosomal profiling analyses will be employed (381, 382). Through RIP-seq analysis, mRNAs that co-purify with endogenous 4E-BP1 from interphase and mitotic cells will be identified and compared. Given the possibility that S83 phosphorylation may abolish the interaction between 4E-BP1 and eIF4E, transcripts that are translationally activated by this S83 modification during mitosis are expected to co-purify with 4E-BP1 from interphase cells, where they are translationally repressed. To confirm these results, ribosomal profiling will be used as in previous studies (244, 245) to identify ribosome-protected, translationally active mRNAs from interphase and mitotic cells. Additionally, ribosomal profiling studies will examine

translation regulation by 4E-BP1 S83 mutants. For this purpose, 4E-BP1 knockout cell lines will be used to stably express wild-type 4E-BP1 and phospho-defective and phospho-mimetic S83 mutants. It is anticipated that differences in translation of mRNAs across wild-type and S83 mutant cell lines will reflect differences observed in mitotic and interphase parental cell populations. Through these studies, mRNA subpopulations that are regulated by CDK1 through 4E-BP1 phosphorylation will be identified, and it is expected that some of these genes may contribute to tumorigenesis.

To address the second objective, pull-down assays will be used to investigate the interaction of the 4E-BP1 ⁷⁹PGVTS⁸³ binding motif with eIF4E, and immunofluorescence assays will be used to investigate the connection between 4E-BP1 and mitotic spindle function. The 7-methyl-guanine cap pull-down assays shown in the previous chapter showed that 4E-BP1 S83 phosphorylation mutants did not differ significantly from the wild-type protein in their interaction with cap-bound eIF4E. Immunoprecipitation and tandem-affinity purification (TAP) assays will be used to pull down wild-type 4E-BP1 and S83 mutants directly to determine whether there are indeed no significant differences between these proteins (383). 4E-BP1 mutants that cannot bind eIF4E through its dorsal surface, with alanine mutations at Y54 and L59, will be included to confirm these results. To determine the role of 4E-BP1 in mitotic spindle function, 4E-BP1 knockout cell lines will also be used as in the previous objective. Immunofluorescence assays staining for tubulin will show any differences in spindle assembly across mitotic cells expressing wild-type 4E-BP1 and S83 phosphorylation mutants. It is expected that cells expressing 4E-BP1 S83A will exhibit spindle defects similar to studies in oocytes (375). All in all, these experiments will hopefully uncover novel functional aspects of 4E-BP1.

5.0 BIBLIOGRAPHY

1. Merrick WC (1992) Mechanism and regulation of eukaryotic protein synthesis. *Microbiol Rev* 56(2):291-315.
2. Sonenberg N & Hinnebusch AG (2009) Regulation of translation initiation in eukaryotes: mechanisms and biological targets. *Cell* 136(4):731-745.
3. Jackson RJ, Hellen CU, & Pestova TV (2010) The mechanism of eukaryotic translation initiation and principles of its regulation. *Nat Rev Mol Cell Biol* 11(2):113-127.
4. Terenin IM, Smirnova VV, Andreev DE, Dmitriev SE, & Shatsky IN (2017) A researcher's guide to the galaxy of IRESs. *Cell Mol Life Sci* 74(8):1431-1455.
5. Meyer KD, *et al.* (2015) 5' UTR m(6)A Promotes Cap-Independent Translation. *Cell* 163(4):999-1010.
6. Sonenberg N, Rupprecht KM, Hecht SM, & Shatkin AJ (1979) Eukaryotic mRNA cap binding protein: purification by affinity chromatography on sepharose-coupled m7GDP. *Proc Natl Acad Sci U S A* 76(9):4345-4349.
7. Sonenberg N, Morgan MA, Merrick WC, & Shatkin AJ (1978) A polypeptide in eukaryotic initiation factors that crosslinks specifically to the 5'-terminal cap in mRNA. *Proc Natl Acad Sci U S A* 75(10):4843-4847.
8. Korneeva NL, Lamphear BJ, Hennigan FL, Merrick WC, & Rhoads RE (2001) Characterization of the two eIF4A-binding sites on human eIF4G-1. *J Biol Chem* 276(4):2872-2879.
9. Korneeva NL, Lamphear BJ, Hennigan FL, & Rhoads RE (2000) Mutually cooperative binding of eukaryotic translation initiation factor (eIF) 3 and eIF4A to human eIF4G-1. *J Biol Chem* 275(52):41369-41376.

10. Gingras AC, Raught B, & Sonenberg N (1999) eIF4 initiation factors: effectors of mRNA recruitment to ribosomes and regulators of translation. *Annu Rev Biochem* 68:913-963.
11. Grosfeld H & Ochoa S (1980) Purification and properties of the double-stranded RNA-activated eukaryotic initiation factor 3 kinase from rabbit reticulocytes. *Proc Natl Acad Sci U S A* 77(11):6526-6530.
12. Pestova TV, Borukhov SI, & Hellen CU (1998) Eukaryotic ribosomes require initiation factors 1 and 1A to locate initiation codons. *Nature* 394(6696):854-859.
13. Trachsel H, Erni B, Schreier MH, & Staehelin T (1977) Initiation of mammalian protein synthesis. II. The assembly of the initiation complex with purified initiation factors. *J Mol Biol* 116(4):755-767.
14. Benne R, Brown-Luedi ML, & Hershey JW (1978) Purification and characterization of protein synthesis initiation factors eIF-1, eIF-4C, eIF-4D, and eIF-5 from rabbit reticulocytes. *J Biol Chem* 253(9):3070-3077.
15. Peterson DT, Safer B, & Merrick WC (1979) Role of eukaryotic initiation factor 5 in the formation of 80 S initiation complexes. *J Biol Chem* 254(16):7730-7735.
16. Chaudhuri J, Chowdhury D, & Maitra U (1999) Distinct functions of eukaryotic translation initiation factors eIF1A and eIF3 in the formation of the 40 S ribosomal preinitiation complex. *J Biol Chem* 274(25):17975-17980.
17. Battiste JL, Pestova TV, Hellen CU, & Wagner G (2000) The eIF1A solution structure reveals a large RNA-binding surface important for scanning function. *Mol Cell* 5(1):109-119.
18. Majumdar R, Bandyopadhyay A, & Maitra U (2003) Mammalian translation initiation factor eIF1 functions with eIF1A and eIF3 in the formation of a stable 40 S preinitiation complex. *J Biol Chem* 278(8):6580-6587.
19. Sachs A (1990) The role of poly(A) in the translation and stability of mRNA. *Curr Opin Cell Biol* 2(6):1092-1098.
20. Kahvejian A, Roy G, & Sonenberg N (2001) The mRNA closed-loop model: the function of PABP and PABP-interacting proteins in mRNA translation. *Cold Spring Harb Symp Quant Biol* 66:293-300.
21. Kozak M (1989) The scanning model for translation: an update. *J Cell Biol* 108(2):229-241.

22. Lopez-Lastra M, Rivas A, & Barria MI (2005) Protein synthesis in eukaryotes: the growing biological relevance of cap-independent translation initiation. *Biol Res* 38(2-3):121-146.
23. Pelletier J & Sonenberg N (1988) Internal initiation of translation of eukaryotic mRNA directed by a sequence derived from poliovirus RNA. *Nature* 334(6180):320-325.
24. Etchison D, Milburn SC, Edery I, Sonenberg N, & Hershey JW (1982) Inhibition of HeLa cell protein synthesis following poliovirus infection correlates with the proteolysis of a 220,000-dalton polypeptide associated with eucaryotic initiation factor 3 and a cap binding protein complex. *J Biol Chem* 257(24):14806-14810.
25. Lomakin IB, Hellen CU, & Pestova TV (2000) Physical association of eukaryotic initiation factor 4G (eIF4G) with eIF4A strongly enhances binding of eIF4G to the internal ribosomal entry site of encephalomyocarditis virus and is required for internal initiation of translation. *Mol Cell Biol* 20(16):6019-6029.
26. Stein I, *et al.* (1998) Translation of vascular endothelial growth factor mRNA by internal ribosome entry: implications for translation under hypoxia. *Mol Cell Biol* 18(6):3112-3119.
27. Ling J, Morley SJ, & Traugh JA (2005) Inhibition of cap-dependent translation via phosphorylation of eIF4G by protein kinase Pak2. *EMBO J* 24(23):4094-4105.
28. Holcik M, Lefebvre C, Yeh C, Chow T, & Korneluk RG (1999) A new internal-ribosome-entry-site motif potentiates XIAP-mediated cytoprotection. *Nat Cell Biol* 1(3):190-192.
29. Qin X & Sarnow P (2004) Preferential translation of internal ribosome entry site-containing mRNAs during the mitotic cycle in mammalian cells. *J Biol Chem* 279(14):13721-13728.
30. Pyronnet S, Pradayrol L, & Sonenberg N (2000) A cell cycle-dependent internal ribosome entry site. *Mol Cell* 5(4):607-616.
31. Kaiser C, *et al.* (2008) Activation of cap-independent translation by variant eukaryotic initiation factor 4G in vivo. *RNA* 14(10):2170-2182.
32. Johannes G & Sarnow P (1998) Cap-independent polysomal association of natural mRNAs encoding c-myc, BiP, and eIF4G conferred by internal ribosome entry sites. *RNA* 4(12):1500-1513.

33. Hundsdorfer P, Thoma C, & Hentze MW (2005) Eukaryotic translation initiation factor 4G1 and p97 promote cellular internal ribosome entry sequence-driven translation. *Proc Natl Acad Sci U S A* 102(38):13421-13426.
34. de Breyne S, Yu Y, Unbehaun A, Pestova TV, & Hellen CU (2009) Direct functional interaction of initiation factor eIF4G with type 1 internal ribosomal entry sites. *Proc Natl Acad Sci U S A* 106(23):9197-9202.
35. Nanbru C, *et al.* (1997) Alternative translation of the proto-oncogene c-myc by an internal ribosome entry site. *J Biol Chem* 272(51):32061-32066.
36. Stoneley M, Paulin FE, Le Quesne JP, Chappell SA, & Willis AE (1998) C-Myc 5' untranslated region contains an internal ribosome entry segment. *Oncogene* 16(3):423-428.
37. Vagner S, *et al.* (1995) Alternative translation of human fibroblast growth factor 2 mRNA occurs by internal entry of ribosomes. *Mol Cell Biol* 15(1):35-44.
38. Kozak M (2005) A second look at cellular mRNA sequences said to function as internal ribosome entry sites. *Nucleic Acids Res* 33(20):6593-6602.
39. Komar AA & Hatzoglou M (2011) Cellular IRES-mediated translation: the war of ITAFs in pathophysiological states. *Cell Cycle* 10(2):229-240.
40. Dominissini D, *et al.* (2012) Topology of the human and mouse m6A RNA methylomes revealed by m6A-seq. *Nature* 485(7397):201-206.
41. Meyer KD, *et al.* (2012) Comprehensive analysis of mRNA methylation reveals enrichment in 3' UTRs and near stop codons. *Cell* 149(7):1635-1646.
42. Wang X, *et al.* (2015) N(6)-methyladenosine Modulates Messenger RNA Translation Efficiency. *Cell* 161(6):1388-1399.
43. Zhou J, *et al.* (2015) Dynamic m(6)A mRNA methylation directs translational control of heat shock response. *Nature* 526(7574):591-594.
44. Lin S, Choe J, Du P, Triboulet R, & Gregory RI (2016) The m(6)A Methyltransferase METTL3 Promotes Translation in Human Cancer Cells. *Mol Cell* 62(3):335-345.
45. Muthukrishnan S, *et al.* (1975) mRNA methylation and protein synthesis in extracts from embryos of brine shrimp, *Artemia salina*. *J Biol Chem* 250(24):9336-9341.

46. Miller AO, Dhont E, De Vreese AM, & Van Nimmen L (1968) Study of messenger like RNA extracted from HeLa cells polysomes. I. Sedimentation and chromatographic data. *Biochem Biophys Res Commun* 33(4):702-708.
47. Prichard PM, Gilbert JM, Shafritz DA, & Anderson WF (1970) Factors for the initiation of haemoglobin synthesis by rabbit reticulocyte ribosomes. *Nature* 226(5245):511-514.
48. Weissbach H & Ochoa S (1976) Soluble factors required for eukaryotic protein synthesis. *Annu Rev Biochem* 45:191-216.
49. Palmiter RD (1972) Regulation of protein synthesis in chick oviduct. II. Modulation of polypeptide elongation and initiation rates by estrogen and progesterone. *J Biol Chem* 247(21):6770-6780.
50. Perry RP & Kelley DE (1975) Methylated constituents of heterogeneous nuclear RNA: presence in blocked 5' terminal structures. *Cell* 6(1):13-19.
51. Shatkin AJ (1976) Capping of eucaryotic mRNAs. *Cell* 9(4 PT 2):645-653.
52. Pillutla RC, Shimamoto A, Furuichi Y, & Shatkin AJ (1998) Human mRNA capping enzyme (RNGTT) and cap methyltransferase (RNMT) map to 6q16 and 18p11.22-p11.23, respectively. *Genomics* 54(2):351-353.
53. Tsukamoto T, Shibagaki Y, Niikura Y, & Mizumoto K (1998) Cloning and characterization of three human cDNAs encoding mRNA (guanine-7-)-methyltransferase, an mRNA cap methylase. *Biochem Biophys Res Commun* 251(1):27-34.
54. Topisirovic I, Svitkin YV, Sonenberg N, & Shatkin AJ (2011) Cap and cap-binding proteins in the control of gene expression. *Wiley Interdiscip Rev RNA* 2(2):277-298.
55. Ishigaki Y, Li X, Serin G, & Maquat LE (2001) Evidence for a pioneer round of mRNA translation: mRNAs subject to nonsense-mediated decay in mammalian cells are bound by CBP80 and CBP20. *Cell* 106(5):607-617.
56. Varani G (1997) A cap for all occasions. *Structure* 5(7):855-858.
57. Izaurralde E, *et al.* (1994) A nuclear cap binding protein complex involved in pre-mRNA splicing. *Cell* 78(4):657-668.

58. Izaurralde E, Stepinski J, Darzynkiewicz E, & Mattaj IW (1992) A cap binding protein that may mediate nuclear export of RNA polymerase II-transcribed RNAs. *J Cell Biol* 118(6):1287-1295.
59. Visa N, *et al.* (1996) A pre-mRNA-binding protein accompanies the RNA from the gene through the nuclear pores and into polysomes. *Cell* 84(2):253-264.
60. Cooke C & Alwine JC (1996) The cap and the 3' splice site similarly affect polyadenylation efficiency. *Mol Cell Biol* 16(6):2579-2584.
61. Sonenberg N, Trachsel H, Hecht S, & Shatkin AJ (1980) Differential stimulation of capped mRNA translation in vitro by cap binding protein. *Nature* 285(5763):331-333.
62. Wei C & Moss B (1977) 5'-Terminal capping of RNA by guanylyltransferase from HeLa cell nuclei. *Proc Natl Acad Sci U S A* 74(9):3758-3761.
63. Cory S, Genin C, & Adams JM (1976) Modified nucleosides and 5'-end groups in purified mouse immunoglobulin light chain mRNA and rabbit globin mRNA detected by borohydride labelling. *Biochim Biophys Acta* 454(2):248-262.
64. Johannes G, Carter MS, Eisen MB, Brown PO, & Sarnow P (1999) Identification of eukaryotic mRNAs that are translated at reduced cap binding complex eIF4F concentrations using a cDNA microarray. *Proc Natl Acad Sci U S A* 96(23):13118-13123.
65. Marzluff WF, Wagner EJ, & Duronio RJ (2008) Metabolism and regulation of canonical histone mRNAs: life without a poly(A) tail. *Nat Rev Genet* 9(11):843-854.
66. Ullrich SJ, Appella E, & Mercer WE (1988) Growth-related expression of a 72,000 molecular weight poly(A)⁺ mRNA binding protein. *Exp Cell Res* 178(2):273-286.
67. Gunnery S, Maivali U, & Mathews MB (1997) Translation of an uncapped mRNA involves scanning. *J Biol Chem* 272(34):21642-21646.
68. Gorgoni B & Gray NK (2004) The roles of cytoplasmic poly(A)-binding proteins in regulating gene expression: a developmental perspective. *Brief Funct Genomic Proteomic* 3(2):125-141.

69. Mangus DA, Evans MC, & Jacobson A (2003) Poly(A)-binding proteins: multifunctional scaffolds for the post-transcriptional control of gene expression. *Genome Biol* 4(7):223.
70. Dever TE (2002) Gene-specific regulation by general translation factors. *Cell* 108(4):545-556.
71. Caponigro G & Parker R (1995) Multiple functions for the poly(A)-binding protein in mRNA decapping and deadenylation in yeast. *Genes Dev* 9(19):2421-2432.
72. Gebauer F & Hentze MW (2004) Molecular mechanisms of translational control. *Nat Rev Mol Cell Biol* 5(10):827-835.
73. Kochetov AV, *et al.* (1998) Eukaryotic mRNAs encoding abundant and scarce proteins are statistically dissimilar in many structural features. *FEBS Lett* 440(3):351-355.
74. Damgaard CK & Lykke-Andersen J (2011) Translational coregulation of 5'TOP mRNAs by TIA-1 and TIAR. *Genes Dev* 25(19):2057-2068.
75. Hamilton TL, Stoneley M, Spriggs KA, & Bushell M (2006) TOPs and their regulation. *Biochem Soc Trans* 34(Pt 1):12-16.
76. Iadevaia V, Caldarola S, Tino E, Amaldi F, & Loreni F (2008) All translation elongation factors and the e, f, and h subunits of translation initiation factor 3 are encoded by 5'-terminal oligopyrimidine (TOP) mRNAs. *RNA* 14(9):1730-1736.
77. Yamashita R, *et al.* (2008) Comprehensive detection of human terminal oligopyrimidine (TOP) genes and analysis of their characteristics. *Nucleic Acids Res* 36(11):3707-3715.
78. Patursky-Polischuk I, *et al.* (2009) The TSC-mTOR pathway mediates translational activation of TOP mRNAs by insulin largely in a raptor- or rictor-independent manner. *Mol Cell Biol* 29(3):640-649.
79. Thoreen CC, *et al.* (2012) A unifying model for mTORC1-mediated regulation of mRNA translation. *Nature* 485(7396):109-113.
80. Hsieh AC, *et al.* (2012) The translational landscape of mTOR signalling steers cancer initiation and metastasis. *Nature* 485(7396):55-61.

81. Ingolia NT, Lareau LF, & Weissman JS (2011) Ribosome profiling of mouse embryonic stem cells reveals the complexity and dynamics of mammalian proteomes. *Cell* 147(4):789-802.
82. Kozak M (1991) An analysis of vertebrate mRNA sequences: intimations of translational control. *J Cell Biol* 115(4):887-903.
83. Kozak M (1991) Structural features in eukaryotic mRNAs that modulate the initiation of translation. *J Biol Chem* 266(30):19867-19870.
84. Kozak M (1987) An analysis of 5'-noncoding sequences from 699 vertebrate messenger RNAs. *Nucleic Acids Res* 15(20):8125-8148.
85. Kozak M (1986) Bifunctional messenger RNAs in eukaryotes. *Cell* 47(4):481-483.
86. Kuersten S & Goodwin EB (2003) The power of the 3' UTR: translational control and development. *Nat Rev Genet* 4(8):626-637.
87. Xie X, *et al.* (2005) Systematic discovery of regulatory motifs in human promoters and 3' UTRs by comparison of several mammals. *Nature* 434(7031):338-345.
88. Gallie DR (1991) The cap and poly(A) tail function synergistically to regulate mRNA translational efficiency. *Genes Dev* 5(11):2108-2116.
89. Pelletier J & Sonenberg N (1985) Insertion mutagenesis to increase secondary structure within the 5' noncoding region of a eukaryotic mRNA reduces translational efficiency. *Cell* 40(3):515-526.
90. Koromilas AE, Lazaris-Karatzas A, & Sonenberg N (1992) mRNAs containing extensive secondary structure in their 5' non-coding region translate efficiently in cells overexpressing initiation factor eIF-4E. *EMBO J* 11(11):4153-4158.
91. Jang SK, *et al.* (1988) A segment of the 5' nontranslated region of encephalomyocarditis virus RNA directs internal entry of ribosomes during in vitro translation. *J Virol* 62(8):2636-2643.
92. Hellen CU & Sarnow P (2001) Internal ribosome entry sites in eukaryotic mRNA molecules. *Genes Dev* 15(13):1593-1612.
93. Bushell M & Sarnow P (2002) Hijacking the translation apparatus by RNA viruses. *J Cell Biol* 158(3):395-399.

94. Holcik M & Sonenberg N (2005) Translational control in stress and apoptosis. *Nat Rev Mol Cell Biol* 6(4):318-327.
95. Chen JM, Ferec C, & Cooper DN (2006) A systematic analysis of disease-associated variants in the 3' regulatory regions of human protein-coding genes II: the importance of mRNA secondary structure in assessing the functionality of 3' UTR variants. *Hum Genet* 120(3):301-333.
96. Joshi B, Cameron A, & Jagus R (2004) Characterization of mammalian eIF4E-family members. *Eur J Biochem* 271(11):2189-2203.
97. Osborne MJ, *et al.* (2013) eIF4E3 acts as a tumor suppressor by utilizing an atypical mode of methyl-7-guanosine cap recognition. *Proc Natl Acad Sci U S A* 110(10):3877-3882.
98. Zuberek J, *et al.* (2007) Weak binding affinity of human 4EHP for mRNA cap analogs. *RNA* 13(5):691-697.
99. Poulin F, Gingras AC, Olsen H, Chevalier S, & Sonenberg N (1998) 4E-BP3, a new member of the eukaryotic initiation factor 4E-binding protein family. *J Biol Chem* 273(22):14002-14007.
100. Mader S, Lee H, Pause A, & Sonenberg N (1995) The translation initiation factor eIF-4E binds to a common motif shared by the translation factor eIF-4 gamma and the translational repressors 4E-binding proteins. *Mol Cell Biol* 15(9):4990-4997.
101. Marcotrigiano J, Gingras AC, Sonenberg N, & Burley SK (1997) Cocystal structure of the messenger RNA 5' cap-binding protein (eIF4E) bound to 7-methyl-GDP. *Cell* 89(6):951-961.
102. Chapat C, *et al.* (2017) Cap-binding protein 4EHP effects translation silencing by microRNAs. *Proc Natl Acad Sci U S A*.
103. Marcotrigiano J, Gingras AC, Sonenberg N, & Burley SK (1999) Cap-dependent translation initiation in eukaryotes is regulated by a molecular mimic of eIF4G. *Mol Cell* 3(6):707-716.
104. Pause A, *et al.* (1994) Insulin-dependent stimulation of protein synthesis by phosphorylation of a regulator of 5'-cap function. *Nature* 371(6500):762-767.

105. Sekiyama N, *et al.* (2015) Molecular mechanism of the dual activity of 4EGI-1: Dissociating eIF4G from eIF4E but stabilizing the binding of unphosphorylated 4E-BP1. *Proc Natl Acad Sci U S A* 112(30):E4036-4045.
106. Peter D, *et al.* (2015) Molecular architecture of 4E-BP translational inhibitors bound to eIF4E. *Mol Cell* 57(6):1074-1087.
107. Igreja C, Peter D, Weiler C, & Izaurralde E (2014) 4E-BPs require non-canonical 4E-binding motifs and a lateral surface of eIF4E to repress translation. *Nat Commun* 5:4790.
108. Ray BK, *et al.* (1983) Role of mRNA competition in regulating translation: further characterization of mRNA discriminatory initiation factors. *Proc Natl Acad Sci U S A* 80(3):663-667.
109. Hershey PE, *et al.* (1999) The Cap-binding protein eIF4E promotes folding of a functional domain of yeast translation initiation factor eIF4G1. *J Biol Chem* 274(30):21297-21304.
110. Prevot D, *et al.* (2003) Characterization of a novel RNA-binding region of eIF4G1 critical for ribosomal scanning. *EMBO J* 22(8):1909-1921.
111. Goyer C, *et al.* (1993) TIF4631 and TIF4632: two yeast genes encoding the high-molecular-weight subunits of the cap-binding protein complex (eukaryotic initiation factor 4F) contain an RNA recognition motif-like sequence and carry out an essential function. *Mol Cell Biol* 13(8):4860-4874.
112. Gradi A, *et al.* (1998) A novel functional human eukaryotic translation initiation factor 4G. *Mol Cell Biol* 18(1):334-342.
113. Yan R & Rhoads RE (1995) Human protein synthesis initiation factor eIF-4 gamma is encoded by a single gene (EIF4G) that maps to chromosome 3q27-qter. *Genomics* 26(2):394-398.
114. Tahara SM, Morgan MA, & Shatkin AJ (1981) Two forms of purified m7G-cap binding protein with different effects on capped mRNA translation in extracts of uninfected and poliovirus-infected HeLa cells. *J Biol Chem* 256(15):7691-7694.
115. Martineau Y, *et al.* (2008) Poly(A)-binding protein-interacting protein 1 binds to eukaryotic translation initiation factor 3 to stimulate translation. *Mol Cell Biol* 28(21):6658-6667.

116. Imataka H, Olsen HS, & Sonenberg N (1997) A new translational regulator with homology to eukaryotic translation initiation factor 4G. *EMBO J* 16(4):817-825.
117. Lamphear BJ, *et al.* (1993) Mapping the cleavage site in protein synthesis initiation factor eIF-4 gamma of the 2A proteases from human Coxsackievirus and rhinovirus. *J Biol Chem* 268(26):19200-19203.
118. Lamphear BJ, Kirchwegger R, Skern T, & Rhoads RE (1995) Mapping of functional domains in eukaryotic protein synthesis initiation factor 4G (eIF4G) with picornaviral proteases. Implications for cap-dependent and cap-independent translational initiation. *J Biol Chem* 270(37):21975-21983.
119. Gross JD, *et al.* (2003) Ribosome loading onto the mRNA cap is driven by conformational coupling between eIF4G and eIF4E. *Cell* 115(6):739-750.
120. Imataka H, Gradi A, & Sonenberg N (1998) A newly identified N-terminal amino acid sequence of human eIF4G binds poly(A)-binding protein and functions in poly(A)-dependent translation. *EMBO J* 17(24):7480-7489.
121. Marcotrigiano J, *et al.* (2001) A conserved HEAT domain within eIF4G directs assembly of the translation initiation machinery. *Mol Cell* 7(1):193-203.
122. Morino S, Imataka H, Svitkin YV, Pestova TV, & Sonenberg N (2000) Eukaryotic translation initiation factor 4E (eIF4E) binding site and the middle one-third of eIF4GI constitute the core domain for cap-dependent translation, and the C-terminal one-third functions as a modulatory region. *Mol Cell Biol* 20(2):468-477.
123. Pyronnet S, *et al.* (1999) Human eukaryotic translation initiation factor 4G (eIF4G) recruits mnk1 to phosphorylate eIF4E. *EMBO J* 18(1):270-279.
124. Tarun SZ, Jr., Wells SE, Deardorff JA, & Sachs AB (1997) Translation initiation factor eIF4G mediates in vitro poly(A) tail-dependent translation. *Proc Natl Acad Sci U S A* 94(17):9046-9051.
125. Pestova TV, Shatsky IN, & Hellen CU (1996) Functional dissection of eukaryotic initiation factor 4F: the 4A subunit and the central domain of the 4G subunit are sufficient to mediate internal entry of 43S preinitiation complexes. *Mol Cell Biol* 16(12):6870-6878.
126. Parsyan A, *et al.* (2011) mRNA helicases: the tacticians of translational control. *Nat Rev Mol Cell Biol* 12(4):235-245.

127. Linder P & Slonimski PP (1989) An essential yeast protein, encoded by duplicated genes TIF1 and TIF2 and homologous to the mammalian translation initiation factor eIF-4A, can suppress a mitochondrial missense mutation. *Proc Natl Acad Sci U S A* 86(7):2286-2290.
128. Ray A, Walden WE, Brendler T, Zenger VE, & Thach RE (1985) Effect of medium hypertonicity on reovirus translation rates. An application of kinetic modeling in vivo. *Biochemistry* 24(26):7525-7532.
129. Rozen F, *et al.* (1990) Bidirectional RNA helicase activity of eucaryotic translation initiation factors 4A and 4F. *Mol Cell Biol* 10(3):1134-1144.
130. Jaramillo M, Dever TE, Merrick WC, & Sonenberg N (1991) RNA unwinding in translation: assembly of helicase complex intermediates comprising eukaryotic initiation factors eIF-4F and eIF-4B. *Mol Cell Biol* 11(12):5992-5997.
131. Lorsch JR & Herschlag D (1999) Kinetic dissection of fundamental processes of eukaryotic translation initiation in vitro. *EMBO J* 18(23):6705-6717.
132. Rogers GW, Jr., Komar AA, & Merrick WC (2002) eIF4A: the godfather of the DEAD box helicases. *Prog Nucleic Acid Res Mol Biol* 72:307-331.
133. Nielsen PJ & Trachsel H (1988) The mouse protein synthesis initiation factor 4A gene family includes two related functional genes which are differentially expressed. *EMBO J* 7(7):2097-2105.
134. Weinstein DC, Honore E, & Hemmati-Brivanlou A (1997) Epidermal induction and inhibition of neural fate by translation initiation factor 4AIII. *Development* 124(21):4235-4242.
135. Yoder-Hill J, Pause A, Sonenberg N, & Merrick WC (1993) The p46 subunit of eukaryotic initiation factor (eIF)-4F exchanges with eIF-4A. *J Biol Chem* 268(8):5566-5573.
136. Oberer M, Marintchev A, & Wagner G (2005) Structural basis for the enhancement of eIF4A helicase activity by eIF4G. *Genes Dev* 19(18):2212-2223.
137. Kapp LD & Lorsch JR (2004) The molecular mechanics of eukaryotic translation. *Annu Rev Biochem* 73:657-704.
138. Rogers GW, Jr., Richter NJ, Lima WF, & Merrick WC (2001) Modulation of the helicase activity of eIF4A by eIF4B, eIF4H, and eIF4F. *J Biol Chem* 276(33):30914-30922.

139. Fleming K, *et al.* (2003) Solution structure and RNA interactions of the RNA recognition motif from eukaryotic translation initiation factor 4B. *Biochemistry* 42(30):8966-8975.
140. Fonseca BD, *et al.* (2014) The ever-evolving role of mTOR in translation. *Semin Cell Dev Biol* 36:102-112.
141. Dowling RJ, *et al.* (2010) mTORC1-mediated cell proliferation, but not cell growth, controlled by the 4E-BPs. *Science* 328(5982):1172-1176.
142. Kleijn M, Scheper GC, Wilson ML, Tee AR, & Proud CG (2002) Localisation and regulation of the eIF4E-binding protein 4E-BP3. *FEBS Lett* 532(3):319-323.
143. Musa J, *et al.* (2016) Eukaryotic initiation factor 4E-binding protein 1 (4E-BP1): a master regulator of mRNA translation involved in tumorigenesis. *Oncogene* 35(36):4675-4688.
144. Martineau Y, Azar R, Bousquet C, & Pyronnet S (2013) Anti-oncogenic potential of the eIF4E-binding proteins. *Oncogene* 32(6):671-677.
145. Yamaguchi S, *et al.* (2008) ATF4-mediated induction of 4E-BP1 contributes to pancreatic beta cell survival under endoplasmic reticulum stress. *Cell Metab* 7(3):269-276.
146. Ueda T, Watanabe-Fukunaga R, Fukuyama H, Nagata S, & Fukunaga R (2004) Mnk2 and Mnk1 are essential for constitutive and inducible phosphorylation of eukaryotic initiation factor 4E but not for cell growth or development. *Mol Cell Biol* 24(15):6539-6549.
147. Takano S, *et al.* (2007) Smad4 is essential for down-regulation of E-cadherin induced by TGF-beta in pancreatic cancer cell line PANC-1. *J Biochem* 141(3):345-351.
148. Balakumaran BS, *et al.* (2009) MYC activity mitigates response to rapamycin in prostate cancer through eukaryotic initiation factor 4E-binding protein 1-mediated inhibition of autophagy. *Cancer Res* 69(19):7803-7810.
149. Rolli-Derkinderen M, *et al.* (2003) ERK and p38 inhibit the expression of 4E-BP1 repressor of translation through induction of Egr-1. *J Biol Chem* 278(21):18859-18867.

150. Azar R, Najib S, Lahlou H, Susini C, & Pyronnet S (2008) Phosphatidylinositol 3-kinase-dependent transcriptional silencing of the translational repressor 4E-BP1. *Cell Mol Life Sci* 65(19):3110-3117.
151. Rong L, *et al.* (2008) Control of eIF4E cellular localization by eIF4E-binding proteins, 4E-BPs. *RNA* 14(7):1318-1327.
152. Richter JD & Sonenberg N (2005) Regulation of cap-dependent translation by eIF4E inhibitory proteins. *Nature* 433(7025):477-480.
153. Gingras AC, *et al.* (1999) Regulation of 4E-BP1 phosphorylation: a novel two-step mechanism. *Genes Dev* 13(11):1422-1437.
154. Fadden P, Haystead TA, & Lawrence JC, Jr. (1997) Identification of phosphorylation sites in the translational regulator, PHAS-I, that are controlled by insulin and rapamycin in rat adipocytes. *J Biol Chem* 272(15):10240-10247.
155. Haystead TA, Haystead CM, Hu C, Lin TA, & Lawrence JC, Jr. (1994) Phosphorylation of PHAS-I by mitogen-activated protein (MAP) kinase. Identification of a site phosphorylated by MAP kinase in vitro and in response to insulin in rat adipocytes. *J Biol Chem* 269(37):23185-23191.
156. Burnett PE, Barrow RK, Cohen NA, Snyder SH, & Sabatini DM (1998) RAFT1 phosphorylation of the translational regulators p70 S6 kinase and 4E-BP1. *Proc Natl Acad Sci U S A* 95(4):1432-1437.
157. Gingras AC, Kennedy SG, O'Leary MA, Sonenberg N, & Hay N (1998) 4E-BP1, a repressor of mRNA translation, is phosphorylated and inactivated by the Akt(PKB) signaling pathway. *Genes Dev* 12(4):502-513.
158. Hara K, *et al.* (1997) Regulation of eIF-4E BP1 phosphorylation by mTOR. *J Biol Chem* 272(42):26457-26463.
159. Mamane Y, Petroulakis E, LeBacquer O, & Sonenberg N (2006) mTOR, translation initiation and cancer. *Oncogene* 25(48):6416-6422.
160. Abraham RT & Wiederrecht GJ (1996) Immunopharmacology of rapamycin. *Annu Rev Immunol* 14:483-510.
161. Hara K, *et al.* (2002) Raptor, a binding partner of target of rapamycin (TOR), mediates TOR action. *Cell* 110(2):177-189.

162. Toschi A, *et al.* (2009) Regulation of mTORC1 and mTORC2 complex assembly by phosphatidic acid: competition with rapamycin. *Mol Cell Biol* 29(6):1411-1420.
163. Herbert TP, Tee AR, & Proud CG (2002) The extracellular signal-regulated kinase pathway regulates the phosphorylation of 4E-BP1 at multiple sites. *J Biol Chem* 277(13):11591-11596.
164. Beugnet A, Wang X, & Proud CG (2003) Target of rapamycin (TOR)-signaling and RAIP motifs play distinct roles in the mammalian TOR-dependent phosphorylation of initiation factor 4E-binding protein 1. *J Biol Chem* 278(42):40717-40722.
165. Schalm SS, Fingar DC, Sabatini DM, & Blenis J (2003) TOS motif-mediated raptor binding regulates 4E-BP1 multisite phosphorylation and function. *Curr Biol* 13(10):797-806.
166. Tee AR & Proud CG (2002) Caspase cleavage of initiation factor 4E-binding protein 1 yields a dominant inhibitor of cap-dependent translation and reveals a novel regulatory motif. *Mol Cell Biol* 22(6):1674-1683.
167. Choi KM, McMahon LP, & Lawrence JC, Jr. (2003) Two motifs in the translational repressor PHAS-I required for efficient phosphorylation by mammalian target of rapamycin and for recognition by raptor. *J Biol Chem* 278(22):19667-19673.
168. Coffman K, *et al.* (2014) Characterization of the Raptor/4E-BP1 interaction by chemical cross-linking coupled with mass spectrometry analysis. *J Biol Chem* 289(8):4723-4734.
169. Schalm SS & Blenis J (2002) Identification of a conserved motif required for mTOR signaling. *Curr Biol* 12(8):632-639.
170. Shuda M, Kwun HJ, Feng H, Chang Y, & Moore PS (2011) Human Merkel cell polyomavirus small T antigen is an oncoprotein targeting the 4E-BP1 translation regulator. *J Clin Invest* 121(9):3623-3634.
171. Matsuo H, *et al.* (1997) Structure of translation factor eIF4E bound to m7GDP and interaction with 4E-binding protein. *Nat Struct Biol* 4(9):717-724.
172. Gingras AC, *et al.* (2001) Hierarchical phosphorylation of the translation inhibitor 4E-BP1. *Genes Dev* 15(21):2852-2864.

173. Heesom KJ & Denton RM (1999) Dissociation of the eukaryotic initiation factor-4E/4E-BP1 complex involves phosphorylation of 4E-BP1 by an mTOR-associated kinase. *FEBS Lett* 457(3):489-493.
174. Miron M, *et al.* (2001) The translational inhibitor 4E-BP is an effector of PI(3)K/Akt signalling and cell growth in *Drosophila*. *Nat Cell Biol* 3(6):596-601.
175. Heesom KJ, Avison MB, Diggle TA, & Denton RM (1998) Insulin-stimulated kinase from rat fat cells that phosphorylates initiation factor 4E-binding protein 1 on the rapamycin-insensitive site (serine-111). *Biochem J* 336 (Pt 1):39-48.
176. Wang X, Li W, Parra JL, Beugnet A, & Proud CG (2003) The C terminus of initiation factor 4E-binding protein 1 contains multiple regulatory features that influence its function and phosphorylation. *Mol Cell Biol* 23(5):1546-1557.
177. Velasquez C, *et al.* (2016) Mitotic protein kinase CDK1 phosphorylation of mRNA translation regulator 4E-BP1 Ser83 may contribute to cell transformation. *Proc Natl Acad Sci U S A* 113(30):8466-8471.
178. Leprivier G, Rotblat B, Khan D, Jan E, & Sorensen PH (2015) Stress-mediated translational control in cancer cells. *Biochim Biophys Acta* 1849(7):845-860.
179. Laplante M & Sabatini DM (2009) mTOR signaling at a glance. *J Cell Sci* 122(Pt 20):3589-3594.
180. Laplante M & Sabatini DM (2013) Regulation of mTORC1 and its impact on gene expression at a glance. *J Cell Sci* 126(Pt 8):1713-1719.
181. Topisirovic I & Sonenberg N (2015) Translation and cancer. *Biochim Biophys Acta* 1849(7):751-752.
182. Laplante M & Sabatini DM (2012) mTOR Signaling. *Cold Spring Harb Perspect Biol* 4(2).
183. Laplante M & Sabatini DM (2012) mTOR signaling in growth control and disease. *Cell* 149(2):274-293.
184. Hardie DG, Ross FA, & Hawley SA (2012) AMPK: a nutrient and energy sensor that maintains energy homeostasis. *Nat Rev Mol Cell Biol* 13(4):251-262.
185. Gwinn DM, *et al.* (2008) AMPK phosphorylation of raptor mediates a metabolic checkpoint. *Mol Cell* 30(2):214-226.

186. Inoki K, Zhu T, & Guan KL (2003) TSC2 mediates cellular energy response to control cell growth and survival. *Cell* 115(5):577-590.
187. Morita M, *et al.* (2013) mTORC1 controls mitochondrial activity and biogenesis through 4E-BP-dependent translational regulation. *Cell Metab* 18(5):698-711.
188. Zoncu R, *et al.* (2011) mTORC1 senses lysosomal amino acids through an inside-out mechanism that requires the vacuolar H(+)-ATPase. *Science* 334(6056):678-683.
189. Bar-Peled L, Schweitzer LD, Zoncu R, & Sabatini DM (2012) Ragulator is a GEF for the rag GTPases that signal amino acid levels to mTORC1. *Cell* 150(6):1196-1208.
190. Sancak Y, *et al.* (2010) Ragulator-Rag complex targets mTORC1 to the lysosomal surface and is necessary for its activation by amino acids. *Cell* 141(2):290-303.
191. Sancak Y, *et al.* (2008) The Rag GTPases bind raptor and mediate amino acid signaling to mTORC1. *Science* 320(5882):1496-1501.
192. Efeyan A, *et al.* (2013) Regulation of mTORC1 by the Rag GTPases is necessary for neonatal autophagy and survival. *Nature* 493(7434):679-683.
193. Foster DA (2007) Regulation of mTOR by phosphatidic acid? *Cancer Res* 67(1):1-4.
194. Brugarolas J, *et al.* (2004) Regulation of mTOR function in response to hypoxia by REDD1 and the TSC1/TSC2 tumor suppressor complex. *Genes Dev* 18(23):2893-2904.
195. DeYoung MP, Horak P, Sofer A, Sgroi D, & Ellisen LW (2008) Hypoxia regulates TSC1/2-mTOR signaling and tumor suppression through REDD1-mediated 14-3-3 shuttling. *Genes Dev* 22(2):239-251.
196. Li Y, *et al.* (2007) Bnip3 mediates the hypoxia-induced inhibition on mammalian target of rapamycin by interacting with Rheb. *J Biol Chem* 282(49):35803-35813.
197. Bernardi R, *et al.* (2006) PML inhibits HIF-1 α translation and neoangiogenesis through repression of mTOR. *Nature* 442(7104):779-785.

198. Corradetti MN, Inoki K, & Guan KL (2005) The stress-induced proteins RTP801 and RTP801L are negative regulators of the mammalian target of rapamycin pathway. *J Biol Chem* 280(11):9769-9772.
199. Reiling JH & Hafen E (2004) The hypoxia-induced paralogs Scylla and Charybdis inhibit growth by down-regulating S6K activity upstream of TSC in *Drosophila*. *Genes Dev* 18(23):2879-2892.
200. Feng Z, Zhang H, Levine AJ, & Jin S (2005) The coordinate regulation of the p53 and mTOR pathways in cells. *Proc Natl Acad Sci U S A* 102(23):8204-8209.
201. Stambolic V, *et al.* (2001) Regulation of PTEN transcription by p53. *Mol Cell* 8(2):317-325.
202. Tee AR & Proud CG (2000) DNA-damaging agents cause inactivation of translational regulators linked to mTOR signalling. *Oncogene* 19(26):3021-3031.
203. Horton LE, *et al.* (2002) p53 activation results in rapid dephosphorylation of the eIF4E-binding protein 4E-BP1, inhibition of ribosomal protein S6 kinase and inhibition of translation initiation. *Oncogene* 21(34):5325-5334.
204. Constantinou C & Clemens MJ (2005) Regulation of the phosphorylation and integrity of protein synthesis initiation factor eIF4GI and the translational repressor 4E-BP1 by p53. *Oncogene* 24(30):4839-4850.
205. Constantinou C, Elia A, & Clemens MJ (2008) Activation of p53 stimulates proteasome-dependent truncation of eIF4E-binding protein 1 (4E-BP1). *Biol Cell* 100(5):279-289.
206. Lee DF, *et al.* (2007) IKK beta suppression of TSC1 links inflammation and tumor angiogenesis via the mTOR pathway. *Cell* 130(3):440-455.
207. Heesom KJ, Gampel A, Mellor H, & Denton RM (2001) Cell cycle-dependent phosphorylation of the translational repressor eIF-4E binding protein-1 (4E-BP1). *Curr Biol* 11(17):1374-1379.
208. Greenberg VL & Zimmer SG (2005) Paclitaxel induces the phosphorylation of the eukaryotic translation initiation factor 4E-binding protein 1 through a Cdk1-dependent mechanism. *Oncogene* 24(30):4851-4860.
209. Shuda M, *et al.* (2015) CDK1 substitutes for mTOR kinase to activate mitotic cap-dependent protein translation. *Proc Natl Acad Sci U S A* 112(19):5875-5882.

210. Shang ZF, *et al.* (2012) 4E-BP1 participates in maintaining spindle integrity and genomic stability via interacting with PLK1. *Cell Cycle* 11(18):3463-3471.
211. Fox CJ, *et al.* (2003) The serine/threonine kinase Pim-2 is a transcriptionally regulated apoptotic inhibitor. *Genes Dev* 17(15):1841-1854.
212. Tamburini J, *et al.* (2009) Protein synthesis is resistant to rapamycin and constitutes a promising therapeutic target in acute myeloid leukemia. *Blood* 114(8):1618-1627.
213. Nawijn MC, Alendar A, & Berns A (2011) For better or for worse: the role of Pim oncogenes in tumorigenesis. *Nat Rev Cancer* 11(1):23-34.
214. Braunstein S, Badura ML, Xi Q, Formenti SC, & Schneider RJ (2009) Regulation of protein synthesis by ionizing radiation. *Mol Cell Biol* 29(21):5645-5656.
215. Imai Y, *et al.* (2008) Phosphorylation of 4E-BP by LRRK2 affects the maintenance of dopaminergic neurons in *Drosophila*. *EMBO J* 27(18):2432-2443.
216. Pons B, *et al.* (2012) Association between LRRK2 and 4E-BP1 protein levels in normal and malignant cells. *Oncol Rep* 27(1):225-231.
217. Yang DQ & Kastan MB (2000) Participation of ATM in insulin signalling through phosphorylation of eIF-4E-binding protein 1. *Nat Cell Biol* 2(12):893-898.
218. Shin S, Wolgamott L, Roux PP, & Yoon SO (2014) Casein kinase 1epsilon promotes cell proliferation by regulating mRNA translation. *Cancer Res* 74(1):201-211.
219. Shin S, *et al.* (2014) Glycogen synthase kinase-3beta positively regulates protein synthesis and cell proliferation through the regulation of translation initiation factor 4E-binding protein 1. *Oncogene* 33(13):1690-1699.
220. Walsh D & Mohr I (2004) Phosphorylation of eIF4E by Mnk-1 enhances HSV-1 translation and replication in quiescent cells. *Genes Dev* 18(6):660-672.
221. Janzen C, Sen S, Cuevas J, Reddy ST, & Chaudhuri G (2011) Protein phosphatase 2A promotes endothelial survival via stabilization of translational inhibitor 4E-BP1 following exposure to tumor necrosis factor-alpha. *Arterioscler Thromb Vasc Biol* 31(11):2586-2594.

222. Liu G, Zhang Y, Bode AM, Ma WY, & Dong Z (2002) Phosphorylation of 4E-BP1 is mediated by the p38/MSK1 pathway in response to UVB irradiation. *J Biol Chem* 277(11):8810-8816.
223. She QB, *et al.* (2010) 4E-BP1 is a key effector of the oncogenic activation of the AKT and ERK signaling pathways that integrates their function in tumors. *Cancer Cell* 18(1):39-51.
224. Yoon SO & Roux PP (2013) Rapamycin resistance: mTORC1 substrates hold some of the answers. *Curr Biol* 23(19):R880-883.
225. Zhang Y & Zheng XF (2012) mTOR-independent 4E-BP1 phosphorylation is associated with cancer resistance to mTOR kinase inhibitors. *Cell Cycle* 11(3):594-603.
226. Fingar DC & Blenis J (2004) Target of rapamycin (TOR): an integrator of nutrient and growth factor signals and coordinator of cell growth and cell cycle progression. *Oncogene* 23(18):3151-3171.
227. Fingar DC, Salama S, Tsou C, Harlow E, & Blenis J (2002) Mammalian cell size is controlled by mTOR and its downstream targets S6K1 and 4EBP1/eIF4E. *Genes Dev* 16(12):1472-1487.
228. Fingar DC, *et al.* (2004) mTOR controls cell cycle progression through its cell growth effectors S6K1 and 4E-BP1/eukaryotic translation initiation factor 4E. *Mol Cell Biol* 24(1):200-216.
229. Ramirez-Valle F, Badura ML, Braunstein S, Narasimhan M, & Schneider RJ (2010) Mitotic raptor promotes mTORC1 activity, G(2)/M cell cycle progression, and internal ribosome entry site-mediated mRNA translation. *Mol Cell Biol* 30(13):3151-3164.
230. Braun-Dullaeus RC, *et al.* (2001) Cell cycle protein expression in vascular smooth muscle cells in vitro and in vivo is regulated through phosphatidylinositol 3-kinase and mammalian target of rapamycin. *Arterioscler Thromb Vasc Biol* 21(7):1152-1158.
231. Zhang H, Stallock JP, Ng JC, Reinhard C, & Neufeld TP (2000) Regulation of cellular growth by the Drosophila target of rapamycin dTOR. *Genes Dev* 14(21):2712-2724.

232. Lynch M, Fitzgerald C, Johnston KA, Wang S, & Schmidt EV (2004) Activated eIF4E-binding protein slows G1 progression and blocks transformation by c-myc without inhibiting cell growth. *J Biol Chem* 279(5):3327-3339.
233. Graff JR & Zimmer SG (2003) Translational control and metastatic progression: enhanced activity of the mRNA cap-binding protein eIF-4E selectively enhances translation of metastasis-related mRNAs. *Clin Exp Metastasis* 20(3):265-273.
234. Zimmer SG, DeBenedetti A, & Graff JR (2000) Translational control of malignancy: the mRNA cap-binding protein, eIF-4E, as a central regulator of tumor formation, growth, invasion and metastasis. *Anticancer Res* 20(3A):1343-1351.
235. Tarnowka MA & Baglioni C (1979) Regulation of protein synthesis in mitotic HeLa cells. *J Cell Physiol* 99(3):359-367.
236. Pyronnet S, Dostie J, & Sonenberg N (2001) Suppression of cap-dependent translation in mitosis. *Genes Dev* 15(16):2083-2093.
237. Fan H & Penman S (1970) Regulation of protein synthesis in mammalian cells. II. Inhibition of protein synthesis at the level of initiation during mitosis. *J Mol Biol* 50(3):655-670.
238. Bonneau AM & Sonenberg N (1987) Involvement of the 24-kDa cap-binding protein in regulation of protein synthesis in mitosis. *J Biol Chem* 262(23):11134-11139.
239. Thoma C, Ostareck-Lederer A, & Hentze MW (2004) A poly(A) tail-responsive in vitro system for cap- or IRES-driven translation from HeLa cells. *Methods Mol Biol* 257:171-180.
240. Fredlund JO, Johansson MC, Dahlberg E, & Oredsson SM (1995) Ornithine decarboxylase and S-adenosylmethionine decarboxylase expression during the cell cycle of Chinese hamster ovary cells. *Exp Cell Res* 216(1):86-92.
241. Wilker EW, *et al.* (2007) 14-3-3sigma controls mitotic translation to facilitate cytokinesis. *Nature* 446(7133):329-332.
242. Dobrikov MI, Shveygert M, Brown MC, & Gromeier M (2014) Mitotic phosphorylation of eukaryotic initiation factor 4G1 (eIF4G1) at Ser1232 by Cdk1:cyclin B inhibits eIF4A helicase complex binding with RNA. *Mol Cell Biol* 34(3):439-451.

243. Coldwell MJ, *et al.* (2013) Phosphorylation of eIF4GII and 4E-BP1 in response to nocodazole treatment: a reappraisal of translation initiation during mitosis. *Cell Cycle* 12(23):3615-3628.
244. Park JE, Yi H, Kim Y, Chang H, & Kim VN (2016) Regulation of Poly(A) Tail and Translation during the Somatic Cell Cycle. *Mol Cell* 62(3):462-471.
245. Tanenbaum ME, Stern-Ginossar N, Weissman JS, & Vale RD (2015) Regulation of mRNA translation during mitosis. *Elife* 4.
246. Sabatini DM (2006) mTOR and cancer: insights into a complex relationship. *Nat Rev Cancer* 6(9):729-734.
247. Thornton S, Anand N, Purcell D, & Lee J (2003) Not just for housekeeping: protein initiation and elongation factors in cell growth and tumorigenesis. *J Mol Med (Berl)* 81(9):536-548.
248. Armengol G, *et al.* (2007) 4E-binding protein 1: a key molecular "funnel factor" in human cancer with clinical implications. *Cancer Res* 67(16):7551-7555.
249. Alain T, *et al.* (2012) eIF4E/4E-BP ratio predicts the efficacy of mTOR targeted therapies. *Cancer Res* 72(24):6468-6476.
250. Wang S, *et al.* (2013) HPV E6 induces eIF4E transcription to promote the proliferation and migration of cervical cancer. *FEBS Lett* 587(6):690-697.
251. Oh KJ, Kalinina A, Park NH, & Bagchi S (2006) Deregulation of eIF4E: 4E-BP1 in differentiated human papillomavirus-containing cells leads to high levels of expression of the E7 oncoprotein. *J Virol* 80(14):7079-7088.
252. Arias C, Walsh D, Harbell J, Wilson AC, & Mohr I (2009) Activation of host translational control pathways by a viral developmental switch. *PLoS Pathog* 5(3):e1000334.
253. George A, *et al.* (2012) Hepatitis C virus NS5A binds to the mRNA cap-binding eukaryotic translation initiation 4F (eIF4F) complex and up-regulates host translation initiation machinery through eIF4E-binding protein 1 inactivation. *J Biol Chem* 287(7):5042-5058.
254. De Benedetti A & Graff JR (2004) eIF-4E expression and its role in malignancies and metastases. *Oncogene* 23(18):3189-3199.

255. Lazaris-Karatzas A, *et al.* (1992) Ras mediates translation initiation factor 4E-induced malignant transformation. *Genes Dev* 6(9):1631-1642.
256. Lazaris-Karatzas A & Sonenberg N (1992) The mRNA 5' cap-binding protein, eIF-4E, cooperates with v-myc or E1A in the transformation of primary rodent fibroblasts. *Mol Cell Biol* 12(3):1234-1238.
257. Lazaris-Karatzas A, Montine KS, & Sonenberg N (1990) Malignant transformation by a eukaryotic initiation factor subunit that binds to mRNA 5' cap. *Nature* 345(6275):544-547.
258. Graff JR, *et al.* (1995) Reduction of translation initiation factor 4E decreases the malignancy of ras-transformed cloned rat embryo fibroblasts. *Int J Cancer* 60(2):255-263.
259. Rinker-Schaeffer CW, Graff JR, De Benedetti A, Zimmer SG, & Rhoads RE (1993) Decreasing the level of translation initiation factor 4E with antisense RNA causes reversal of ras-mediated transformation and tumorigenesis of cloned rat embryo fibroblasts. *Int J Cancer* 55(5):841-847.
260. Graff JR, *et al.* (2009) eIF4E activation is commonly elevated in advanced human prostate cancers and significantly related to reduced patient survival. *Cancer Res* 69(9):3866-3873.
261. Jones RM, *et al.* (1996) An essential E box in the promoter of the gene encoding the mRNA cap-binding protein (eukaryotic initiation factor 4E) is a target for activation by c-myc. *Mol Cell Biol* 16(9):4754-4764.
262. Mamane Y, *et al.* (2004) eIF4E--from translation to transformation. *Oncogene* 23(18):3172-3179.
263. Murata T & Shimotohno K (2006) Ubiquitination and proteasome-dependent degradation of human eukaryotic translation initiation factor 4E. *J Biol Chem* 281(30):20788-20800.
264. Pyronnet S (2000) Phosphorylation of the cap-binding protein eIF4E by the MAPK-activated protein kinase Mnk1. *Biochem Pharmacol* 60(8):1237-1243.
265. Waskiewicz AJ, Flynn A, Proud CG, & Cooper JA (1997) Mitogen-activated protein kinases activate the serine/threonine kinases Mnk1 and Mnk2. *EMBO J* 16(8):1909-1920.

266. Ueda T, *et al.* (2010) Combined deficiency for MAP kinase-interacting kinase 1 and 2 (Mnk1 and Mnk2) delays tumor development. *Proc Natl Acad Sci U S A* 107(32):13984-13990.
267. Shveygert M, Kaiser C, Bradrick SS, & Gromeier M (2010) Regulation of eukaryotic initiation factor 4E (eIF4E) phosphorylation by mitogen-activated protein kinase occurs through modulation of Mnk1-eIF4G interaction. *Mol Cell Biol* 30(21):5160-5167.
268. Avdulov S, *et al.* (2004) Activation of translation complex eIF4F is essential for the genesis and maintenance of the malignant phenotype in human mammary epithelial cells. *Cancer Cell* 5(6):553-563.
269. Hsieh AC, *et al.* (2010) Genetic dissection of the oncogenic mTOR pathway reveals druggable addiction to translational control via 4EBP-eIF4E. *Cancer Cell* 17(3):249-261.
270. Jacobson BA, *et al.* (2006) Repression of cap-dependent translation attenuates the transformed phenotype in non-small cell lung cancer both in vitro and in vivo. *Cancer Res* 66(8):4256-4262.
271. Boussemart L, *et al.* (2014) eIF4F is a nexus of resistance to anti-BRAF and anti-MEK cancer therapies. *Nature* 513(7516):105-109.
272. Petroulakis E, *et al.* (2009) p53-dependent translational control of senescence and transformation via 4E-BPs. *Cancer Cell* 16(5):439-446.
273. Walsh D, Mathews MB, & Mohr I (2013) Tinkering with translation: protein synthesis in virus-infected cells. *Cold Spring Harb Perspect Biol* 5(1):a012351.
274. Crosbie EJ, Einstein MH, Franceschi S, & Kitchener HC (2013) Human papillomavirus and cervical cancer. *Lancet* 382(9895):889-899.
275. Chang Y, *et al.* (1994) Identification of herpesvirus-like DNA sequences in AIDS-associated Kaposi's sarcoma. *Science* 266(5192):1865-1869.
276. Martin D, Nguyen Q, Molinolo A, & Gutkind JS (2014) Accumulation of dephosphorylated 4EBP after mTOR inhibition with rapamycin is sufficient to disrupt paracrine transformation by the KSHV vGPCR oncogene. *Oncogene* 33(18):2405-2412.
277. Feng H, Shuda M, Chang Y, & Moore PS (2008) Clonal integration of a polyomavirus in human Merkel cell carcinoma. *Science* 319(5866):1096-1100.

278. Moore PS & Chang Y (2010) Why do viruses cause cancer? Highlights of the first century of human tumour virology. *Nat Rev Cancer* 10(12):878-889.
279. Agelli M & Clegg LX (2003) Epidemiology of primary Merkel cell carcinoma in the United States. *J Am Acad Dermatol* 49(5):832-841.
280. Hodgson NC (2005) Merkel cell carcinoma: changing incidence trends. *J Surg Oncol* 89(1):1-4.
281. Lemos B & Nghiem P (2007) Merkel cell carcinoma: more deaths but still no pathway to blame. *J Invest Dermatol* 127(9):2100-2103.
282. Lucarz A & Brand G (2007) Current considerations about Merkel cells. *Eur J Cell Biol* 86(5):243-251.
283. Engels EA, Frisch M, Goedert JJ, Biggar RJ, & Miller RW (2002) Merkel cell carcinoma and HIV infection. *Lancet* 359(9305):497-498.
284. Chang Y & Moore PS (2012) Merkel cell carcinoma: a virus-induced human cancer. *Annu Rev Pathol* 7:123-144.
285. Miller RW & Rabkin CS (1999) Merkel cell carcinoma and melanoma: etiological similarities and differences. *Cancer Epidemiol Biomarkers Prev* 8(2):153-158.
286. Rodig SJ, *et al.* (2012) Improved detection suggests all Merkel cell carcinomas harbor Merkel polyomavirus. *J Clin Invest* 122(12):4645-4653.
287. Linzer DI & Levine AJ (1979) Characterization of a 54K dalton cellular SV40 tumor antigen present in SV40-transformed cells and uninfected embryonal carcinoma cells. *Cell* 17(1):43-52.
288. Pallas DC, *et al.* (1990) Polyoma small and middle T antigens and SV40 small t antigen form stable complexes with protein phosphatase 2A. *Cell* 60(1):167-176.
289. Kaplan DR, *et al.* (1987) Common elements in growth factor stimulation and oncogenic transformation: 85 kd phosphoprotein and phosphatidylinositol kinase activity. *Cell* 50(7):1021-1029.
290. Poulin DL & DeCaprio JA (2006) Is there a role for SV40 in human cancer? *J Clin Oncol* 24(26):4356-4365.
291. Berrios C, *et al.* (2015) Malawi polyomavirus is a prevalent human virus that interacts with known tumor suppressors. *J Virol* 89(1):857-862.

292. Nicol JT, *et al.* (2014) Seroprevalence of human Malawi polyomavirus. *J Clin Microbiol* 52(1):321-323.
293. van der Meijden E, *et al.* (2011) Seroprevalence of trichodysplasia spinulosa-associated polyomavirus. *Emerg Infect Dis* 17(8):1355-1363.
294. Viscidi RP, *et al.* (2011) Age-specific seroprevalence of Merkel cell polyomavirus, BK virus, and JC virus. *Clin Vaccine Immunol* 18(10):1737-1743.
295. Alexiev BA, Randhawa P, Drachenberg CB, & Papadimitriou JC (2013) BK virus-associated urinary bladder carcinoma in transplant recipients: productive or nonproductive polyomavirus infections in tumor cells?--reply. *Hum Pathol* 44(12):2871-2872.
296. Shuda M, Chang Y, & Moore PS (2014) Merkel cell polyomavirus-positive Merkel cell carcinoma requires viral small T-antigen for cell proliferation. *J Invest Dermatol* 134(5):1479-1481.
297. Richards KF, *et al.* (2015) Merkel cell polyomavirus T antigens promote cell proliferation and inflammatory cytokine gene expression. *J Gen Virol* 96(12):3532-3544.
298. Carter JJ, *et al.* (2013) Identification of an overprinting gene in Merkel cell polyomavirus provides evolutionary insight into the birth of viral genes. *Proc Natl Acad Sci U S A* 110(31):12744-12749.
299. DeCaprio JA & Garcea RL (2013) A cornucopia of human polyomaviruses. *Nat Rev Microbiol* 11(4):264-276.
300. Feng H, *et al.* (2011) Cellular and viral factors regulating Merkel cell polyomavirus replication. *PLoS One* 6(7):e22468.
301. Lee S, *et al.* (2011) Identification and validation of a novel mature microRNA encoded by the Merkel cell polyomavirus in human Merkel cell carcinomas. *J Clin Virol* 52(3):272-275.
302. Seo GJ, Chen CJ, & Sullivan CS (2009) Merkel cell polyomavirus encodes a microRNA with the ability to autoregulate viral gene expression. *Virology* 383(2):183-187.
303. Spurgeon ME & Lambert PF (2013) Merkel cell polyomavirus: a newly discovered human virus with oncogenic potential. *Virology* 435(1):118-130.

304. Neumann F, *et al.* (2011) Replication, gene expression and particle production by a consensus Merkel Cell Polyomavirus (MCPyV) genome. *PLoS One* 6(12):e29112.
305. Tolstov YL, *et al.* (2009) Human Merkel cell polyomavirus infection II. MCV is a common human infection that can be detected by conformational capsid epitope immunoassays. *Int J Cancer* 125(6):1250-1256.
306. Schowalter RM, Pastrana DV, & Buck CB (2011) Glycosaminoglycans and sialylated glycans sequentially facilitate Merkel cell polyomavirus infectious entry. *PLoS Pathog* 7(7):e1002161.
307. Pastrana DV, *et al.* (2009) Quantitation of human seroresponsiveness to Merkel cell polyomavirus. *PLoS Pathog* 5(9):e1000578.
308. Erickson KD, Garcea RL, & Tsai B (2009) Ganglioside GT1b is a putative host cell receptor for the Merkel cell polyomavirus. *J Virol* 83(19):10275-10279.
309. Neu U, Stehle T, & Atwood WJ (2009) The Polyomaviridae: Contributions of virus structure to our understanding of virus receptors and infectious entry. *Virology* 384(2):389-399.
310. Neu U, *et al.* (2012) Structures of Merkel cell polyomavirus VP1 complexes define a sialic acid binding site required for infection. *PLoS Pathog* 8(7):e1002738.
311. Lane DP & Crawford LV (1979) T antigen is bound to a host protein in SV40-transformed cells. *Nature* 278(5701):261-263.
312. DeCaprio JA, *et al.* (1988) SV40 large tumor antigen forms a specific complex with the product of the retinoblastoma susceptibility gene. *Cell* 54(2):275-283.
313. Wendzicki JA, Moore PS, & Chang Y (2015) Large T and small T antigens of Merkel cell polyomavirus. *Curr Opin Virol* 11:38-43.
314. Pipas JM (1992) Common and unique features of T antigens encoded by the polyomavirus group. *J Virol* 66(7):3979-3985.
315. Shuda M, *et al.* (2008) T antigen mutations are a human tumor-specific signature for Merkel cell polyomavirus. *Proc Natl Acad Sci U S A* 105(42):16272-16277.

316. Kwun HJ, *et al.* (2009) The minimum replication origin of merkel cell polyomavirus has a unique large T-antigen loading architecture and requires small T-antigen expression for optimal replication. *J Virol* 83(23):12118-12128.
317. Nakamura T, *et al.* (2010) Nuclear localization of Merkel cell polyomavirus large T antigen in Merkel cell carcinoma. *Virology* 398(2):273-279.
318. Liu X, *et al.* (2011) Merkel cell polyomavirus large T antigen disrupts lysosome clustering by translocating human Vam6p from the cytoplasm to the nucleus. *J Biol Chem* 286(19):17079-17090.
319. Borchert S, *et al.* (2014) High-affinity Rb binding, p53 inhibition, subcellular localization, and transformation by wild-type or tumor-derived shortened Merkel cell polyomavirus large T antigens. *J Virol* 88(6):3144-3160.
320. An P, Saenz Robles MT, & Pipas JM (2012) Large T antigens of polyomaviruses: amazing molecular machines. *Annu Rev Microbiol* 66:213-236.
321. Arora R, *et al.* (2012) Survivin is a therapeutic target in Merkel cell carcinoma. *Sci Transl Med* 4(133):133ra156.
322. Houben R, *et al.* (2012) An intact retinoblastoma protein-binding site in Merkel cell polyomavirus large T antigen is required for promoting growth of Merkel cell carcinoma cells. *Int J Cancer* 130(4):847-856.
323. Dresang LR, *et al.* (2013) Response of Merkel cell polyomavirus-positive merkel cell carcinoma xenografts to a survivin inhibitor. *PLoS One* 8(11):e80543.
324. Harrison CJ, *et al.* (2011) Asymmetric assembly of Merkel cell polyomavirus large T-antigen origin binding domains at the viral origin. *J Mol Biol* 409(4):529-542.
325. Diaz J, Wang X, Tsang SH, Jiao J, & You J (2014) Phosphorylation of large T antigen regulates merkel cell polyomavirus replication. *Cancers (Basel)* 6(3):1464-1486.
326. Fischer N, Brandner J, Fuchs F, Moll I, & Grundhoff A (2010) Detection of Merkel cell polyomavirus (MCPyV) in Merkel cell carcinoma cell lines: cell morphology and growth phenotype do not reflect presence of the virus. *Int J Cancer* 126(9):2133-2142.
327. Li J, *et al.* (2013) Merkel cell polyomavirus large T antigen disrupts host genomic integrity and inhibits cellular proliferation. *J Virol* 87(16):9173-9188.

328. Li J, Diaz J, Wang X, Tsang SH, & You J (2015) Phosphorylation of Merkel cell polyomavirus large tumor antigen at serine 816 by ATM kinase induces apoptosis in host cells. *J Biol Chem* 290(3):1874-1884.
329. Cheng J, Rozenblatt-Rosen O, Paulson KG, Nghiem P, & DeCaprio JA (2013) Merkel cell polyomavirus large T antigen has growth-promoting and inhibitory activities. *J Virol* 87(11):6118-6126.
330. Verhaegen ME, *et al.* (2015) Merkel cell polyomavirus small T antigen is oncogenic in transgenic mice. *J Invest Dermatol* 135(5):1415-1424.
331. Shuda M, *et al.* (2015) Merkel Cell Polyomavirus Small T Antigen Induces Cancer and Embryonic Merkel Cell Proliferation in a Transgenic Mouse Model. *PLoS One* 10(11):e0142329.
332. Rodriguez-Viciano P, Collins C, & Fried M (2006) Polyoma and SV40 proteins differentially regulate PP2A to activate distinct cellular signaling pathways involved in growth control. *Proc Natl Acad Sci U S A* 103(51):19290-19295.
333. Sontag E, *et al.* (1993) The interaction of SV40 small tumor antigen with protein phosphatase 2A stimulates the map kinase pathway and induces cell proliferation. *Cell* 75(5):887-897.
334. Hwang JH, Jiang T, Kulkarni S, Faure N, & Schaffhausen BS (2013) Protein phosphatase 2A isoforms utilizing Abeta scaffolds regulate differentiation through control of Akt protein. *J Biol Chem* 288(44):32064-32073.
335. Griffiths DA, *et al.* (2013) Merkel cell polyomavirus small T antigen targets the NEMO adaptor protein to disrupt inflammatory signaling. *J Virol* 87(24):13853-13867.
336. Kwun HJ, *et al.* (2015) Restricted protein phosphatase 2A targeting by Merkel cell polyomavirus small T antigen. *J Virol* 89(8):4191-4200.
337. Knight LM, *et al.* (2015) Merkel cell polyomavirus small T antigen mediates microtubule destabilization to promote cell motility and migration. *J Virol* 89(1):35-47.
338. Kwun HJ, *et al.* (2013) Merkel cell polyomavirus small T antigen controls viral replication and oncoprotein expression by targeting the cellular ubiquitin ligase SCFFbw7. *Cell Host Microbe* 14(2):125-135.

339. Tsang SH, *et al.* (2015) The Oncogenic Small Tumor Antigen of Merkel Cell Polyomavirus Is an Iron-Sulfur Cluster Protein That Enhances Viral DNA Replication. *J Virol* 90(3):1544-1556.
340. Wang X & Proud CG (2011) mTORC1 signaling: what we still don't know. *J Mol Cell Biol* 3(4):206-220.
341. Prescott DM & Bender MA (1962) Synthesis of RNA and protein during mitosis in mammalian tissue culture cells. *Exp Cell Res* 26:260-268.
342. Konrad CG (1963) Protein Synthesis and Rna Synthesis during Mitosis in Animal Cells. *J Cell Biol* 19:267-277.
343. Schrama D, Ugurel S, & Becker JC (2012) Merkel cell carcinoma: recent insights and new treatment options. *Curr Opin Oncol* 24(2):141-149.
344. Terasima T & Tolmach LJ (1963) Growth and nucleic acid synthesis in synchronously dividing populations of HeLa cells. *Exp Cell Res* 30:344-362.
345. Vassilev LT, *et al.* (2006) Selective small-molecule inhibitor reveals critical mitotic functions of human CDK1. *Proc Natl Acad Sci U S A* 103(28):10660-10665.
346. Kanie T, *et al.* (2012) Genetic reevaluation of the role of F-box proteins in cyclin D1 degradation. *Mol Cell Biol* 32(3):590-605.
347. Feldman ME, *et al.* (2009) Active-site inhibitors of mTOR target rapamycin-resistant outputs of mTORC1 and mTORC2. *PLoS Biol* 7(2):e38.
348. Tyler RK, Shpiro N, Marquez R, & Eyers PA (2007) VX-680 inhibits Aurora A and Aurora B kinase activity in human cells. *Cell Cycle* 6(22):2846-2854.
349. Chung J, Kuo CJ, Crabtree GR, & Blenis J (1992) Rapamycin-FKBP specifically blocks growth-dependent activation of and signaling by the 70 kd S6 protein kinases. *Cell* 69(7):1227-1236.
350. Magnuson B, Ekim B, & Fingar DC (2012) Regulation and function of ribosomal protein S6 kinase (S6K) within mTOR signalling networks. *Biochem J* 441(1):1-21.
351. Vassilev LT (2006) Cell cycle synchronization at the G2/M phase border by reversible inhibition of CDK1. *Cell Cycle* 5(22):2555-2556.

352. Kiick KL, Saxon E, Tirrell DA, & Bertozzi CR (2002) Incorporation of azides into recombinant proteins for chemoselective modification by the Staudinger ligation. *Proc Natl Acad Sci U S A* 99(1):19-24.
353. Wang Q, *et al.* (2003) Bioconjugation by copper(I)-catalyzed azide-alkyne [3 + 2] cycloaddition. *J Am Chem Soc* 125(11):3192-3193.
354. Nielsen DA & Shapiro DJ (1986) Preparation of capped RNA transcripts using T7 RNA polymerase. *Nucleic Acids Res* 14(14):5936.
355. Stepinski J, Waddell C, Stolarski R, Darzynkiewicz E, & Rhoads RE (2001) Synthesis and properties of mRNAs containing the novel "anti-reverse" cap analogs 7-methyl(3'-O-methyl)GpppG and 7-methyl (3'-deoxy)GpppG. *RNA* 7(10):1486-1495.
356. Cencic R, *et al.* (2011) Reversing chemoresistance by small molecule inhibition of the translation initiation complex eIF4F. *Proc Natl Acad Sci U S A* 108(3):1046-1051.
357. Mazroui R, Di Marco S, Kaufman RJ, & Gallouzi IE (2007) Inhibition of the ubiquitin-proteasome system induces stress granule formation. *Mol Biol Cell* 18(7):2603-2618.
358. Stehelin D, Varmus HE, Bishop JM, & Vogt PK (1976) DNA related to the transforming gene(s) of avian sarcoma viruses is present in normal avian DNA. *Nature* 260(5547):170-173.
359. Werness BA, Levine AJ, & Howley PM (1990) Association of human papillomavirus types 16 and 18 E6 proteins with p53. *Science* 248(4951):76-79.
360. Chang HW, *et al.* (1997) Transformation of chicken cells by the gene encoding the catalytic subunit of PI 3-kinase. *Science* 276(5320):1848-1850.
361. Moore PS & Chang Y (1998) Antiviral activity of tumor-suppressor pathways: clues from molecular piracy by KSHV. *Trends Genet* 14(4):144-150.
362. Shahbazian D, *et al.* (2006) The mTOR/PI3K and MAPK pathways converge on eIF4B to control its phosphorylation and activity. *EMBO J* 25(12):2781-2791.
363. Wang X, *et al.* (2001) Regulation of elongation factor 2 kinase by p90(RSK1) and p70 S6 kinase. *EMBO J* 20(16):4370-4379.

364. Carew JS, Kelly KR, & Nawrocki ST (2011) Mechanisms of mTOR inhibitor resistance in cancer therapy. *Target Oncol* 6(1):17-27.
365. Mertins P, *et al.* (2014) Ischemia in tumors induces early and sustained phosphorylation changes in stress kinase pathways but does not affect global protein levels. *Mol Cell Proteomics* 13(7):1690-1704.
366. Brown JN, *et al.* (2012) Morphine produces immunosuppressive effects in nonhuman primates at the proteomic and cellular levels. *Mol Cell Proteomics* 11(9):605-618.
367. Enserink JM & Kolodner RD (2010) An overview of Cdk1-controlled targets and processes. *Cell Div* 5:11.
368. Skoufias DA, Indorato RL, Lacroix F, Panopoulos A, & Margolis RL (2007) Mitosis persists in the absence of Cdk1 activity when proteolysis or protein phosphatase activity is suppressed. *J Cell Biol* 179(4):671-685.
369. Li DW, *et al.* (2005) Dynamic distribution of Ser-10 phosphorylated histone H3 in cytoplasm of MCF-7 and CHO cells during mitosis. *Cell Res* 15(2):120-126.
370. Paku KS, *et al.* (2012) A conserved motif within the flexible C-terminus of the translational regulator 4E-BP is required for tight binding to the mRNA cap-binding protein eIF4E. *Biochem J* 441(1):237-245.
371. Gosselin P, *et al.* (2011) The translational repressor 4E-BP called to order by eIF4E: new structural insights by SAXS. *Nucleic Acids Res* 39(8):3496-3503.
372. Webb NR, Chari RV, DePillis G, Kozarich JW, & Rhoads RE (1984) Purification of the messenger RNA cap-binding protein using a new affinity medium. *Biochemistry* 23(2):177-181.
373. Rousseau D, Gingras AC, Pause A, & Sonenberg N (1996) The eIF4E-binding proteins 1 and 2 are negative regulators of cell growth. *Oncogene* 13(11):2415-2420.
374. Li S, *et al.* (2002) Translational control of cell fate: availability of phosphorylation sites on translational repressor 4E-BP1 governs its proapoptotic potency. *Mol Cell Biol* 22(8):2853-2861.
375. Jansova D, *et al.* (2017) Regulation of 4E-BP1 activity in the mammalian oocyte. *Cell Cycle*:1-13.

376. Gruner S, *et al.* (2016) The Structures of eIF4E-eIF4G Complexes Reveal an Extended Interface to Regulate Translation Initiation. *Mol Cell* 64(3):467-479.
377. Tcherkezian J, *et al.* (2014) Proteomic analysis of cap-dependent translation identifies LARP1 as a key regulator of 5'TOP mRNA translation. *Genes Dev* 28(4):357-371.
378. Lahr RM, *et al.* (2017) La-related protein 1 (LARP1) binds the mRNA cap, blocking eIF4F assembly on TOP mRNAs. *Elife* 6.
379. Fonseca BD, *et al.* (2015) La-related Protein 1 (LARP1) Represses Terminal Oligopyrimidine (TOP) mRNA Translation Downstream of mTOR Complex 1 (mTORC1). *J Biol Chem* 290(26):15996-16020.
380. Fehr AR & Yu D (2013) Control the host cell cycle: viral regulation of the anaphase-promoting complex. *J Virol* 87(16):8818-8825.
381. Zambelli F & Pavesi G (2015) RIP-Seq data analysis to determine RNA-protein associations. *Methods Mol Biol* 1269:293-303.
382. Aramayo R & Polymenis M (2017) Ribosome profiling the cell cycle: lessons and challenges. *Curr Genet*.
383. Li Y (2011) The tandem affinity purification technology: an overview. *Biotechnol Lett* 33(8):1487-1499.